Infectious Bronchitis Virus

Ding Xiang Liu[1]*, Yan Ling Ng[2] and To Sing Fung[1]

5

[1]South China Agricultural University, Guangdong Province Key Laboratory Microbial Signals & Disease Co, and Integrative Microbiology Research Centre, Guangzhou, Guangdong, People's Republic of China.
[2]School of Biological Sciences, Nanyang Technological University, Singapore.

*Correspondence: dxliu0001@163.com

https://doi.org/10.21775/9781912530106.05

Abstract

Infectious bronchitis virus (IBV) is one of the major avian viral pathogens that afflict the global poultry industry. Since its first isolation in 1931, astounding numbers of IBV variants have been identified around the world. With the continuous emergence of pathogenic variants and the lack of efficacious IBV vaccines that provide a broad spectrum of protection, it is crucial to study and understand the biology of this economically important pathogen. In fact, using IBV as a prototype coronavirus, research over the past few decades have unravelled some of the most fundamental concepts in the molecular cell biology and pathogenesis of coronavirus. Also, IBV is among the few coronaviruses that reverse genetics systems were first successfully established. In this chapter, we first briefly revisit the history of IBV, followed by an up-to-date review of its molecular biology and effects on the infected cells, with a focus on the molecular mechanisms of viral replication and the strategies exploited by this virus to regulate and interact with critical cellular signalling pathways, such as ER stress response, autophagy and apoptosis. We then review the pathogenesis of IBV, and end with a discussion on the current status of IBV epizootiology, prevention and control.

History

Infectious bronchitis virus (IBV), the first known member of the genus *Gammacoronavirus* in the family *Coronaviridae*, came to light in North Dakota, USA, in 1931 as the causative agent of infectious bronchitis (IB), described as 'an apparently new respiratory disease of baby chicks' (Schalk and Hawn, 1931). IB is an acute, contagious respiratory disease marked by gasping, nasal discharge, coughing and tracheal rales. Following the identification of IBV, the virus was subsequently found in various regions around the world with an intensive poultry industry, including Africa (Ahmed, 1954), Asia (Song *et al.*, 1998), South America (Hipólito, 1957) and Europe (Dawson and Gough, 1971). Although it was commonly thought that Massachusetts (Mass) strain was the only IBV variant, a breakthrough study by Jungherr and co-workers (1956) reported that the Connecticut (Conn) isolate found in 1951 did not cross-protect against the Mass strain isolated in the 1940s, indicating the presence of multiple IBV variants circulating around the world. In the same year, drastic drops in egg production and quality were also reported, reflecting the economic impact upon farms hit by IB outbreaks (Broadfoot *et al.*, 1956).

Although IBV is known to primarily infect the respiratory tract of chickens, some strains displayed a preference for the oviduct, kidney and muscles of the chickens; M41 for the first two (Jones and Jordan, 1972; Jones, 1974) and 793/B for the latter (Gough *et al.*, 1992). Despite initial success in controlling the disease through commercially available IB vaccines, IB outbreaks continue to occur in well-vaccinated flocks. Particularly, there is an unprecedented increase in the incidence of flocks with renal problems (Choi *et al.*, 2009), as illustrated by the Kllb type IBV field strain that emerged in Korea, known as Kr/Q43/06. Following challenge with Kr/Q43/06, specific pathogen free (SPF) 1-week-old chicks developed dyspnoea and nephropathogenic lesions. This finding fuelled the interest in developing new vaccines against nephropathogenic and myopathogenic strains of IBV.

With the advances in IB detection and diagnostic techniques, numerous IBV variants had been identified based on serological tests, such as virus neutralization (VN) test for classifying field isolates in the following decades (Hofstad, 1958; Hitchner *et al.*, 1966; Hopkins, 1974; Cowen and Hitchner, 1975a; Johnson and Marquardt, 1976). Reverse transcription-polymerase chain reaction (RT-PCR) has proved to be an important tool for detection and diagnosis of IB (Jackwood *et al.*, 1992; Adzhar *et al.*, 1996). Using RT-PCR surveying, Jackwood and colleagues (2005) have identified 82 different IBV variants over an 11-year period, with some are widely distributed and of economic significance. The most significant of these were the Ark, Conn, and Mass strains, against which vaccines were developed in the USA, either singly or in combination (Gelb and Cloud, 1983). While most of these variants were only present for a brief period, some transient variants have occasionally caused major disease outbreaks. This is best exemplified by IBV variant B1648, which is associated with renal problems in vaccinated flocks in the 1990s (Lambrechts *et al.*, 1993; Pensaert and Lambrechts, 1994). Of the IBV variants

identified in Europe, perhaps the ones of major importance are 4/91, 793B, CR88 (Gough *et al.*, 1992; Parsons *et al.*, 1992). Some IBV variants may be geographically restricted, and multiple studies have employed molecular methods to identify IBV variants unique to the region (Escorcia *et al.*, 2000; Collison *et al.*, 2001; Gelb *et al.*, 2001; Alvarado *et al.*, 2005).

Nomenclature

IBV is an enveloped, positive sense, single-stranded RNA virus classified under the family *Coronaviridae* of the order *Nidovirales*, along with families *Arteriviridae*, *Mesoniviridae*, and *Roniviridae* (International Committee on Taxonomy of viruses, http://www.ictvonline.org/virustaxonomy.asp). Virus taxonomy of the family *Coronaviridae* is shown in Fig. 5.1. Nidoviruses are set apart from other RNA viruses by four distinctive characteristics: (a) an invariant genome organization comprising a large replicase gene occupying the 5′ two-thirds of the viral genome, (b) translation of the replicase-transcriptase polyprotein is performed via ribosomal frame-shifting, (c) the structural and accessory genes downstream of the replicase gene are expressed via a 3′-nested subgenomic messenger RNAs (sgRNAs) and (d) a collection of viral enzymatic activities are encoded within the replicase-transcriptase protein products.

The classification systems of IBV strains are divided into two major groups, namely the functional and non-functional tests (Table 5.1). Functional tests look into the biological functions of the said IBV strains, and categorize IBV into various pathotypes, protectotypes and antigenic types. On the other hand, the non-functional tests probe into the viral genome, and this usually results in grouping IBVs based on genotype (de Wit, 2000; Valastro *et al.*, 2016).

Sequence comparisons of the complete genome, spike (S) protein subunits 1 and 2 (S1 and S2), envelope (E) protein, membrane (M) protein and nucleocapsid (N) protein of IBV strains from distinct geographical regions have contributed great strides in the construction of the IBV phylogenetic tree (Fig. 5.2) (Lin *et al.*, 2016).

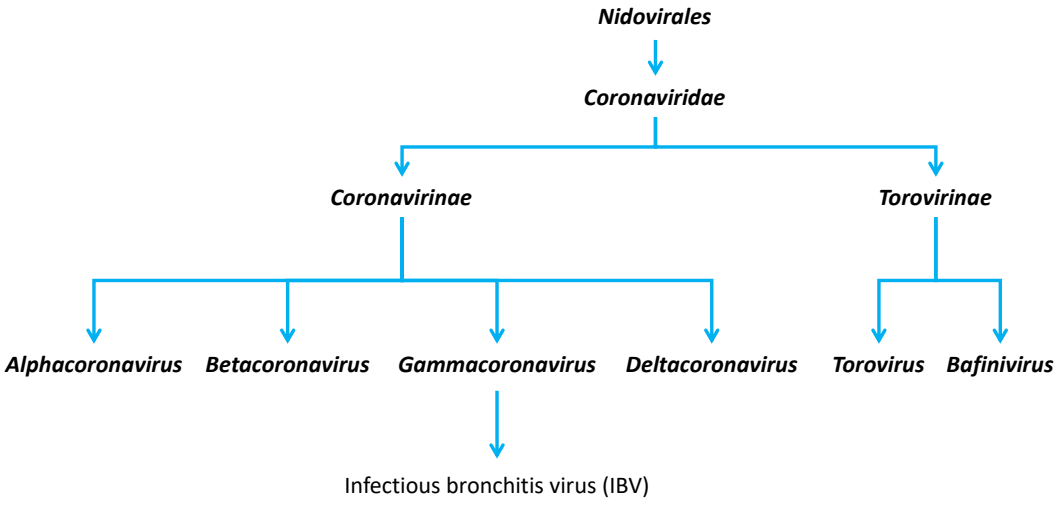

Figure 5.1 Taxonomy of the family *Coronaviridae*. Infectious bronchitis virus (IBV) is a *Gammacoronavirus*, under the family *Coronaviridae* within the order *Nidovirales*.

Table 5.1 Classification of infectious bronchitis virus (IBV) into pathotypes, protectotypes, antigenic types and genotypes

	Parameter measured	Features
Functional tests		
Pathotypes	Clinical signs, gross lesions, and virus pathogenicity; same pathotype when both tested strains induce similar pathological signs	Pros: practical in the field for vaccine strategy
Protectotypes	Complete immune response against an IBV strain; same protectotype when strains induce protection against each other	Pros: provides valuable information about vaccine efficacy Cons: laborious and expensive; requires high-level facilities for vaccination-challenge studies
Antigenic types (serotypes and epitope type)	Reaction between IBV strain and chicken-induced IBV serotype-specific antibodies; same serotype when heterologous neutralization titres differ less than 20-fold from homologous titres	Cons: less practical when more IB variants are found in the area as every serotype requires its own neutralization test. For new IB strains, an antiserum has to be raised in SPF birds.
Non-functional tests		
Genotypes	Genetic characterization of viral genome; same genotype when sequence of tested strain matches	Pros: objective; provides useful information for epidemiological studies

IB, infectious bronchitis; IBV, infectious bronchitis virus; SPF, specific pathogen free.

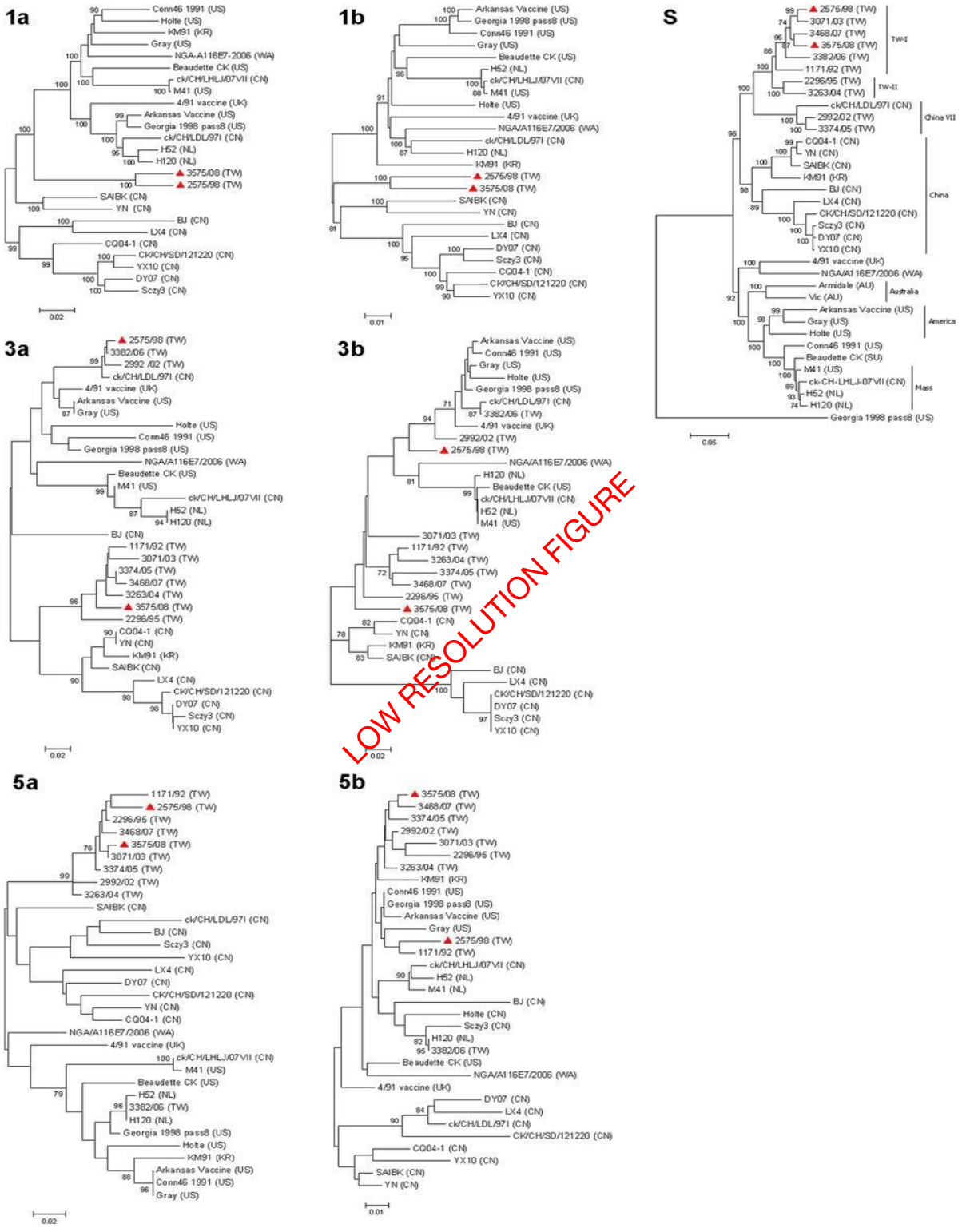

Figure 5.2 Phylogenetic tree of infectious bronchitis virus (IBV) proteins 1a, 1b, 3a, 3b, 5a, 5b and S based on neighbour-joining method. The red triangle represents IBV strains 3575/08 and 2575/98. AU, Australia; CN, China; NL, Netherlands; TW, Taiwan; UK, United Kingdom; US, United States; WA, Western Africa. Taken from 'Identification of an infectious bronchitis coronavirus strain exhibiting a classical genotype but altered antigenicity, pathogenicity, and innate immunity profile' by Lin, S.Y., Li, Y.T., Chen, Y.T., Chen T.C., Hu, C.M.J, and Chen, H.W., licensed under CC BY. https://doi.org/10.1038/srep37725. [108]

Morphology

Under the electron microscope, CoV virions appear roughly spherical and 82 nm in diameter (Becker *et al.*, 1967), and have distinct 'club-like' projections radiating from the virion surface. The exterior projections formed by trimers of S protein render the virus particle to resemble like a crown and based on this morphological feature these group of viruses are called 'coronaviruses' (the rootword '*corona*' means *crown* in Latin) (Fig. 5.3). In addition to the S protein, structural M and E proteins are also found on the membrane, while the helically symmetrical nucleocapsid which contains the N protein and viral RNA genome (Fig. 5.3). The genome is enclosed within the N protein core (Fig. 5.3).

Propagation

Embryonated eggs

Embryonated chicken eggs are utilized as a laboratory host system for isolation and propagation of a variety of avian CoVs, such as turkey CoV (TCoV) (Adams and Hofstad, 1971) and pheasant CoVs (Gough *et al.*, 1996). Pioneering work on IBV propagation in embryonated chicken eggs in the 1970s established that IBV grows well in embryonated chicken eggs, and the passage of IBV field isolate via the allantoic route of 9-day-old embryos became the method of choice for virus isolation (Cunningham, 1970; Fabricant, 1998). Furthermore, embryonated chicken eggs have been utilized for production of IBV vaccines on a commercial scale (Britton *et al.*, 2012). Collectively, embryonated chicken eggs provide a potential host system for isolation and propagation of CoVs, and it may be used for studies aimed for identifying novel CoVs.

The embryonated chicken egg comprises the developing embryo and supporting membrane which enclose cavities or 'sacs' within the egg (Hawkes, 1979). The shell membrane lies directly under the shell, a tough fibrinous membrane forming the air sac in the region of the broader end of the egg (Fig. 5.4). In contrast to the shell membrane, the chorioallantoic (CAM), amniotic and yolk membranes comprised largely of epithelium, providing potential sites for IBV replication. CAM, which lies directly underneath the shell membrane, is a highly vascular membrane serving as the respiratory organ of the embryo. In addition, the CAM is the largest of all embryo membranes, and consequently encloses the largest cavity within the egg known as the allantoic cavity. In an embryonated chicken egg, this cavity can hold up to 10 ml of fluid depending on the stage of embryonation. The amniotic membrane encloses the embryo and forms the amniotic cavity and may contain approximately 1 ml of fluid in an embryonated chicken egg. The yolk sac attached to the embryo contains nutrients for use during embryonic development and post-hatch period.

The developing embryo and its membranes (CAM, amniotic and yolk) provide diverse cell types necessary for successful replication of different viruses, including IBV. Virus may be inoculated into embryonated eggs through depositing onto the CAM or within the allantoic, amniotic and yolk sacs (Senne, 2008). For avian CoVs, inoculation of eggs by allantoic or amniotic routes has been shown to provide access to specific cell types which support their replication (Gough *et al.*, 1996; Cavanagh and Naqi, 2003; Guy, 2013). IBV is an epitheliotropic virus that replicates in a variety of epithelial tissues in post-hatch chickens such as the respiratory tract, gastrointestinal tract, kidney, bursa of Fabricius and oviduct (Cavanagh, 2003), and replicates well regardless of inoculation route in the embryonated egg. However, the allantoic route is favoured as the virus replicates extensively in the epithelium of CAM and high titres of IBV are shed into the allantoic fluid (Jordan and Nassar, 1973).

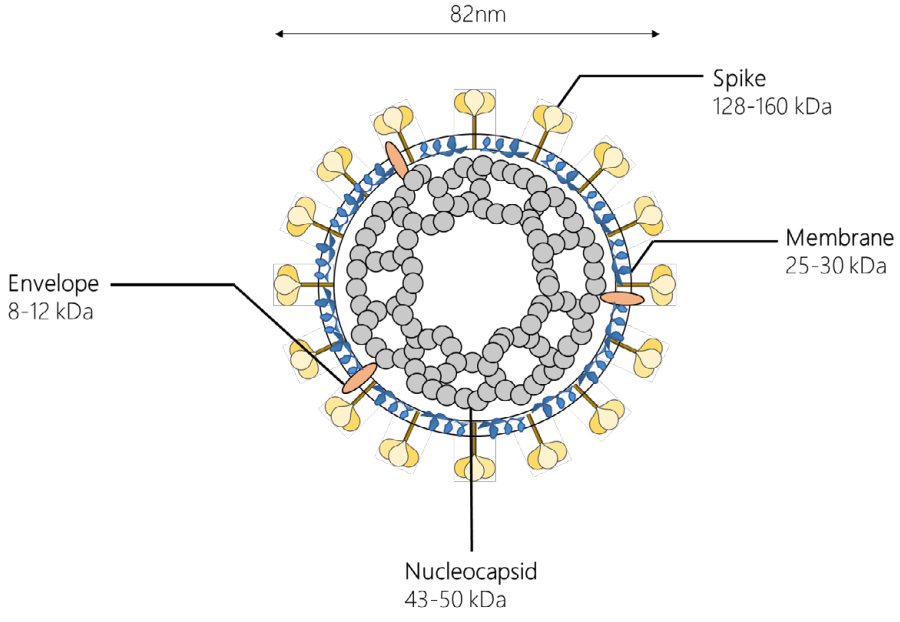

Figure 5.3 Schematic of a coronavirus virion. The structural proteins of coronaviruses, the spike, membrane, nucleocapsid and envelope proteins are shown along with the nucleocapsid encapsidated (+)sense RNA genome. The molecular weight of each structural protein monomer is shown. The size of an infectious bronchitis virus (IBV) virion is approximately 82 nm.

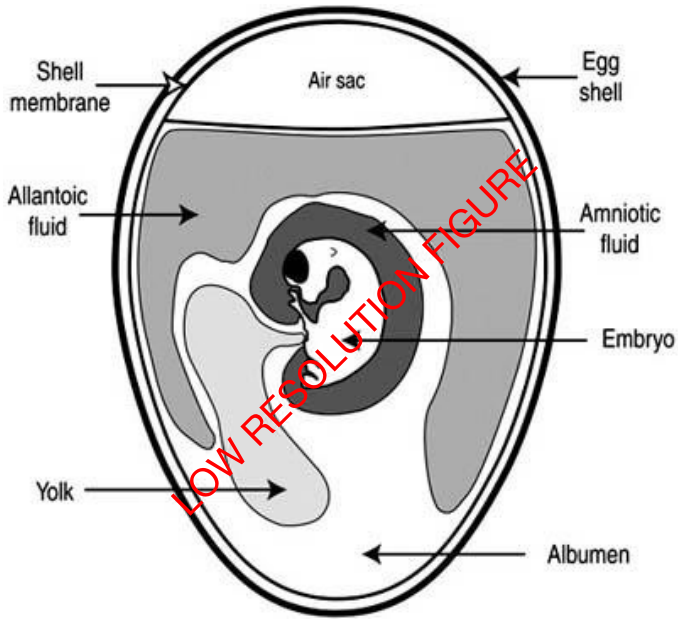

[109] **Figure 5.4** Anatomy of an embryonated egg. Taken from 'A Basic Laboratory Manual for the Small-Scale Production and Testing of I-2 Newcastle Disease Vaccine' by Sally E Grimes (ISBN-974-7946-26-2). http://www.fao.org/docrep/005/ac802e/ac802e0v.htm

Tracheal organ cultures (TOCs)

TOCs are a common method used for propagation of numerous respiratory tract pathogens (McGee and Woods, 1987). Some of the first reports include human CoVs (HCoVs) (Tyrrell and Bynoe, 1965), Newcastle disease virus (Cummiskey *et al.*, 1973) and influenza A2 virus variant (Higgins and Ellis, 1972). TOC have been used in studies of pathogenicity and induction of protective immunity (Hodgson *et al.*, 2004). This system has been successfully prepared for IBV using multiwell-plates (Yachida *et al.*, 1978) and chicken embryo TOCs on a rolling tube assembly (Cherry and Taylor-Robinson, 1970). The latter propagation protocol appears to maintain the ciliary activity of TOCs longer than static cultures, perhaps as a result of lower debris accumulation within the TOCs rings, making the observation of ciliary activity easier.

Chicken kidney cell cultures

Chicken kidney (CK) cell cultures have historically proved useful for the isolation of IBV. The techniques for preparing monolayer cultures from adult CK cells suitable for growth and quantification of viruses have been available for decades. The first technique involves the preparation of monkey kidney cultures in 1953 (Dulbecco and Vogt, 1954) and the modification of the process came in 1954 (Youngner, 1954). In 1959, the preparation of CK monolayer cultures from 4- to 5-day-old chicks were described (Maassab, 1959), and its use in the study of avian viruses including IBV were reported in 1965 using 3- to 8-week-old chickens (Churchill, 1965).

While IBV titration in CK cells yields lower titres compared with embryonated chicken eggs (Darbyshire *et al.*, 1975) and TOCs (Cook *et al.*,1976), the propagation of many IBV strains in CK cells is well proven. Following adaptation in embryonated eggs, IBV strains Beaudette and Mass are capable of producing characteristic cytopathic effects within two CK passages (Churchill, 1965), with the Beaudette strain displaying syncytium formation 6 h post infection (Alexander and Collins, 1975). The growth curves of IBV in CK cells exhibit a lag phase of 2–4 h and maximum virus yield in 18–20 h (Darbyshire *et al.*, 1975).

The ability of CK cells to support the growth of IBV has been utilized in numerous studies including the assessment of pH stability of different IBV strains (Cowen and Hitchner, 1975b), identification of the presence of leader sequence on IBV mRNA (Brown *et al.*, 1984), identification of IBV S protein as a determinant of cell tropism (Casais *et al.*, 2003), induction of innate immunity with recombinant IBV Beaudette (Hodgson *et al.*, 2004) to identification of novel zippered ER and associated spherules induced by IBV (Maier *et al.*, 2013).

Other cultured cell lines

The Beaudette strain of IBV has been adapted to replicate in a number of animal cultured cell lines, such as African green monkey kidney (Vero) cells (Cunningham *et al.*, 1972; Alonso-Caplen *et al.*, 1984; Ng and Liu, 1998) and BHK-21 cells (Otsuki *et al.*, 1979). Using a Vero-adapted IBV Beaudette strain, infection was established in another four human cell lines: H1299, HepG2, Hep3B and Huh7 (Tay *et al.*, 2012). An investigation into the furin abundance of these cell lines was reported to be positively associated with an efficient IBV infection, suggesting that IBV can likely infect a variety of human and animal cell lines of different tissue origin, with the relative abundance of furin as a restrictive factor (Tay *et al.*, 2012).

Genome structure and organization

The CoV RNA genome, as with the genomes of Ateriviruses and Roniviruses, is characterized by four unique hallmarks which set them apart from other RNA viruses: (1) the presence of a large replicase gene occupying the upstream 5′ two thirds of their genome, (2) expression of the replicase gene is proceeded by means of ribosomal frame-shifting, (3) multiple viral enzymatic products are embedded within the replicase-transcriptase protein products and (4) production of downstream gene products via transcription of subgenomic mRNAs (van Vliet *et al.*, 2002). The CoV genome acts as an mRNA, a template RNA and a substrate in the viral transcription, replication and packaging stages of the replication cycle, respectively.

To cater for its function as a + ssRNA virus, all CoV genomes are 5′ capped and 3′ polyadenylated to allow for immediate translation of its genome upon entry into the cell (Fig. 5.5). The 5′ end begins with a leader sequence and an untranslated region (UTR) containing multiple stem loops which regulates viral genome replication and transcription (Fig. 5.6). In addition to these regulatory features, each structural and accessory gene is preceded by a transcriptional regulatory sequence (TRS) required for gene expression. The 3′UTR region also contains RNA structures required for replication and synthesis of viral

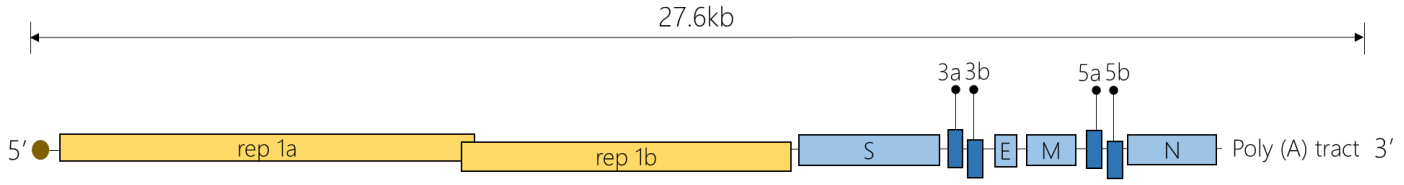

Figure 5.5 Genome organization of infectious bronchitis virus (IBV). The IBV viral RNA genome is approximately 27.6 kilobases (kb) long and is arranged in an invariant order of 5′-rep 1a-rep 1b-S-3a-3b-E-M-5a-5b-N-3′.

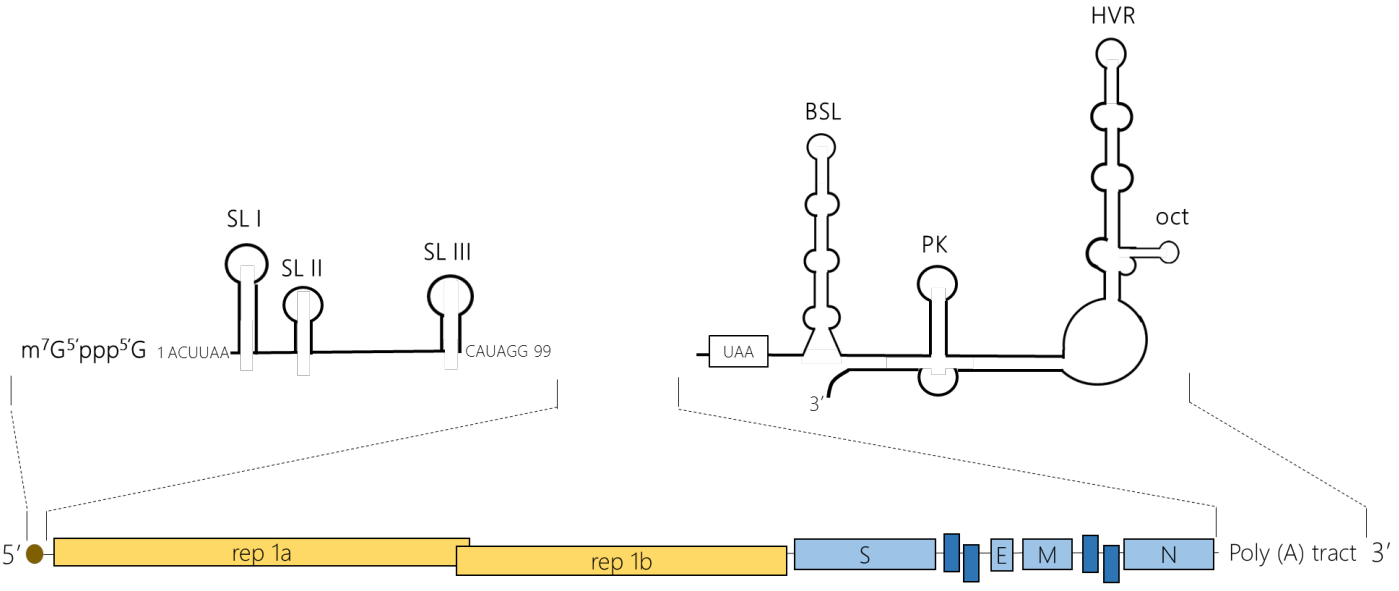

Figure 5.6 The predicted secondary and tertiary structures of the 5′ and 3′ UTR regions of the infectious bronchitis virus (IBV) genomic RNA. The structures shown are those characterized for IBV (SL I to III) for the first 100 nucleotides of the 5′ UTR. The predicted secondary structures of the rest 428 nucleotides of the 5′ UTR are not shown. The 3′ expanded region represents the 301 nucleotides of the 3′ UTR. The elements shown are the bulged stem loop (BSL), the pseudoknot (PK), the hypervariable region (HVR), and the conserved coronavirus octanucleotide motif (oct); the stop codon for the upstream N gene is boxed. SL, stem loop; UTR, untranslated region.

RNA. As previously mentioned, IBV contains an RNA genome that is 27.6 kilobases (kb) long. The IBV genome is arranged as 5′ORF1a-ORF1b-S-3-E-M-5-N-3 propagation, with various accessory genes interspersed within the structural genes at the 3′ one-third region. While these accessory genes were reported to be non-essential for viral replication in cell culture, they proved to play a critical role in viral pathogenesis (Casais *et al.*, 2005).

Structural proteins: structure and function

S protein

The S protein is the largest amongst all CoV structural proteins, with the S monomer at 128 kDa to 160 kDa. S protein is a class I transmembrane protein with a large N-terminal ectodomain and a small C-terminal endodomain, and is heavily N-glycosylated (Belouzard *et al.*, 2012; Fung and Liu, 2018). It plays a critical role in infection by binding to the host cell receptors and mediates the earliest steps of a viral infection (Cavanagh, 1995). During infection, the S protein is cleaved by host cell proteases into an N-terminal S1 subunit and a C-terminal S2 subunit, two subunits of roughly the same size (Bosch *et al.*, 2004). Cryo-EM studies of the structure of IBV S protein showed that while S2 region is structurally similar across the CoV genera, S1 region contains unique structural features that suggest the evolutionary spectrum of CoV S proteins to be in the order of the genera *Alphacoronavirus*, *Deltacoronavirus*, *Gammacoronavirus*, and *Betacoronavirus* (Shang *et al.*, 2018).

The S1 subunit forms the receptor-binding domain (RBD) and the S2 subunit forms the stalk of the spike molecule. The RBD of IBV M41 S protein was mapped to the N-terminal 253 amino acid residues, with amino acids 19–272 both required and sufficient for binding to α-2,3-sialic acid in the respiratory tract (Promkuntod *et al.*, 2014). The critical attachment site for M41 spike was pinpointed to four residues, namely N38, H43, P63 and T69 (Promkuntod *et al.*, 2014). Interestingly, during a cold-adaptation of the Beaudette strain of IBV to Vero cells, a single amino acid mutation of Q294 to L294 in the S1 subunit was found to hamper the processing and translocation of S protein, thus abolishing mediation of cell–cell fusion and incorporation into virions at the non-permissive temperature (Shen *et al.*, 2004). A recent study using iterative threading assembly refinement (I-TASSER), an automated homology modelling platform, has predicted the tertiary structure for IBV S1 of the vaccine strains Ma5 and ArkDPI

(Leyson *et al.*, 2016). The predicted structures were consistent with existing experimental data, as residues previously shown to be critical for receptor binding were found at the surface of the predicted structures (Fig. 5.7). Also, the predicted S1 structures exhibited two distinct domains, a N-terminal domain where the minimal receptor-binding domain was previously mapped and a C-terminal domain (Leyson *et al.*, 2016).

The S2 subunit contains the buried fusion peptide and two heptad repeats (HR), HR1 and HR2. Collectively, the fusion peptide, HR1 and HR2 are essential for viral fusion upon RBD binding to its cognate receptor. Using a series of recombinant IBVs expressing chimeric S glycoproteins, it was reported that S2 of the IBV Beaudette is a determinant of cellular tropism (Bickerton *et al.*, 2018). Interestingly, the S1 subunit of IBV Beaudette spike was not sufficient for binding to host tissues (Promkuntod *et al.*, 2013). Although the S2 subunit did not contain an independent RBD, it could contribute to the avidity of S1 subunit, thus affecting the specificity of virus attachment and viral host range (Promkuntod *et al.*, 2013). In other cases, the S protein may also be cleaved by furin or furin-like proteases during IBV exocytosis (Tay *et al.*, 2012), or by endosomal cathepsin proteases during SARS-CoV entry (Huang *et al.*, 2006; Bosch *et al.*, 2008). There are two furin consensus motifs in IBV, namely RRFRR(537)/S and RRRR(690)/S (Yamada and Liu, 2009). Furin cleavage in S protein has been shown to promote the entry, syncytium formation and infectivity of IBV in Vero cells (Yamada and Liu, 2009).

The cytoplasmic tail of IBV S protein contains a canonical dilysine endoplasmic reticulum (ER) retrieval signal sequence (-KKXX-COOH), which could retain the chimeric reporter protein (VSVG) in the ERGIC, similar to a dibasic motif (-KXHXX-COOH) identified in alphacoronaviruses and SARS-CoV (Lontok *et al.*, 2004). However, later studies have shown that overexpressed S proteins lacking this dilysine motif was still retained intracellularly and not transported to the plasma membrane (Winter *et al.*, 2008b). In contrast, Y1143 in the dityrosine motif was shown to be crucial for the intracellular retention of the S protein (Winter *et al.*, 2008b). A similar tyrosine dependent signal is present in the S protein of transmissible gastroenteritis virus (TGEV), also serving as an intracellular retention signal (Schwegmann-Wessels *et al.*, 2004). The importance of these trafficking signals was further validated by reverse genetics. Infectious cDNA clone lacking the dilysine signal was viable, but it had a growth defect at late stage of infection and produced larger plaques than wild type (Youn *et al.*, 2005b). In contrast, recombinant viruses lacking the tyrosine motif could not be recovered, although transient syncytia were observed in the transfected cells (Youn *et al.*, 2005b).

N-linked glycosylation of IBV S protein at different positions may differentially affect the folding, cleavage and fusogenicity of IBV S protein, as revealed in a recent study using bioinformatics and proteomics tools to predict and determine the N-linked glycosylation sites on IBV S protein (Zheng *et al.*, 2018). Asparagine to aspartic acid or glutamine substitution at N212 and N276 was reported to abolish the fusogenicity of IBV S protein and decrease

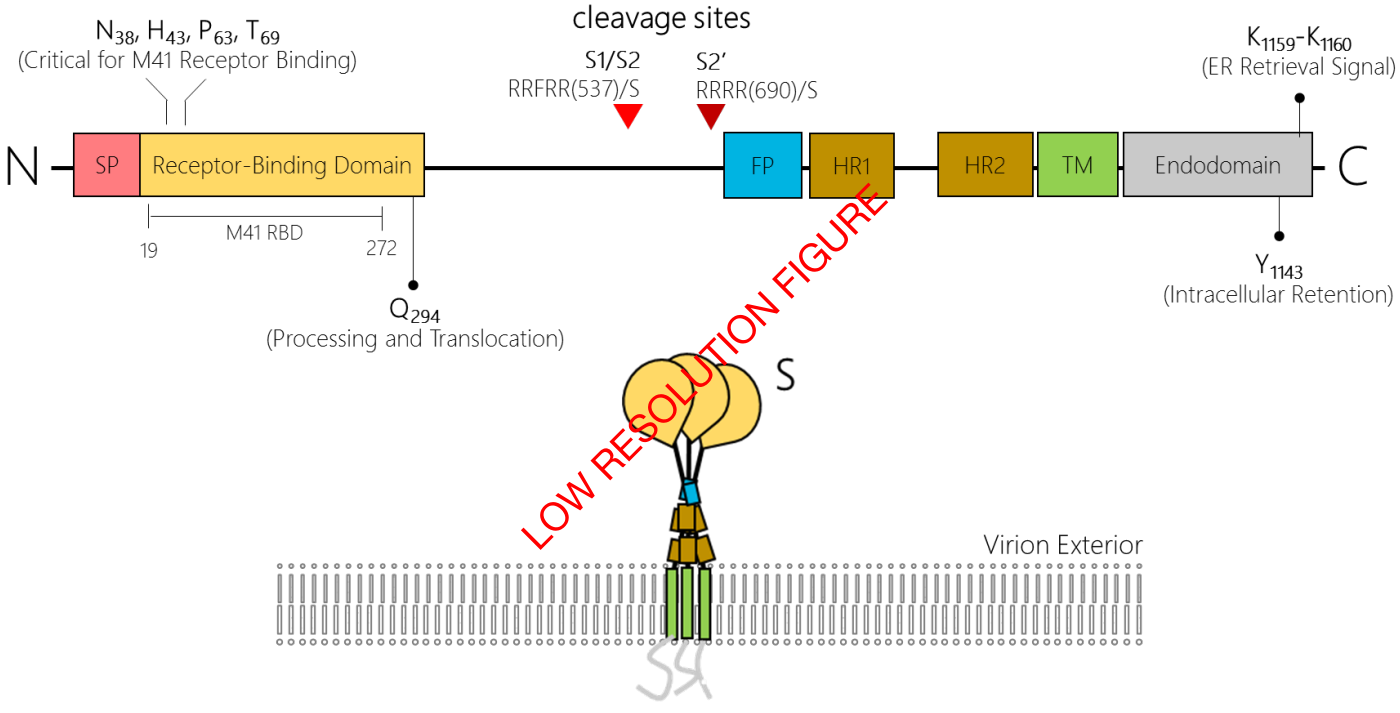

Figure 5.7 Linear and folded representations of coronavirus spike (S) protein. The S protein comprise two subunits, S1 and S2 (demarcated by the S1/S2 cleavage site in red triangle). Critical receptor binding sites for infectious bronchitis virus (IBV) M41 (N_{38}, H_{43}, P_{63} and T_{69}) lies within amino acids 19–272 of the receptor binding domain. A second furin cleavage site (S2') is located downstream of S1/S2 cleavage site. Important residues of the S protein are Q_{294} (processing and translocation), Y_{1143} (intracellular retention) and K_{1159}-K_{1160} (ER retrieval signal). FP, fusion peptide; HR, heptad repeat; SP, signal peptide; TM, transmembrane domain.

the infectivity of the recombinant viruses, while N283 is critically involved in IBV replication and infectivity independent of N-linked glycosylation (Zheng *et al.*, 2018).

Interestingly, S protein can also inhibit host gene translation in SARS-CoV and IBV through interactions with eukaryotic initiation factor 3f (eIF3F), a subunit of eIF3 (Xiao *et al.*, 2008). In cells stably expressing a FLAG-tagged eIF3f, IBV infection induced significantly higher protein translation of interleukin 6 (IL-6) and IL-8, compared with the control. Therefore, S protein mediated translational inhibition might function as a novel mechanism to regulate viral pathogenesis.

M protein

While S protein is a key defining feature for CoVs, they are surprisingly not the most abundant structural protein found in CoVs. The most abundant structural protein is the M protein, which ranges from 25–30 kDa and accounts for ≈ 40% of the mass of virus particles (Stern *et al.*, 1982). M protein monomer contains a small N-terminal ectodomain and a large C-terminal endodomain and is thought to give CoVs their shape (Machamer and Rose, 1987) (Fig. 5.8). While the M protein is co-translationally inserted into the ER, most coronavirus M proteins, including IBV, contain no signal sequences (Kapke *et al.*, 1988; Fung and Liu, 2018). Ectodomain of IBV M protein is modified by N-linked glycosylation, which is different from the O-linked glycosylation observed in the M proteins of murine coronavirus and bovine coronavirus L9 (Cavanagh, 1983). M protein is a polytopic membrane protein that is embedded within the envelope by three transmembrane domains (Armstrong *et al.*, 1984). The cytoplasmic tail of IBV M protein is required for its interaction with the E protein (Lim and Liu, 2001) and, similar to other CoVs, when overexpressed together, IBV M and E protein could support the formation of virus-like particles (Lim and Liu, 2001; Corse and Machamer, 2003). Recent studies suggest that M protein exists as a dimer in the virion and adopts two different conformations to promote curvature of the virion (Neuman *et al.*, 2011). It also helps to regulate the virion size and virus assembly through interactions with other structural proteins (Neuman *et al.*, 2011).

Coimmunoprecipitation and immunofluorescence microscopy also revealed interactions between M protein and beta-actin in the assembly and budding phases of the viral life cycle (Wang, J. *et al.*, 2009). The A159 and K160 in the M protein were found to be essential for binding to actin, and recombinant viruses harbouring mutations in A159-K160 could no longer generate infectious virions, although the genome could still be replicated and transcribed normally (Wang, J. *et al.*, 2009). This M protein–actin interaction was supported by the observation that purified IBV particles contain a certain amount of beta-actin (Kong *et al.*, 2010).

E protein

Contrary to the abundance of the M protein, the E protein is a small polypeptide (8–12 kDa) found in limited amounts in the virion envelope (Liu and Inglis, 1991; Fung and Liu, 2018). Current evidence supports the membrane topology of IBV E protein as a transmembrane protein with an N-terminal ectodomain,

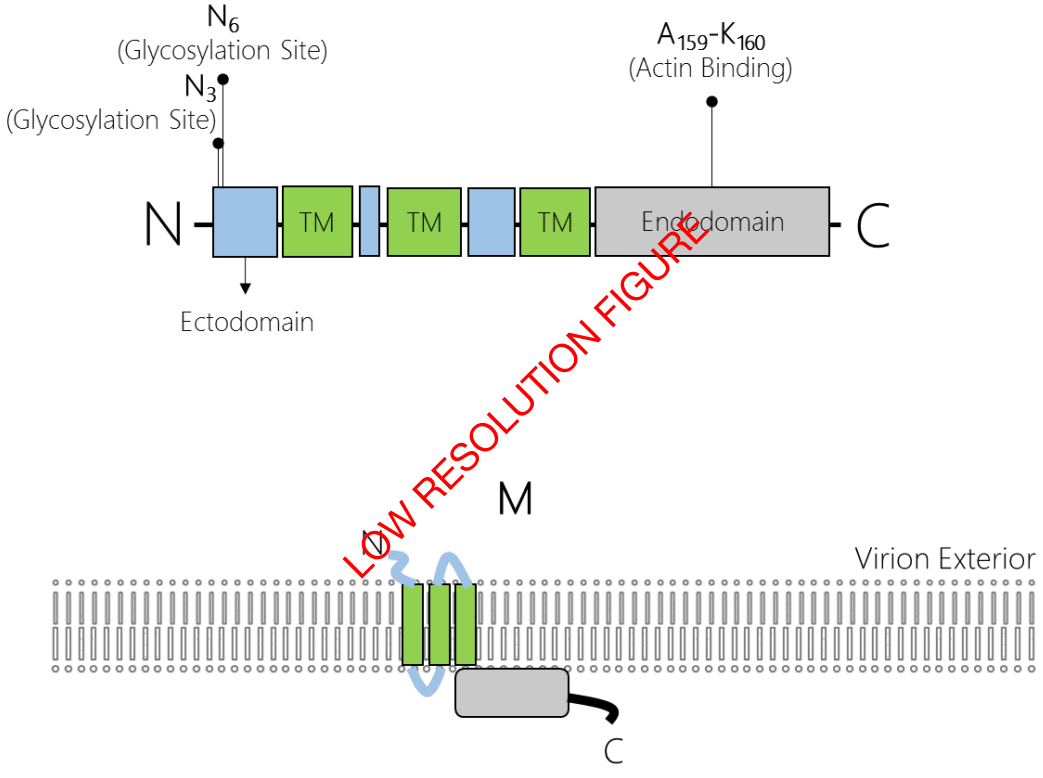

Figure 5.8 Linear and folded representations of coronavirus membrane (M) protein. Important residues for the infectious bronchitis virus (IBV) M protein are N_3 and N_6 (glycosylation sites) and A_{159}-K_{160} (Actin-binding). TM, transmembrane domain.

a hydrophobic domain (HD) and a C-terminal endodomain (Fig. 5.9). The major function of the E protein is to facilitate virus assembly and release (Liu *et al.*, 2007; Ye and Hogue, 2007), which is mediated by the physical interaction between E and M (Lim and Liu, 2001). In fact, when coexpressed in cells, the E protein can relocate M to the same subcellular compartments that E resides in (Lim and Liu, 2001). The six residues at the C-terminal (RDKLYS) serves as the ER retention signal of E, and mutation of the fourth lysine to glutamine resulted in the accumulation of E in the Golgi apparatus (Lim and Liu, 2001).

As opposed to other structural proteins, deletion of the E protein is not always lethal. In fact, recombinant viruses with the E gene deleted have been successfully generated for MHV and SARS-CoV, although the mutants formed severely crippled virions with significantly reduced titres (Kuo and Masters, 2003; DeDiego *et al.*, 2007). However, recombinant IBV with the E gene deleted could not be recovered, indicating that E protein plays a critical role during IBV replication (unpublished data). In fact, simply swapping the HD domain of IBV E protein with the transmembrane domain of VSV-G resulted in ≈200-fold reduction of virion release into the supernatant (Machamer and Youn, 2006).

Biophysical and computational studies have supported a model that five molecules of SARS-CoV E protein form a homopentameric α-helical bundle, with the hydrophobic domains embedded in the lipid bilayer, forming a voltage-independent ion channel (Torres *et al.*, 2006; Verdiá-Báguena *et al.*, 2012). Ion channel activity of SARS-CoV E protein could be readily determined *in vitro*, and its overexpression also altered membrane permeability in both E. coli and mammalian cells (Liao *et al.*, 2004, 2006). Two mutations within the HD of SARS-CoV E protein, namely N15A and V25F, have been shown to completely abolish the ion channel activity (Verdiá-Báguena *et al.*, 2012).

It is very likely that IBV E protein adopts similar membrane topology and forms a homopentamer as the SARS-CoV E protein (Fig. 5.9). Biophysical analysis has shown that IBV E protein also exhibited ion channel activity and either of the corresponding mutations in the HD domain, T16A and A26F, completely abolishes the channel conductance (To *et al.*, 2017). Interestingly, overexpression of IBV E protein, but not the T16A mutant, disrupted the intracellular trafficking of VSV-G protein and the morphology of the Golgi complex (Ruch and Machamer, 2012). Later biochemical analysis has shown that in both infected cells and virions, the IBV E protein is present in two distinct pools: a high molecular weight (HMW) pool and a low molecular weight (LMW) pool (Westerbeck and Machamer, 2015). The virion-associated IBV E was mainly in the HMW pool and formed homo-oligomers. Interestingly, at steady state, the T16A protein was nearly exclusively in the HMW pool, while the A26F protein was enriched in the LMW pool (Westerbeck and Machamer, 2015). Consistently, the T16A mutant could support the production of virus like particles (VLPs) similar to the wild type IBV E protein, whereas the A26F mutant did not support VLP production (Westerbeck and Machamer, 2015).

To better understand the importance of the ion channel activity of E protein during IBV replication, a recombinant IBV with

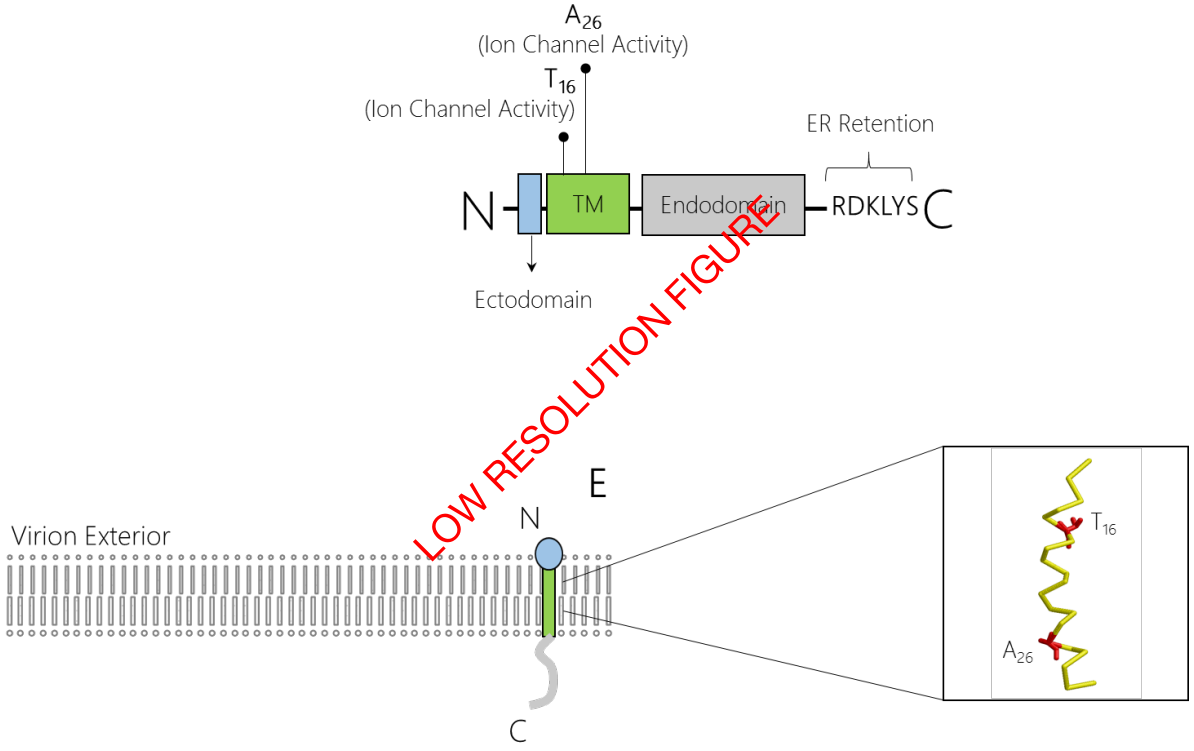

Figure 5.9 Linear and folded representations of coronavirus envelop (E) protein. *Top* Important residues for the infectious bronchitis virus (IBV) E protein are T_{16} and A_{26} (ion channel activity). The C-terminal RDKLYS contains an endoplasmic reticulum (ER) retention signal. *Below* The positions of T_{16} and A_{26} are shown (boxed). TM, transmembrane domain.

either T16A or A26F mutation was generated (To *et al.*, 2017). Both mutant rIBVs could be recovered, although A26F formed smaller plaques compared with wild type. The two ion channel mutants were very similar to wild type IBV in terms of genome replication and transcription, structural protein synthesis and virion assembly. However, the release of mature virion to the culture supernatant was significantly reduced in the mutants, indicating that ion channel activity is required for efficient release of infectious virus particles (To *et al.*, 2017).

N protein

Residing within the virion interior, N protein is the sole protein constituent of the helical nucleocapsid (Fung and Liu, 2018). Monomers of this 43–50 kDa protein bind the RNA genome in a 'beads on a string' configuration. Crystal structures of IBV N protein revealed a protein core composed of antiparallel beta sheets, hairpin extension and a hydrophobic platform which may be implicated in RNA binding (Fan *et al.*, 2005). The N monomer is composed of two domains: N-terminal domain (NTD) and the C-terminal domain (CTD), each with a different binding mechanism (Fig. 5.10). Within the NTD of the N protein, site-directed mutagenesis has revealed Arg76 and Tyr94 to be critical for its RNA-binding activity (Tan *et al.*, 2006). While both domains are capable of binding to the viral RNA genome *in vitro*, binding contributions from both domains are required to achieve optimal RNA binding (Chang *et al.*, 2006; Hurst *et al.*, 2009).

Additionally, the N protein is a phosphoprotein, modified at a limited number of serine and threonine residues. Ser190, Ser192, Thr378, and Ser379 have been revealed as the phosphorylation sites in IBV (Chen *et al.*, 2005), and a cellular kinase is responsible for the phosphorylation in the N protein (Fang *et al.*, 2013). This heavy phosphorylation is thought to play a role in increasing the N protein affinity to bind viral versus non-viral RNA (Spencer *et al.*, 2008). The most conspicuous function of the N protein is to bind viral RNA. While two RNA substrates were identified for the N protein before 2000, namely the TRS (Stohlman *et al.*, 1988) and the genomic packaging signal (Molenkamp and Spaan, 1997), the N protein is also known to bind to non-structural protein 3 (nsp3) and M protein to help tether the viral genome into the replicase-transcriptase complex (RTC) and packaged the genome into virion particles (Sturman *et al.*, 1980; Hurst *et al.*, 2013).

Using stable isotope labelling with amino acid in cell culture (SILAC), Emmott and colleagues have identified numerous cellular proteins as potentially binding to the IBV N protein (Emmott *et al.*, 2013). Among the identified proteins, siRNA-mediated knockdown of nucleolin, RPL19 and GSK3 has been shown to significantly inhibit IBV replication in cell culture, suggesting the important functions of these host proteins during IBV infection (Emmott *et al.*, 2013).

Previous studies have shown that the N protein of TGEV is cleaved at the late stage of infection, presumably by the activated

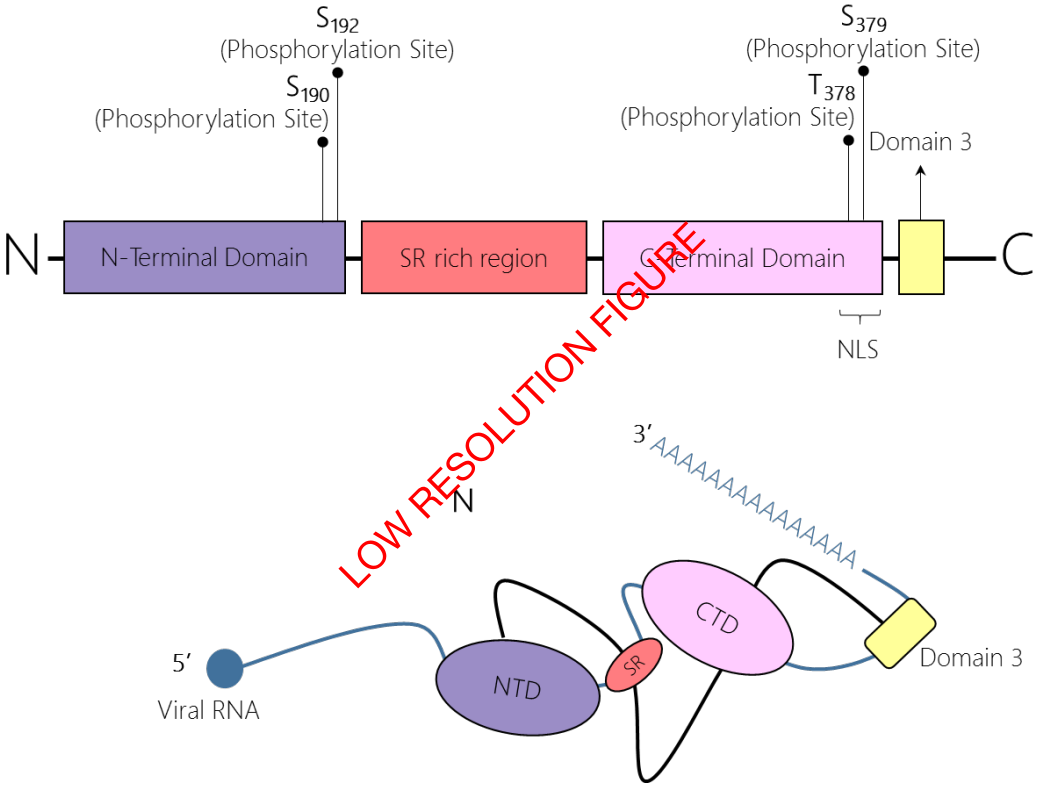

Figure 5.10 Linear and folded representations of coronavirus nucleocapsid (N) protein. Important residues for the infectious bronchitis virus (IBV) N protein are S_{190}, S_{192}, T_{378}, S_{379} (phosphorylation sites). CTD, C-terminal domain; NLS, nuclear localization signal; NTD, N-terminal domain; SR, serine–arginine-rich region.

caspase-6 and -7 during TGEV-induced apoptosis (Eléouët *et al.*, 2000). Similarly, the N protein of SARS-CoV has been shown to be cleaved by caspases during lytic infection in Vero E6 and A549 cells, but not cleaved during persistent infection in Caco-2 and N2a cells (Diemer *et al.*, 2008). Cleavage of the SARS-CoV N protein is mediated by caspase-6 and/or caspase-3 and is dependent on the nuclear localization of the N protein (Diemer *et al.*, 2008). Interestingly, a recent study has shown that the N protein of porcine epidemic diarrhoea virus (PEDV) interacts with the nucleolar protein nucleophosmin (NPM1), thus protecting it from capspase-3-mediated cleavage and promoting cell survival during PEDV infection (Shi *et al.*, 2017). The cleavage of IBV N protein in IBV-induced apoptosis was also observed, suggesting that caspase-dependent cleavage of the N protein may be a common phenomenon in CoV-infected cells. It is likely that by acting itself as a caspase substrate, the N protein can protect host proteins from cleavage by activated caspase, thus promote cell survival and prolong the duration of virion release.

Host proteins recruited to mature virions

Apart from the viral structural proteins, recent studies have also identified host proteins recruited to the mature IBV particles. In a study by Kong and colleagues (2010), 10-day-old SPF embryonated chicken eggs were infected with IBV strain H52, and IBV particles were purified from allantoic fluid by sucrose gradient ultracentrifugation. The proteins in purified IBV particles were resolved by 2-dimensional gel electrophoresis (2-DE) and protein spots were in-gel digested with trypsin before subjected to matrix-assisted laser desorption/ionization time of flight (MALDI-TOF) mass spectrometry analysis. The IBV S and N protein, as well as 60 host proteins were identified. Using Western blot analysis and immunogold labelling of the bromelain protease treated IBV particles, the presence of heat shock protein 90 kDa beta member 1 (HSP90B1, also known as glucose-regulated protein 94 kDa, or GRP94) and Annexin A2 were validated (Kong *et al.*, 2010).

In another study by Dent and co-workers, IBV strain Beau-R was cultured in the same way and purified using polyethylene glycol (PEG) precipitation followed by ultracentrifugation (Dent *et al.*, 2015). Three IBV structural proteins, S, M and N, as well as 35 host proteins were identified. Interestingly, another member of the HSP90 family, HSP90AA1 and Annexin A2 were again found to be associated with IBV virion (Dent *et al.*, 2015). Both HSP90B1 (located inside the ER) and HSP90AA1 (located in the cytoplasm) are molecular chaperones that may facilitate the folding of structural and/or non-structural proteins during IBV replication. On the other hand, Annexin A2 belongs to the annexin family proteins, and is a calcium-regulated membrane-binding protein that has been implicated in exocytosis and cross-linking plasma membrane phospholipids with actin. Further functional studies are required to unravel the involvement of these host factors in the replication cycle of IBV and other CoVs.

Non-structural and accessory proteins: structure and function

Accessory genes

In general, accessory genes are numbered according to the subgenomic RNA in whose unique region they appear. As such, identically numbered genes in two different viruses, such as 3a in SARS-CoV and IBV, do not necessarily share any sequence homology. While it is often speculated that CoV accessory genes were horizontally acquired from cellular or heterologous viral sources, most ORFs of accessory genes have no obvious homology to any other viral or cellular sequence in public databases. Therefore, it is conceivable that many of them evolved in individual CoV by scavenging ORFs from the viral genome through duplication and subsequent mutations, as proposed for several accessory proteins of SARS-CoV (Inberg and Linial, 2004). It also needs to be considered that, although there is evidence that some accessory genes encode 'luxury' functions for their respective viruses, other accessory genes may be genetic junk. This is evident in isolates of IBV, in which many contain an extremely divergent segment of ≈200 nucleotides between the N gene and the 3′ UTR (Sapats *et al.*, 1996). This region was long considered to be an HVR of the 3′UTR, although it has been demonstrated to be dispensable for RNA synthesis.

The IBV genome (Fig. 5.5) contains two accessory genes, 3 and 5, that each encode two (3a and 3b, 5a and 5b) gene products (Liu *et al.*, 1991; Liu and Inglis, 1992; Cook *et al.*, 2012). Accessory gene 3 proteins are translated from subgenomic mRNA 3, a functionally polycistronic mRNA via leaky ribosome scanning (Liu *et al.*, 1991; Liu and Inglis, 1992). The E protein (previously known as 3c) is also translated from the same mRNA by an internal ribosome entry site (Liu and Inglis, 1991). IBV 3a and 3b polypeptide sequences are well-conserved within the gammacoronaviruses, with the similarities among different field isolates to be as high as 82.2% and 95%, respectively (Jia and Naqi, 1997).

There is growing interest in the field pertaining to the functional characterization of IBV gene 3 and 5 proteins. A previous study demonstrated the emergence of a truncated form of Beaudette-IBV 3b in Vero cells, indicating that IBV 3b may not be essential for virus replication, but may be a virulence determinant (Shen *et al.*, 2003). This is the same case for gene 5 of IBV, which has been demonstrated to be non-essential for replication using reverse genetics (Casais *et al.*, 2005; Armesto *et al.*, 2009). On the other hand, IBV 3a protein appears to be cytoplasmic and tightly associated with membranes, suggesting a potentially novel function for this protein (Pendleton and Machamer, 2005). Individual deletion of 3a, 3b, 5a, and 5b and recovery of their resultant rIBVs have shown that 5b is involved in delaying the activation of interferon response and induces an attenuated phenotype *in vitro* and *in vivo* (Laconi *et al.*, 2018). In another study, a recombinant live attenuated vaccine containing deletions in 3ab and 5ab has been reported to show protection against IBV infection in chickens (van Beurden *et al.*, 2018).

Non-structural proteins

CoV non-structural proteins (nsps) are derived from the replicase polyproteins and constitute the viral replication complex (Table 5.2). To maximize the production of viral proteins, CoVs have evolved strategies to interfere with the host cell machinery at various levels (Walsh and Mohr, 2011). To date, functional studies of most of these nsps were conducted with other members of the family *Coronaviridae*, and the demonstrated functions of these proteins are discussed as follows.

To inhibit host protein translation, many alpha- and betacoronaviruses encode nsp1, which works to selectively induce host RNA degradation and acts as an interferon antagonist (Kamitani *et al.*, 2006; Lokugamage *et al.*, 2012). Interestingly, gamma- and deltacoronaviruses do not encode nsp1, but there is early evidence in IBV suggesting that these CoVs can continue to induce host shutoff via accessory proteins by antagonizing the host innate immune response (Kint *et al.*, 2016).

Downstream of nsp1 is nsp2, a 65 kDa protein in its mature form (Denison *et al.*, 1995). The counterpart in IBV is an 87 kDa protein, which is the N-terminal cleavage product of polyproteins 1a and 1ab (Liu *et al.*, 1994). Deletion of nsp2 in MHV and SARS-CoV through reverse genetics have found this protein to be dispensable in viral replication, as infectious mutants have been recovered with intact polyprotein processing, albeit with defects in RNA synthesis and growth kinetics (Graham *et al.*, 2005). However, IBV nsp2 has been known to act as a protein kinase R (PKR) antagonist (Wang, X. *et al.*, 2009), and may play a role in inhibiting the dsRNA-triggered RNase L system.

MHV nsp3 is a multi-domain protein, containing two papain-like protease (PLP) domains, PLP1 and PLP2, as well as a transmembrane domain (Kanjanahaluethai *et al.*, 2007). This transmembrane domain has been demonstrated to play a significant role in tethering PLP2 during processing at cleavage site 3, as well as mediating the ER membrane association of cytosolic proteins (Kanjanahaluethai *et al.*, 2007). Besides acting as a protease in polyprotein processing, nsp3 can also function as a deubiquitinating enzyme to degrade polyubiquitin-associated proteins in the host antiviral signalling pathway (Yu *et al.*, 2017), as well as an interferon antagonist (Yang *et al.*, 2014).

Nsp4 was reported to be localized at the ER and engages in homotypic and heterotypic interactions with nsp3 and nsp6, respectively (Hagemeijer *et al.*, 2011). It assembles in the membrane as a tetraspanning transmembrane protein with a Nendo/Cendo topology and appears to play a role in the early secretory pathway in replication (Oostra *et al.*, 2007). IBV nsp4 is post-translationally modified by glycosylation (Lim and Liu, 1998a,b).

Nsp5 encodes a 3C-like protease (3CLpro), or also known as the main protease (Mpro). It is responsible for all downstream

Table 5.2 Functions and structures of coronavirus non-structural proteins. With the exception of nsp11, the enzymatic functions of each coronavirus nsp have been confirmed. Structures for nsp2, nsp12, and nsp13 has not yet been solved. Nsp11 is not known to produce protein, and therefore do not have a structure

Non-structural protein	Function	PDB ID	Method	Coronavirus	References
1	IFN antagonist	2HSX	NMR	SARS-CoV	Almeida *et al*. (2007)
2	IFN antagonist				
3	Papain-like protease (PL_{pro}) for polyprotein processing, deubiquitinas, IFN antagonist	2FE8	X-ray diffraction	SARS-CoV	Ratia *et al*. (2006)
4	Transmembrane scaffold				
5	Main protease (M_{pro}, $3CL_{pro}$) for polyprotein processing, IFN antagonist	2BX3	X-ray diffraction	SARS-CoV	Tan *et al*. (2005)
6	Transmembrane scaffold				
7	Hexadecameric complex	2KYS	NMR	SARS-CoV	Johnson *et al*. (2010)
8	Hexadecameric complex; primase	2AHM	X-ray diffraction	SARS-CoV	Zhai *et al*. (2005)
9	RNA-binding protein	2J97	X-ray diffraction	HCoV-229E	Ponnusamy *et al*. (2008)
10	Zinc-binding domain (ZBD), 2′-O-methyltransferase (2′-O-MTase) cofactor	2FYG	X-ray diffraction	SARS-CoV	Joseph *et al*. (2006)
11	Unknown				
12	RNA-dependent RNA polymerase (RdRP)				
13	ZBD, RNA 5′triphosphatase, RNA helicase				
14	3′–5′ exoribonuclease (ExoN), 7-methyltransferase	5C8U	X-ray diffraction	SARS-CoV	Ma *et al*. (2015)
15	Endoribonuclease (NendoU)	2H85	X-ray diffraction	SARS-CoV	Ricagno *et al*. (2006)
16	2′-O-MTase	2XYR	X-ray diffraction	SARS-CoV	Decroly *et al*. (2011)

cleavage events beyond nsp4. Nsp5 exists as a three-domain structure containing a chymotrypsin-like fold formed by domains 1 and 2. Domain 3 appears to be crucial for nsp5 dimerization, although the function of this domain remains to be investigated (Anand *et al.*, 2002). Since Mpro is only active as a homodimer, the crystal structure analysis revealed that Arg298 is a key residue in maintaining dimerization (Shi *et al.*, 2008). Mutations in nsp3 and nsp10 have been known to adversely affect nsp5-mediated polyprotein processing (Donaldson *et al.*, 2007; Stokes *et al.*, 2010).

Nsp6 produces two products of approximately 23 and 25 kDa, and analysis into its transmembrane topology revealed six-membrane-spanning segments and a conserved hydrophobic domain at the C-terminus on the cytosolic side (Baliji *et al.*, 2009). In SARS-CoV, nsp3, nsp 4 and nsp 6 are required to induce double-membrane vesicles (DMVs) in virus infected cells (Angelini *et al.*, 2013). Mutations in MHV nsp3 has been reported to impair DMV-formation (Stokes *et al.*, 2010). IBV nsp6 has been shown to generate autophagosomes from the ER, indicating that it can induce autophagy in cells when expressed (Cottam *et al.*, 2011).

Nsp7 forms the hexadecameric complex with nsp8. Alone, nsp7 consists of an antiparallel three-helix bundle with an α-helix at the C-terminus. The C-terminal portion of nsp7 is flexible and can associate with nsp8. This interaction between nsp7 and nsp8 within the hexadecameric complex is stabilized by the aliphatic side-chains on the N-terminus of the three-helix bundle of nsp7 and the hydrophobic interactions involving the C-terminal helix of nsp7 and the C-terminus of nsp 8 (Zhai *et al.*, 2005).

Many positive-sense RNA viruses utilize the Vpg (viral protein genome-linked) oligonucleotides as a primer for the RNA-dependent RNA polymerase (RdRP) (Pettersson *et al.*, 1978; Steil *et al.*, 2010). Since the CoV RNA synthesis is primer-dependent (Cheng *et al.*, 2005), and the CoV genome does not encode a Vpg, nsp8 serves as a primase by synthesizing short primers for the RdRP and a second RdRP in SARS-CoV (Imbert *et al.*, 2006). In synthesizing primers in a manganese-dependent reaction, nsp8 selectively synthesizes primers specific to the 5′-(G/U)CC-3′ sites on the template RNA. By observing the 3D structure of nsp8, the inner diameter within the hexadecameric complex is approximately 30Å, and can accommodate double-stranded RNA, suggesting that the hexadecameric complex may act as a processivity factor for RdRP (Zhai *et al.*, 2005). Alongside Nsp7, Nsp8 is also known to form a stable complex with NSP12, independent of the UTRs of viral RNA and other viral proteins (Tan *et al.*, 2018).

Nsp9 plays an essential role in viral replication by forming a homodimer which binds ssRNA (Egloff *et al.*, 2004). Structurally, nsp9 comprises a single beta-barrel with an OB-fold and a C-terminal extension related to the subdomains of the Mpro of SARS-CoV (Sutton *et al.*, 2004). Crystal structure solved for SARS-CoV nsp9 suggests that this protein may be dimeric (Sutton *et al.*, 2004), and this has been recently confirmed by Hu and colleagues (2017) on IBV nsp9. Indeed, IBV nsp9 forms a homodimer via interactions across the hydrophobic surface containing two parallel alpha helices near the C-terminal of nsp9. Moreover, dimeric nsp9 resembles SARS-CoV nsp9, indicating that the dimerization may be conserved among all CoVs. Although the function of nsp9 remains elusive other than a ssRNA-binding protein, it is presumed to be involved in viral RNA synthesis, since yeast-2-hybrid and coimmunoprecipitation have found nsp9 to be associated with nsp7, nsp8 and nsp10 (von Brunn *et al.*, 2007). Furthermore, there is evidence supporting the role of nsp9 in reducing the disorder of nsp8 N-terminus in an analytical ultracentrifugation experiment (Sutton *et al.*, 2004).

Nsp10 is among the most well conserved nsps among different CoVs. It contains two zinc fingers acting as a zinc binding domain and acts as a co-factor for nsp14 and nsp16 to elicit 3′–5′ exoribonuclease and 2′-O-methyltransferase (2′-O-MTase) activities, respectively. Moreover, nsp9 and nsp10 was found to be membrane-associated in the replicase complex by immunofluorescence (van der Meer *et al.*, 1998). Using the mouse hepatitis virus strain A59 (MHV-A59), a single amino-acid mutation in nsp10 (Q65E) was found to be defective in negative-strand synthesis of viral RNA and activation of Mpro (Donaldson *et al.*, 2007). The structure of both monomeric and dodecameric forms of nsp10 has been solved for SARS-CoV by X-ray crystallography (Su *et al.*, 2006). The monomeric nsp10 contains a helical-hairpin at the N-terminus, followed by an irregular β-sheet surrounded by additional helices, and finally a C-terminal subdomain loop. The first zinc-finger module of nsp10 is CCHC-type with a C-(X)2-C-(X)5-H-(X)6-C sequence motif, while the second zinc-binding site is a CCCC-type with a C-(X)2-C-(X)7-C-(X)-C sequence motif (Su *et al.*, 2006). Recently, the key residues on nsp10 surface responsible for its interactions with nsp14 have been identified (Bouvet *et al.*, 2014). Interestingly, the same nsp10 surface interacting with nsp14 has been demonstrated to overlap with nsp10-mediated activation of nsp16 2′-O-MTase, indicating that nsp10 is a major regulator of CoV replicase function (Bouvet *et al.*, 2014).

Nsp11 forms the C-terminus of pp1a. This 13-residue oligopeptide in SARS-CoV sits at the ribosomal frame-shifting site and is produced when no ribosomal frame-shifting occurs at the slippery sequence. So far, nsp11 protein has not been detected in infected cells. Nsp11 shares its N-terminus with nsp12, the RdRP. Obviously, since most of nsp11 coding sequence overlaps with the RNA frame-shifting sequence and nsp12 coding sequence, no functional role for nsp11 has been assigned.

Nsp12 is arguably the most conserved nsp of the CoV replicase transcriptase. The RdRP activity of nsp12 was confirmed in 2005 when a bacterially expressed nsp12 could extend an oligouridylate (U) primer hybridized to a poly(A) template (Cheng *et al.*, 2005). Phylogenetic clustering studies have found CoV nsp12 to be closely related to RdRPs of other positive-sense RNA viruses whose genome RNAs have 5′-end covalently linked to viral protein genome-linked (VPg) (Koonin, 1991). RdRPs of VPg-containing viruses share a conserved sequence motif G implicated in the recognition of primer-template RNA complex (Barrette-Ng *et al.*, 2002; Thompson and Peersen, 2004); this same motif was also conserved in CoVs, implying that nsp12 contains VPg-like activities (Gorbalenya *et al.*, 2002). Nsp12 contains 932 residues and conserved RdRP motifs which function as the catalytic domain

at the C-terminus (Gorbalenya *et al.*, 1989; Koonin, 1991). A 3D-homology model proposed by Xu and colleagues (2003) for SARS-CoV nsp12 showed a cupped right-hand palm-finger-thumb structure surrounding a nucleic acid-binding tunnel. It is important to note that the expression of nsp12 requires ribosomal frame-shifting, implying that nsp12–16 are therefore produced at a much lower level than pp1a-encoded products.

SARS-CoV nsp13 contains 601 residues and comprises of multiple domains. Interestingly, this nsp is trifunctional, working as a zinc-binding domain (ZBD), a 5′RNA triphosphatase and a RNA helicase. The N-terminus contains a ZBD and the helicase domain is located on the C-terminus (Gorbalenya *et al.*, 1989). The ZBD comprises of 12 conserved cysteine and histidine residues and is conserved in all Nidoviruses for its helicase activity (Seybert *et al.*, 2005), unwinding RNA and DNA duplexes in the 5′ to 3′ direction according to the ssRNA they bind to initially (Ivanov and Ziebhur, 2004; Ivanov *et al.*, 2004a). Apart from RNA helicase activity, nsp13 was also proposed to mediate the catalysis of the first step of 5′capping of viral mRNAs (Ivanov and Ziebhur, 2004; Ivanov *et al.*, 2004a). Moreover, nsp13 can also interact with p125 subunit of DNA polymerase delta (δ) to induce DNA replication stress following IBV infection (Xu *et al.*, 2011).

The N-terminus of nsp14 contains a 3′–5′ exoribonuclease (ExoN) domain which is related to the DEDD superfamily of exonucleases (Moser *et al.*, 1997; Snijder *et al.*, 2003). The ExoN activity in SARS-CoV was demonstrated *in vitro* and is reported to be specific to ss- and ds-RNA (Minskaia *et al.*, 2006). Genetic inactivation of nsp14 in MHV has been found to accumulate 15-fold more mutations than the wild-type virus, significantly reducing the replication fidelity (Eckerle *et al.*, 2007). However, the requirement of metal ions for enzymatic activity was revealed by isothermal titration calorimetry, in which nsp14 binds to two magnesium ions per molecule (Chen *et al.*, 2007). This suggests that nsp14 activity occurs via two metal ion mechanism, similar to those used by cellular enzymes catalysing phosphoryl-transfer reactions (Beese and Steitz, 1991). Cellular RNA helicase DDX1 has been demonstrated to interact with nsp14 to enhance IBV replication (Xu *et al.*, 2010).

For redundancy, CoVs encode a second conserved ribonuclease, NendoU (Nidoviral endoribonuclease, U-specific) located in nsp15 (Snijder *et al.*, 2003). Because NendoU homologues could not be found in other RNA viruses, NendoU became the genetic marker for nidoviruses (Ivanov *et al.*, 2004b). SARS-CoV nsp15 preferentially cleaves at 3'uridylates, generating 2′–3′ cyclic phosphate ends (Ivanov *et al.*, 2004b). Although manganese ions have been demonstrated to increase the RNA-binding activity of NendoU (Bhardwaj *et al.*, 2006), current crystal structures of nsp15 does not reveal the presence of Mn^{2+} ion-binding sites in any CoVs studied (Ricagno *et al.*, 2006). Additionally, NendoUs form hexamers comprising dimers of trimers in crystals and solutions (Bhardwaj *et al.*, 2006; Ricagno *et al.*, 2006). Mutational analyses on key hexamerization residues have been reported to impair the nucleolytic activity and RNA affinity of SARS-CoV NendoU, implying that hexamerization is crucial for its activity (Guarino *et al.*, 2005).

Located at the C-terminus of pp1ab, nsp16 is proposed to be a 2′-O-MTase related to the RrmJ/FtsJ family (Snijder *et al.*, 2003). Nsp16 MTase activity was only recently confirmed in feline coronavirus (FCoV), methylating $^{7Me}GpppAC_n$ at the ribose-2′-O moiety of adenosine, converting a cap-0 to cap-1 structure (Decroly *et al.*, 2008). Moreover, nsp16 serves as a molecular signature to distinguish between foreign and cellular mRNA through RNA sensor Mda5 (Züst *et al.*, 2011). Deletion or ablation of nsp16 expression has led to abolishment of RNA synthesis in SARS-CoV, implying its critical role in CoV replication (Almazán *et al.*, 2006).

Stages of viral replication

Attachment and entry

CoV infections are initiated by the binding of the S protein to its cognate receptor (Fig. 5.11). The S protein/host receptor interaction forms a major factor in determining the host range, pathogenicity and tissue tropism of the virus. The RBD sites within the S1 subunit of each CoV may vary depending on the virus, with the MHV having the RBD at the N-terminus while SARS-CoV has their RBD at the C-terminus (Kubo *et al.*, 1994; Wong *et al.*, 2004). For IBV M41, RBD is located at the N-terminal 253 residues (Promkuntod *et al.*, 2014). However, it is unclear if all IBV variants share the same RBD sites. Even though the putative host receptor for IBV has not yet been fully determined, there is increasing evidence supporting sialic acid as a receptor determinant for infection (Winter *et al.*, 2006, 2008a; Abd El Rahman *et al.*, 2009). These reports also suggest that successful infection may require a co-receptor to reinforce the attachment process/trigger the fusion event between the viral and cellular membranes. Recently, lipid rafts have also been revealed to play an important role in the attachment and entry of IBV and SARS CoV (Lu *et al.*, 2008; Guo *et al.*, 2017).

Upon receptor binding, the virus must gain access to the cytoplasm through proteolytic cleavage of the S protein, into S1 and S2 subunits. Mutations in the S protein can affect the cell–cell fusion of IBV in cultured cells and consequently affect its infectivity during virus propagation (Yamada *et al.*, 2009). The S protein cleavage proceeds in two sequential steps at distinct sites within the S2 subunit – the first cleavage for separating the RBD and fusion domains and the second for fusion peptide exposure (Belouzard *et al.*, 2009). The insertion of the fusion peptide into the membrane is proceeded by the joining of two heptad repeats in S2 to form an antiparallel six-helix bundle (Bosch *et al.*, 2003). This conformation is crucial as it permits the mixing of both the viral and cellular membranes, resulting in fusion and release of the viral genome into the cytoplasm. For HCoVs, this process is generally accomplished by endosomal cysteine protease cathepsins and other host proteases, such as transmembrane protease serine 2 (TMPRSS2) (Shirato *et al.*, 2013) and airway trypsin-like protease TMRPSS11D (Zumla *et al.*, 2016). S protein cleavage in IBV usually occurs at a furin consensus motif RRFRR(537)/S in virus-infected cell (Cavanagh *et al.*, 1986). Recently, a second furin site at RRRR(690)/S was found to be essential for the

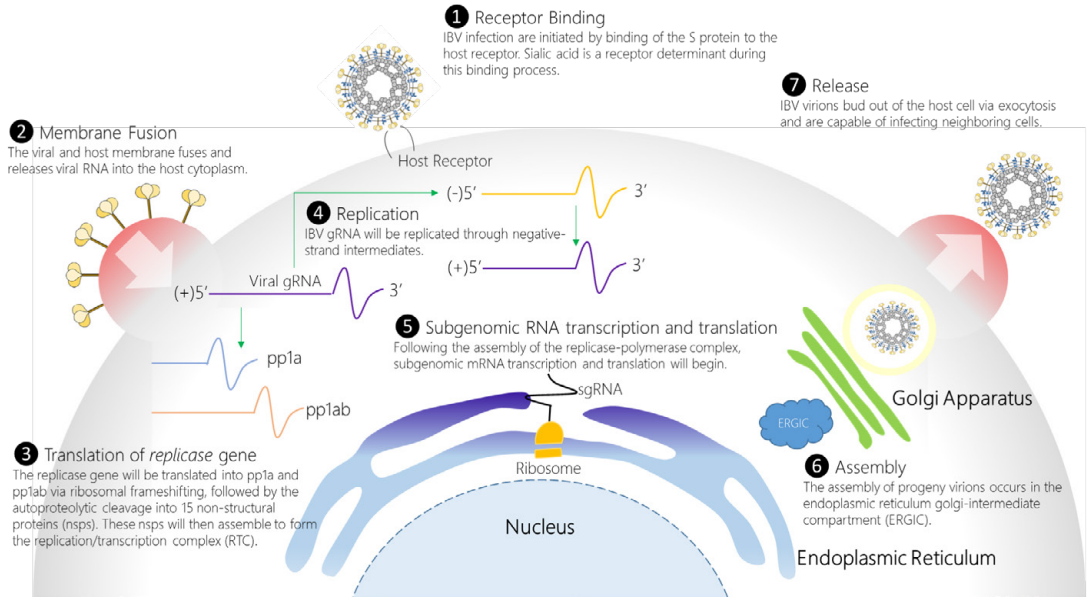

Figure 5.11 Infectious bronchitis virus (IBV) life cycle.

infectivity of IBV in cultured cells (Yamada and Liu, 2009). A previous study on the susceptibility of different cell lines to IBV infection has revealed that cellular furin content is a cellular restriction factor for susceptibility. If a cell line contains higher furin abundance, it would be exhibiting a more efficient infection (Tay *et al.*, 2012). Following fusion of the viral and cellular membranes, the virus enters the cell via endocytosis. Here, IBV fusion occurs at a pH-dependent manner, with a half-maximal fusion rate occurring at pH 5.5, indicating that endosomal pH acidification may be a fusion trigger for IBV as well as other CoVs (Chu *et al.*, 2006a). Several entry routes have been described for CoVs following infection, such as clathrin- and caveolae-independent and caveolae-dependent pathways (Nomura *et al.*, 2004; van Hamme *et al.*, 2008). Inhibitors of clathrin-dependent pathway such as chlorpromazine have been shown to abolish IBV infection (Chu *et al.*, 2006b). More recent studies suggest that the cellular sites of the uncoating events may be at the late endosomes (White and Whittaker, 2016; Wong *et al.*, 2015).

Replicase translation and processing

Following the release of the viral genomic RNA (gRNA) into the cytoplasm, the next step in the CoV replication cycle is to translate the replicase genes, rep1a and rep1b, into polyproteins pp1a and pp1ab (Fig. 5.12). Translation of the rep1b gene does not follow the usual rules of translation. It is instead, translated via an alternate mechanism of translation known as ribosomal frame-shifting, in which the translating ribosome shifts, with a fixed probability, in the –1 direction, from rep1a reading frame into rep1b reading frame. Two RNA elements are essential for ribosome repositioning: (1) a slippery sequence (5′-UUUAAAC-3′) and (2) an RNA pseudoknot. Usually, the ribosome works by unwinding the pseudoknot and carrying on with translation in rep 1a until it encounters the stop codon. When that occurs, the pseudoknot could sometimes prevent the translating ribosome from further elongation. Under this circumstance, the ribosome would pause on the slippery sequence and shifts the reading frame by –1 position before the ribosome can overcome the pseudoknot structure and resume translation on the CDS of rep1b (Brierley *et al.*, 1987, 1989). Currently, the incidence of ribosomal frameshifting is still under debate, with a range from 15% to as high as 60% depending on the *in vitro* studies performed (Baranov *et al.*, 2005; Plant *et al.*, 2005; Su *et al.*, 2005). It is also not known exactly the rationale behind the adoption of ribosomal frameshifting in CoVs. Two schools of thought have been proposed: one which holds that by adopting this translation mechanism, the ratio of pp1a and pp1ab could be regulated, while the other believes that the expression of rep1b products could be delayed until a suitable cellular environment has been created for RNA replication by the products of rep1a (Liu *et al.*, 1994; Fehr and Perlman, 2015).

Next, pp1a and pp1ab are further processed to form 15 nsps (Fig. 5.12) (Liu *et al.*, 1994, 1997). The size (amino acids) and cleavage sites of these 15 final products are summarized in Table 5.3. All CoVs would encode at least two proteases required for this cleavage. These are the papain-like proteases (PLpro) encoded by nsp3 and the main protease (Mpro) encoded by nsp5. With the exception of the gammacoronaviruses, SARS-CoV and MERS-CoV, most CoVs would encode two PLpros in nsp3 (Woo *et al.*, 2010). These PLpros would cleave nsps 1–4 at the nsp 1/2, 2/3, 3/4 boundaries, while Mpro is involved in the downstream cleavage events. Prediction and comparative analyses of Mpro cleavage sites in seven CoVs revealed that the substrate specificity of Mpro is exclusively occupied by glutamine (Gln) at the P1 position, and this is essential for efficient cleavage (Ziebuhr *et al.*, 2000). Amino acid substitutions of Gln in the P1 position at different cleavage sites display variable degrees of growth defects in IBV, with some sites being well-tolerated while others impede virus recovery (Fang *et al.*, 2008, 2010). Collectively, the nsps generated would assemble to form a larger complex known as the

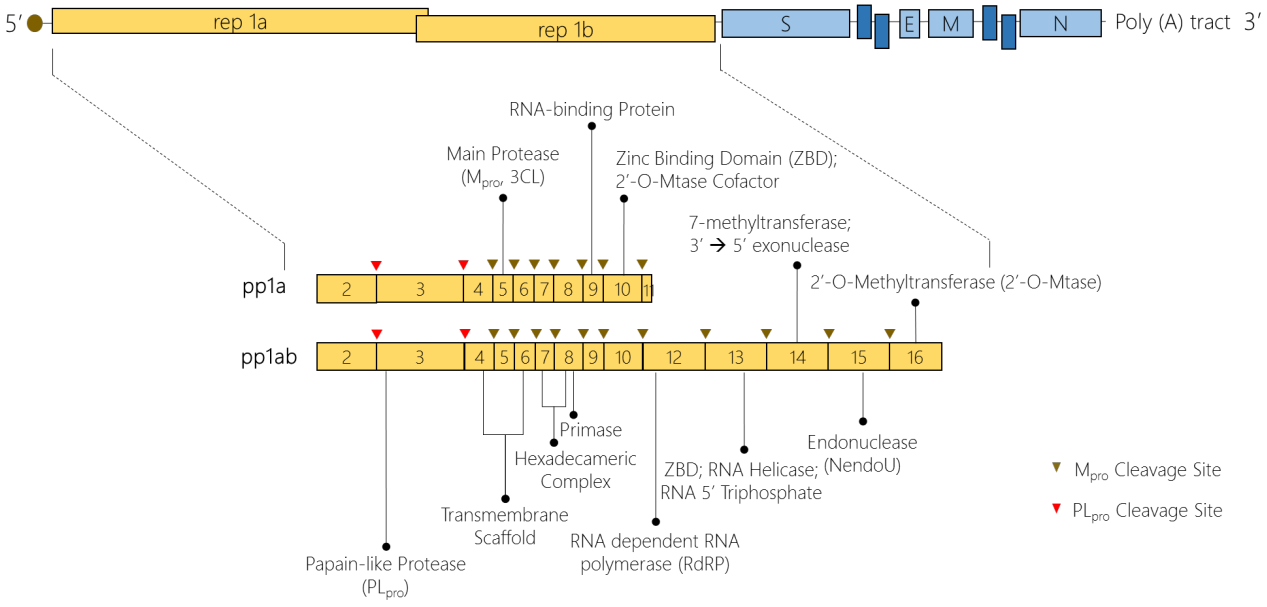

Figure 5.12 Infectious bronchitis virus (IBV) replicase gene and processing scheme of replicase protein products. Translation of the replicase gene would begin once the viral genome is released into the host cytoplasm. Replicase 1a and 1b are the only gene to be translated at this step of the virus life cycle, forming polyprotein (pp) 1a and 1ab via ribosomal frameshifting. Pp1a and pp1ab will then be autoproteolytically cleaved at cleavage sites by papain-like protease (PLpro) (in red triangles) and main protease (Mpro) (in brown triangles) into 15 non-structural proteins.

Table 5.3 Cleavage site and size (amino acid number) of IBV (strain Beaudette) non-structural proteins

IBV strain Beaudette non-structural Protein	Size (amino acids)	Start (nucleotide)	Stop (nucleotide)	References
2	673	529	2547	Liu *et al*. (1995a,b,c); Lim and Liu (1998a)
3	1592	2548	7323	Lim *et al*. (2000)
4	514	7324	8865	Lim *et al*. (2000)
5	307	8866	9786	Liu *et al*. (1994); Ng and Liu (2000)
6	293	9787	10665	Ng and Liu (2000)
7	83	10666	10914	Ng and Liu (2000)
8	210	10915	11544	Ng and Liu (1998)
9	111	11545	11877	Liu *et al*. (1997)
10	145	11878	12312	Ng and Liu (2002)
11	13	12313	12351	Fang *et al*. (2007)
12	932	12313	15131	Liu *et al*. (1994)
13	601	15132	16931	Liu *et al*. (1998a,b,c)
14	521	16932	18494	Liu *et al*. (1998a,b,c)
15	338	18495	19508	Liu *et al*. (1998a,b,c)
16	302	19509	20414	Liu *et al*. (1998a,b,c)

replication-transcription complex (RTC), responsible for RNA replication and subgenomic RNA transcription.

Replication and transcription

Viral RNA synthesis quickly ensues following the formation of the RTC. In CoVs, viral RNA synthesis produces two types of RNAs, the genome-sized gRNAs and subgenome-sized RNAs (sgRNAs), both generated through negative-strand intermediates. These negative-strand intermediates are only ≈ 1% as abundant as their positive-stranded counterparts, and they also contain anti-leader and poly-U sequences (Sethna *et al*., 1991). The sgRNAs serve as mRNAs for various structural and accessory genes residing 3′ downstream of the replicase gene.

Replication of viral RNAs are not without the *cis*-acting sequences. Within the 5′ UTR of the CoV genome, there are many stem–loop structures which extend into rep1a while the 3′

UTR also contains varied *cis*-acting elements from stem–loops, pseudoknots and HVRs (Raman *et al.*, 2003; Brown *et al.*, 2007). While exactly how each of these different structures works in the regulation of RNA synthesis remains to be deeply investigated, host factors such as zinc finger CCHC-type and RNA-binding motif 1 (MADP1) is revealed to interact with the 5′ UTR of IBV RNA and enhance viral replication and transcription (Tan *et al.*, 2012).

On the other hand, during RNA transcription, perhaps the most intriguing issue involves the leader and body TRS fusion during sgRNA production (Fig. 5.13). Each subgenomic mRNA transcript contains a 5′ leader sequence corresponding to the 5′ end of the genome. This 5′ leader is joined to an mRNA 'body', which contains sequences from the 3′-poly(A) to a position upstream of each genomic ORF, coding for either a structural or niche-specific (accessory) protein. At the junction of the leader and body elements in each sgRNA, a characteristic short, AU-rich motif can be found, and is known as TRS.

Although this phenomenon was once thought to occur during positive-stranded RNA synthesis, it became clear that CoV follows a discontinuous transcription model during negative-strand RNA extension (Sawicki and Sawicki, 1995) (Fig. 5.14). In this model, it was proposed that when RdRP transcribes the genome and encounters a TRS body (TRS-B), it is able to pause; following that the RdRP either continues the elongation to the next TRS-B, or switch to the leader sequence located at the 5′ end of the genome by binding complementarily to the leader TRS (TRS-L), leading to the synthesis of a nested set of sgRNAs characteristic to the *Nidovirales*. Recently, a novel sgRNA localized between the M gene and accessory gene 5a was identified in IBV and other gammacoronaviruses, expanding the total sgRNA transcribed to six (Bentley *et al.*, 2013). Nsp9, which functions as an RNA-binding protein, also plays a crucial role in supporting sgRNA transcription. Mutations of a conserved glycine (G98) residue in the C-terminal α-helical domain of nsp9 can abolish sgRNA transcription in Vero cells (Chen *et al.*, 2009).

Assembly and release

With the replication of the gRNA and the transcription of the sgRNAs, the viral proteins can now be translated using the host translation machinery. Following translation, the S, E and M proteins are co-translationally inserted into the ER. Moving along the secretory pathway, these proteins will gather at the assembly point known as the ER-Golgi intermediate compartment (ERGIC). In the ERGIC, viral genomes encapsidated by the N protein are incorporated and mature virions are formed by budding (de Haan and Rottier, 2005).

In the assembly stage of the life cycle, the M protein plays a significant role in directing most of the protein–protein interactions in CoVs. Despite this, M protein is found to be insufficient for virion formation, as virus-like particle (VLPs) cannot be formed by M protein expression alone (Bos *et al.*, 1996; Vennema *et al.*, 1996). Through radioimmunoprecipitation and immunofluorescence studies, IBV E and M proteins were revealed to physically interact with each other via a putative peripheral domain (Lim and Liu, 2001); this interaction is crucial for the formation of the CoV envelope and VLP formation (Lim *et al.*, 2001; Corse and Machamer, 2003).

Further work by other groups has also identified the N protein as an enhancer of VLP (Siu *et al.*, 2008). However, given the contrasting abundance of the M and E proteins, it remains unknown how the E protein aids in virion assembly. Work in this area is rarely explored, with some suggesting the role of E protein in averting M protein aggregation, while others citing the E protein in promoting viral egress through secretory pathway manipulation (Ye and Hogue, 2007; Boscarino *et al.*, 2008). Recently, the ion channel activity of E protein appears to play a role in this process. SARS-CoV equivalent mutations in T16A and A26F of IBV can result in much reduced virion release in cells infected with the two mutants (To *et al.*, 2017). Surprisingly, the S protein, although inserted to the ER during assembly, is not essential for assembly. However, the ability of the S protein to interact with the M protein is crucial to ensure it is incorporated into the progeny virions.

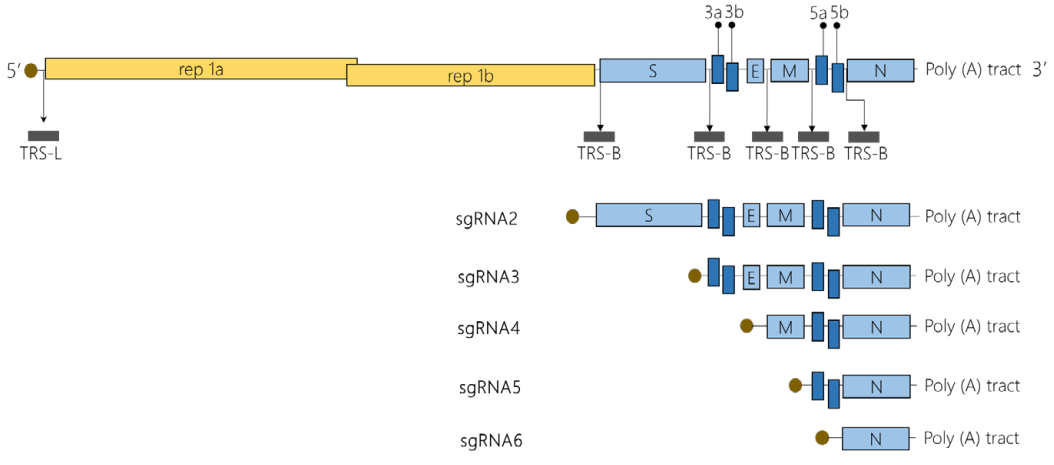

Figure 5.13 Infectious bronchitis virus (IBV) RNA synthesis. Viral RNA synthesis of coronaviruses produces two types of RNAs, the genomic and subgenomic RNAs (sgRNAs). To produce these nested set of sgRNAs requires the leader-to-body fusion of transcriptional regulatory sequences (TRS). The consensus TRS for IBV is 5′-CUUAACAA-3'. TRS-B, transcriptional regulatory sequence body; TRS-L, transcriptional regulatory sequences leader.

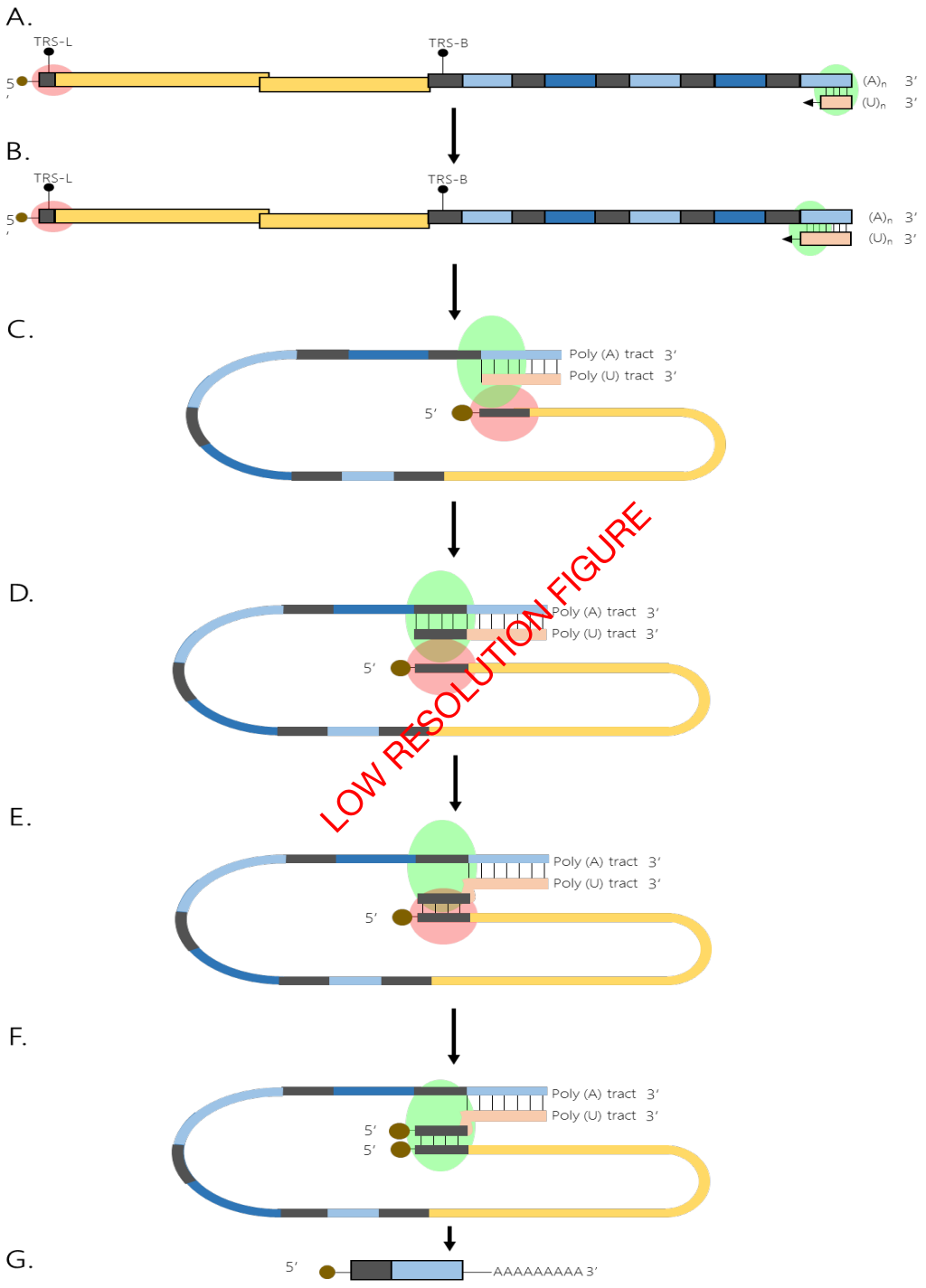

Figure 5.14 Discontinuous transcriptional model of RNA synthesis. (A, B) Subgenomic RNA (sgRNA) synthesis begins at the 3′ end of the positive sense genomic RNA template. (C) To monitor the base-pair complementarity of the negative-strand RNA with the TRS-L by a component of the replicase-transcriptase complex, the genomic template loops out for this purpose. (D) As transcription proceeds towards the 5′ of the genomic RNA, it encounters a TRS-B and pauses. (E) At this point, the nascent negative strand may choose to bypass the TRS-B and resume elongation. Alternatively, it may switch templates by binding to TRS-L. (F) If elongation is resumed, this would result in the complete synthesis of the antileader containing negative-strand sgRNA. (G) These genome and negative-strand sgRNA can then act as templates for the synthesis of positive-sense sgRNA.

Upon the completion of virion assembly, the virions are transported in vesicles and released by exocytosis. However, it remains to be clearly defined whether the virions exit using the traditional exocytosis pathway, or if specialized pathway is used for their exit. This is exemplified in some CoVs, where a proportion of S protein which has not yet been assembled into the virions would transit to the plasma membrane to mediate fusion with neighbouring uninfected cells (Godeke *et al.*, 2000). This permits the formation of large multinucleate syncytia, which poses attractive advantages to increase the

spread of infection and averting any virus-specific antibody neutralization.

Effects on the host cell

During a viral infection, various cellular signalling pathways may be activated to elicit an antiviral response against the invading pathogen. In this section, some of the well-studied signalling pathways activated during IBV infection will be discussed.

ER stress and unfolded protein response

In eukaryotic cells, the ER plays a pivotal role in the synthesis and folding of secretory or transmembrane proteins to mediate a range of post-translational modifications (Schröder, 2008). As such, the ER maintains a homeostasis suitable to regulate the processing and prevent the aggregation of these proteins. Perturbations in the ER homeostasis due to accumulation of nascent, unfolded polypeptides, can result in ER stress and activates the unfolded protein response (UPR) when the protein load exceeds the ER folding and processing capacity (Welihinda *et al.*, 1999).

UPR signalling activates three branches of downstream signalling pathways – PKR-like ER kinase (PER-K), activating transcription factor 6 (ATF6) and inositol-requiring protein 1 (IRE1). UPR works to restore the function of the ER by enhancing protein folding, attenuating protein translation and up-regulating genes related to protein folding, chaperoning and ER-assisted degradation (ERAD). It can also initiate apoptosis if the ER stress levels remain unchanged. ER stress response is induced in CoV infection, allowing the cell to mount UPR as a response (Versteeg *et al.*, 2007; Bechill *et al.*, 2008; Minakshi *et al.*, 2009; Fung *et al.*, 2014a).

PERK signalling pathway

PERK activation is initiated by the dissociation of binding immunoglobulin protein (BiP, GRP78) from the ER chaperone, leading to the oligomerization and autophosphorylation of PERK. An activated PERK can phosphorylate the α-subunit of eukaryotic initiation factor 2 (eIF2α) on Ser51 to attenuate protein translation (Dever *et al.*, 1998).

Activation of PERK is known to play a pro-survival role in cells, as demonstrated using $PERK^{-/-}$ mouse embryonic fibroblasts, which exhibited higher cell mortality when treated with an ER stress-inducing agent cycloheximide (Harding *et al.*, 2000a). While phosphorylated eIF2α can trigger a shutdown of global protein synthesis, it can also enhance the translation of activating transcription factor 4 (ATF4) (Harding *et al.*, 2000b; Lewerenz and Maher, 2009). ATF4 stimulates target gene expression such as GADD153 (growth arrest/DNA damage inducible protein 153, also known as CHOP or C/EBP-homologous protein) to enhance the transcription of pro-apoptotic genes. Furthermore, eIF2α may also be phosphorylated by other kinases, such as protein kinase RNA-activated (PKR), haem-regulated inhibitor kinase (HRI) and general control non-depressible-2 (GCN2) (Ron and Walter, 2007), which together form the integrated stress response when activated (Teske *et al.*, 2011; Fung *et al.*, 2014b).

IBV infection was found to activate the eIF2α-ATF4-GADD153 pathway (Liao *et al.*, 2013). Activation of this pathway modulates stress-induced apoptosis, in which GADD153 plays a critical role in IBV-induced apoptosis (Liao *et al.*, 2013). At late stages of IBV infection, it was also demonstrated that eIF2α phosphorylation was suppressed in both human and animal cells (Wang, X. *et al.*, 2009). At similar time points, phosphorylated PKR levels were greatly reduced in IBV-infected cells and nsp2 may be a weak antagonist against PKR (Wang, X. *et al.*, 2009).

GADD34, a component of protein phosphatase 1 (PP1) complex which dephosphorylated eIF2α, was significantly induced in IBV-infected cells. Supporting evidence from the inhibition of PP1 and overexpression of wild-type and mutant GADD34, eIF2α and PKR have suggested that these virus-modulated pathways play a synergistic role in enhancing IBV replication. It was also postulated that IBV may employ a combination of two mechanisms, i.e. blocking PKR activation and inducing GADD34 expression, to maintain *de novo* protein synthesis in infected cells to enhance viral replication (Wang, X. *et al.*, 2009).

Activating transcription factor 6

ATF6 is a member of the basic-leucine zipper family of transcription factors. Residing in the ER, ATF6 is a transmembrane protein that detects the presence of misfolded/unfolded proteins. Under ER stress, ATF6 is translocated to the Golgi and cleaved by Site-1 (S1P) and Site-2 proteases (S2P) (Ye *et al.*, 2000). This cleavage event releases the cytosolic basic leucine zipper (bZIP) domain, which translocates into the nucleus to activate genes harbouring the ER stress response element (ERSE) (Yoshida *et al.*, 1998; Kokame *et al.*, 2001). These ATF6 targeted genes include the ER chaperones (such as GRP78 and GRP94), PDI and UPR transcription factors GADD153 and XBP1 (Okada *et al.*, 2002). While ATF6 pathway was previously reported as mainly pro-survival, recent studies have demonstrated otherwise. Under certain circumstances, the ATF-6-mediated signals may also contribute to ER-stress-induced apoptosis, possibly via CHOP activation and/or myeloid cell leukaemia sequence 1 suppression (Morishima *et al.*, 2011).

Activation of ATF6 pathway in CoVs has not been deeply investigated, although several studies have demonstrated that ATF6 activation can enhance virus replication and persistent infection and pathogenesis *in vivo*. In MHV-infected cells, ATF6 cleavage has been observed as early as 7 hours post infection (Bechill *et al.*, 2008). However, both full-length and cleaved ATF6 proteins would diminish at later time points during infection. Furthermore, activation of ATF6 target genes were not detected at the mRNA level determined by luciferase reporter constructs under the control of ERSE promoters (Bechill *et al.*, 2008). As such, it is unlikely that MHV infection suppresses downstream signalling of the ATF6 pathway as the reporter induction by overexpressed ATF6 was not inhibited by MHV infection. It was thus concluded that the global translation shutdown via eIF2α phosphorylation prevents the accumulation of ATF6 and activation of ATF6 target genes. The involvement of ATF6 in IBV has not been characterized.

IRE1

In response to unfolded proteins, IRE1 undergoes oligomerization (Korennykh *et al.*, 2009), resulting in trans-autophosphorylation of the kinase domain and activation of the RNase domain. So far, the only known substrate for IRE1 RNase activity is mRNA of the X box binding protein 1 (XBP1) (Yoshida *et al.*, 2001). IRE1 cuts the XBP1 mRNA twice to remove a 26-nt intron, forming a frame-shifted transcript known as spliced XBP1 ($XBP1_S$), opposite from the unspliced XBP1 ($XBP1_U$), which exhibits UPR inhibitory activities. $XBP1_S$ encodes a potent transcriptional activator which translocates to the nucleus to enhance the expression of various UPR genes, such as molecular chaperones and protein contributing to ER-associated degradation (Lee *et al.*, 2003).

Other than the XBP1 pathway, activated IRE1 may also recruit TNF receptor-associated factor 2 (TRAF2) and induce apoptosis by activating JNK (Tabas and Ron, 2011). While IRE1-JNK pathway is distinct from the RNase activity of IRE1, the kinase domain of IRE1 is still required, in addition to TRAF2-dependent activation of caspase-12 (Yoneda *et al.*, 2001). Moreover, one study has demonstrated that IRE1-JNK pathway is required for autophagy activation after pharmacological induction of ER stress. It was found that the kinase domain of IRE1 was required, and treatment with a JNK inhibitor (SP600125) abolished autophagosome formation following ER stress (Ogata *et al.*, 2006). Collectively, the IRE1 branch of UPR is closely associated with the JNK pathway and is involved in JNK-mediated apoptosis and autophagy signalling.

IRE1-XBP1 is activated in IBV-infected cells. In IBV-infected Vero cells, significant splicing of XBP1 mRNA was detected from 12 to 16 hours post infection (Fung *et al.*, 2014a). Moreover, the mRNA levels of XBP1 effector genes (EDEM1, ERDj4 and $p58^{IPK}$) were up-regulated. The activation of IRE1-XBP1 pathway was also detectable in other cell lines such as H1299 and Huh7 cells. IRE1 inhibitor treatment effectively blocked IBV-induced XBP1 mRNA splicing and up-regulation of effector genes in a dosage-dependent manner. Consistently, IRE1 knockdown has effectively inhibited IBV-induced XBP1 mRNA splicing, whereas overexpression of wild-type IRE1 has enhanced IBV-induced XBP1 mRNA splicing. Interestingly, the hyper-phosphorylation of pro-apoptotic kinase (JNK) and hypo-phosphorylation of pro-survival kinase RAC-alpha serine/threonine-protein kinase (Akt) have been associated with earlier onset and more aggressive apoptosis induction in IRE1-knockdown cells upon IBV-infection. As such, IRE1 may modulate IBV-induced apoptosis and act as a survival factor during IBV infection.

Apoptosis

Programmed cell death, or apoptosis, is a highly regulated process in cells characterized by cell shrinkage, blebbing and nuclear pyknosis, DNA fragmentation and asymmetrical distribution of the plasma membrane (Deschesnes *et al.*, 2001). The mechanisms of apoptosis are complex and highly sophisticated, and it usually involves an energy-dependent cascade of events (Elmore, 2007). There are two main apoptotic pathways: the extrinsic or death receptor pathway and the intrinsic or mitochondrial pathway. However, there is now evidence that these two pathways are connected and the molecules in one pathway can influence the other (Igney and Krammer, 2002). Additionally, there is an additional pathway which involves T-cell mediated cytotoxicity and perforin-granzyme-dependent killing of the cell. This perforin/granzyme B pathway can induce apoptosis via granzyme A or B, each with different downstream events. Granzyme A pathway, upon activation, can result in a parallel, caspase-independent cell death pathway via single-stranded DNA damage (Martinvalet *et al.*, 2005). Conversely, the extrinsic, intrinsic and granzyme B pathways converge on the same execution pathway. This pathway is initiated by the cleavage of caspase-3 and results in DNA fragmentation, degradation of cytoskeletal and nuclear proteins, cross-linking of proteins, formation of apoptotic bodies, expression of ligands for phagocytic cell receptor and uptake by phagocytic cells (Elmore, 2007).

During viral infections, apoptosis is often induced as a form of antiviral response towards virus replication and production. To combat this antiviral response, many viruses have evolved various strategies to subvert apoptosis by interfering with apoptotic signalling at multiple control points of the apoptotic pathway (Benedict *et al.*, 2002; Kvansakul and Hinds, 2013). These viral interferences can include inhibiting death receptor activation (Wilson *et al.*, 2009), mimicking prosurvival Bcl-2 family action (Tait and Green, 2010), directly inhibiting caspase (Stennicke *et al.*, 2002) and encoding Bcl-2 family protein homologues (Kvansakul and Hinds, 2013). Besides acting directly on the apoptotic pathways, viruses may also inhibit apoptosis through other signalling pathways, such as nuclear factor kappa-beta (NF-κB) (Tamura *et al.*, 2011).

IBV infection is known to induce caspase-dependent apoptosis in culture cells (Liu *et al.*, 2001). In this study, it was demonstrated that both necrosis and apoptosis may have contributed to cell death of the infected cells in lytic IBV infection. In a follow up study, it was found that IBV-induced apoptosis during the late stages of the infection cycle is p53-independent (Li *et al.*, 2007). Global gene expression profiles via microarray have also revealed pro-apoptotic genes (Bak and Fas) and anti-apoptotic genes (myeloid cell leukaemia-1 (Mcl-1), clusterin and microphthalmia associated transcription factor) to be up-regulated following IBV infection, which has implications in apoptosis modulation and viral replication (Zhong *et al.*, 2012; Cong *et al.*, 2013). As mentioned above, IBV infection-induced ER stress responses can also regulate apoptosis (Liao *et al.*, 2013; Fung *et al.*, 2014a). Recently, there has been evidence illustrating the positive correlation between IBV pathogenicity to apoptosis and innate immune responses. Following the infection of chick embryo kidney cells and TOCs with the M41, 885 and QX strains, it was shown that IBV induction is cell-type dependent. 885 and QX displays a greater induction of TLR3, MDA5 and interferon (IFN)-β and apoptosis in chick embryo kidney cells, while M41 can only generate a greater induction in TOCs (Chhabra *et al.*, 2016).

Autophagy

Autophagy, literally meaning self (auto-) eating (-phagy), is a highly conserved cellular process, in which cytoplasmic contents are sequestered within double membrane vesicles (known as

autophagosomes) and targeted for degradation by the lysosomes (Yang and Klionsky, 2010). Under normal circumstances, basal level of autophagy allows cells to break down mis-folded proteins and damaged organelles (such as mitochondria). Cells can also activate autophagy when starved or deprived of growth factors, so that amino acids and fatty acids can be recycled to maintain metabolism for survival. Autophagy is also activated by a variety of internal and external stimuli, such as hypoxia, oxidative stress, DNA damage, protein aggregation, or infection with intracellular pathogens (Kroemer *et al.*, 2010). In most cases, autophagy facilitates stress adaptation and promotes cell survival. However, autophagy has also been associated with a special type of programmed cell death (PCD) known as autophagic PCD (Maiuri *et al.*, 2007).

The whole process of autophagy, regulated by the highly conserved Atg (autophagy-related gene) proteins, is subdivided into four stages: initiation, nucleation, elongation and lysosomal fusion (Mizushima *et al.*, 2008). Initiation involves the inactivation of mammalian target of rapamycin (mTOR) and hypo-phosphorylation of Unc-51-like kinase (ULK), leading to the formation of the ULK complex and its translocation to the ER where autophagy is initiated (Hosokawa *et al.*, 2009). Next, the ULK complex recruits a class III phosphotidylinositol-3 kinase (PI3K) complex, generating phosphotidylinositol-3-phosphate (PI3P) at the site of membrane nucleation. PI3P then recruits effector proteins that transform the ER into Ω-shape isolated membrane structures (Levine and Deretic, 2007). In the elongation stage, two ubiquitin-like conjugating systems induce elongation of the isolated membranes and their detachment from the ER to form autophagosomes. During this process, a small protein called microtubule-associated proteins 1A/1B light chain 3 (LC3) is conjugated to a phosphatidylethanolamine. This lipidated form of LC3, known as LC3-II, is stably associated with the inner and outer membrane of autophagosomes, making it a classical marker of autophagy induction (Klionsky *et al.*, 2016). In the final stage of autophagy, lysosomes or late endosomes fuse with autophagosomes to form autolysosomes, and the cytoplasmic cargoes are degraded by lysosomal enzymes, releasing amino acid and lipid molecules for recycle in the cytoplasm (Mehrpour *et al.*, 2010).

Numerous DNA and RNA viruses from different families have been shown to induce autophagy during replication (Chiramel *et al.*, 2013). Since coronavirus-induced DMVs are morphologically similar to autophagosomes, early studies with MHV and SARS-CoV observed colocalization of replicase protein with LC3 and proposed autophagosomes as the sites of genome replication/transcription (Prentice *et al.*, 2004a,b). However, similar colocalization was not observed in later studies (Snijder *et al.*, 2006), and the host ATG5 gene was shown to be dispensable for replication of MHV (Zhao *et al.*, 2007) and IBV (Cottam *et al.*, 2011). Subsequent studies using electron microscopy have confirmed that coronavirus-induced DMVs and spherules are derived from modified ER membrane networks (Knoops *et al.*, 2008; Maier *et al.*, 2013). Importantly, Reggiori *et al.* (2010) have demonstrated that MHV-induced DMVs are coated with non-lipidated form of LC3, and that knockdown of LC3 significantly reduces MHV replication in cells, which can be completely restored by transfection of non-lipidable form of LC3. Therefore, although coronavirus replication is not dependent on host cell autophagy, the autophagy-independent role for non-lipidated LC3 is essential for DMV formation.

Interestingly, overexpressing nsp6 of IBV, MHV or SARS-CoV could induce formation of autophagosomes in the transfected cells (Cottam *et al.*, 2011). Nsp6 contains multiple transmembrane domains, and coexpression of SARS-CoV nsp3, nsp4 and nsp6 has been shown to induce DMV formation in the transfected cells (Angelini *et al.*, 2013). However, inhibition of mTOR kinase activity, up-regulation of CHOP mRNA or splicing of XBP1 mRNA could not be observed in cells overexpressing nsp6, suggesting that nsp6-induced autophagosome formation is independent of the mTOR or the ER stress pathways (Cottam *et al.*, 2011).

Our unpublished studies have also shown that IBV induces complete autophagy in the infected cells, as determined by the tandem fluorescence LC3 reporter as developed by Kimura *et al.* (2007) and the autophagic flux study using lysosomal inhibitor chloroquine as reported by Klionaky *et al.* (2016). Moreover, using RNA interference, IBV-induced autophagy was found to be independent of Beclin1, a subunit of the class III PI3K complex, indicating that autophagosome formation in IBV-infected cells might utilize alternative signalling cascades distinct from the canonical autophagic pathway. Furthermore, inhibition of autophagy was found to be associated with enhanced IBV-induced apoptosis in the infected cells, suggesting a prosurvival role of autophagy during infection (unpublished data).

Mitogen-activated protein kinase (MAPK) pathway

MAPKs are a group of evolutionarily conserved serine/threonine kinases which have been shown to play a key role in cell proliferation, programmed cell death, transcription regulation, mRNA stability, protein translation and production of pro-inflammatory cytokines (Dhillon *et al.*, 2007). In mammalian cells, three MAPK pathways are characterized, namely, the ERK, JNK and p38 kinases. Unlike the ERK pathway which is activated by mitogenic and proliferative stimuli, the JNK and p38 MAPK pathways are activated by environmental stress.

MAP kinases lie within protein kinase cascades. In each protein cascade, there are at least three enzymes which are activated in a series: a MAPK kinase kinase (MAPKKK), a MAPK kinase (MAPKK) and a MAP kinase (MAPK). Once activated, MAPK pathways can relay, amplify, and integrate signals from a diverse range of stimuli to elicit an appropriate response in regulating cell proliferation, survival, motility, and apoptosis (Keshet and Seger, 2010). Among them, MKK7 has been reported to be responsible for IBV-induced JNK activation, with JNK serving as a pro-apoptotic protein during IBV infection through modulation of anti-apoptotic protein B-cell lymphoma 2 (Bcl2) (Fung and Liu, 2017).

MAPKs are negatively regulated through dephosphorylating events on both phospho-threonine and phospho-tyrosine residues on the activated MAPKs via dual-specificity phosphatases

(DUSPs). DUSPs constitute a structurally distinct family of 11 proteins, with DUSP1 being the archetype of the family (Lang *et al.*, 2006). DUSP1 can be activated by pro-inflammatory stress stimuli such as ultraviolet (UV) irradiation, IL-1 and lipopolysaccharide (LPS) (Abraham and Clark, 2006; Liu *et al.*, 2007). Studies which involve DUSP1-deficient macrophages reported a prolonged activation of p38 MAPK, indicating that p38 MAPK is a target of DUSP1 (Franklin and Kraft, 1997). Furthermore, the increase in pro-inflammatory cytokines TNFα and IL-6 and anti-inflammatory cytokine IL-10 was reported in DUSP1$^{-/-}$ macrophages following LPS stimulation (Hammer *et al.*, 2006; Salojin *et al.*, 2006; Zhao *et al.*, 2006). Conversely, the up-regulation of DUSP1 in virus infection was reported (Abraham and Clark, 2006), indicating the physiological regulatory role of DUSP1 in innate immunity.

Activation of p38 MAPK was reported in IBV-infected cells, which may be involved in induction of pro-inflammatory cytokines IL-6 and IL-8 expression (Liao *et al.*, 2011). To counteract this induction, one strategy developed by IBV is to induce the expression of DUSP1 to limit the production of IL-6 and IL-8 in cells, which may help modulate the pathogenesis of IBV.

Evolution

As shown in Fig. 5.2, sequence comparisons of the genome, S, E, M, N proteins of IBV strains have been used to construct the IBV phylogenetic tree. As a rule, isolates with less than 89% similarity belong to different serotypes, except for Conn46 and Fla18288, which are 96% similar but are different serotypes, indicating that only minor changes in the S1 are required to change the serotype (Cavanagh *et al.*, 2005; Ammayappan and Vakharia, 2009). Often, the evolution of these IBV serotypes distributed worldwide is facilitated by genomic substitutions, deletion, insertion and/or RNA recombination of the S1 gene (Gelb *et al.*, 1991; Lee and Jackwood, 2000; Alvarado *et al.*, 2005). This wide diversity of IBV serotypes, on top of its rapid evolution rate, is a major contributing factor to the failure or partially efficacious commercial vaccines and continual IB outbreaks in regions around the globe, making this virus extremely difficult to diagnose and control (Cavanagh, 2003; Marandino *et al.*, 2015).

Rapid evolution in IBV is facilitated by strong selection, large population sizes and high genetic diversity within hosts and transmission bottlenecks between hosts. Genetic diversity within hosts arises primarily from mutations, which include substitutions, insertions and deletions. Substitutions are caused by both the high error rate and limited proofreading capability of the viral RdRP, and by recombination, which generates new haplotype diversity from existing variants. On the other hand, insertions and deletions are caused by recombination events or by RdRP stuttering or slippage. These genetic variations occur continuously in nature and lead to the emergence of multiple phenotypes in terms of pathotypes and immuno-types (Cavanagh, 2007). So far, VN tests performed by many groups have reported several serotypes which are poorly cross-protective (Cavanagh, 2007; Marandino *et al.*, 2015). Furthermore, the high error rate of IBV genomic transcription can generate a population of quasispecies which is significant for the IBV evolution and persistence (Montassier, 2010; Jackwood *et al.*, 2012). New dominant strains can emerge by selection from and recombination among minor variants (Fang *et al.*, 2005).

Broad genetic diversity facilitates survival of the virus in a constantly changing environment (Jackwood *et al.*, 2012; Marandino *et al.*, 2015). While the evolutionary progression of IBV is quite complex and poorly understood, investigations carried out to date have highlighted the role of three factors: (1) lack of RNA polymerase proof reading, leading to replication in RNA genomes with the mutation rate that ranges approximately from 10^{-2} to 10^{-6} substitutions/site/year (Holmes, 2009; Umar *et al.*, 2016); (2) interference of continuous use of live and often multiple attenuated vaccines formulated with different IBV strains; and (3) immune pressure exerted on circulating viruses by the constant presence of partially immune bird populations. In many cases, new IBV variants have emerged due to spontaneous mutations and recombination during virus replication, followed by replication of those phenotypes which are favoured by selection (Liu *et al.*, 2013; Awad *et al.*, 2014). Despite the mutation efforts made by the virus to persist in the environment, only a few variants are able to persist for an extended period of time and spread in new territories to become evolutionary and economic significance.

Recombination commonly occurs between two or more viruses infecting the same cell. It is believed that a high rate of recombination events occurs in the genomes of non-segmented RNA viruses such as IBV (Jackwood *et al.*, 2012). Recombination can reduce mutational load, create genetic variants that may be very different from the parental strains, and result in the emergence of new strains (Holmes, 2009; Sumi *et al.*, 2012). Recombination has been reported in many IBVs (Cavanagh *et al.*, 1992; Thor *et al.*, 2011). Recombination hot spots, or regions of the viral genome with higher incidences of recombination breakpoints, have been reported in IBV (Lee and Jackwood, 2000). These hot spots tend to lie immediately upstream of the S glycoprotein gene, as well as in nsp 2, 3 and 16 (Thor *et al.*, 2011; Jackwood *et al.*, 2012). Recombination in the non-structural proteins associated with RdRP can alter the replication efficiency of IBV, which can in turn affect viral pathogenicity.

Mutations and selective pressure in genes, especially in hypervariable regions (HVRs), enable viruses to cross the species barrier and adapt to new host species, hence contribute to viral evolution (Lim *et al.*, 2011). The average rate of synonymous mutation in all CoVs, including IBV is approximately 1.2×10^{-3} substitutions/site/year (Holmes, 2009; Jackwood *et al.*, 2012). For other RNA viruses with smaller genomes, the mutation rate can be as high as 1×10^{-1} substitutions/site/year. The difference is presumably due to the presence of a 3′ to 5′ exoribonuclease (ExoN) domain in nsp 14, which contains similarities to host proteins involved in proofreading and repair (Snijder *et al.*, 2003). A study which involves SARS-CoV nsp 14-ExoN mutant revealed impaired growth and a 21-fold increase in mutation rates for the mutant virus compared with wild type (Eckerle *et al.*, 2010). This study and previous work with an MHV ExoN mutant (Eckerle *et al.*, 2007), confirmed that ExoN, which is conserved in all

CoVs, contributes to the fidelity of the viral RdRP. Relatively high fidelity of polymerase results in a greater 'error threshold' and may permit the virus to maintain a large genome size (Holmes, 2009; Jackwood *et al.*, 2012). The emergence of new IBV strains and serotypes is largely due to the accumulation of mutations in the S gene over time as opposed to recombination events. This is thought to be the primary method of cross-species transmission and was shown to lead to the emergence of SARS-CoV (Hon *et al.*, 2008).

Different environmental determinants within the host, i.e. immune responses, affinity for cell receptors, physical and biochemical conditions are implicated in the selection process (Toro *et al.*, 2012). Amino acid changes within the three S1 glycoprotein HVRs, described in the first 395 amino acid region of the S1 subunit, determine the most relevant phenotypic changes, resulting in new serotypes and the induction of non-cross protecting VN antibodies. Thus, it is assumed that due to widespread vaccination, the immune selection pressure involving the S1 subunit of the S gene and the high mutation rate of the viral genome altogether can result in the emergence of many serotypes and variants (Abro *et al.*, 2012). Variants may attain increased virulence, efficient receptor binding, rapid transmission and persistence in host system causing significant disease in vaccinated flocks of all ages. Many variant viruses have been reported in China, Italy, Brazil, and Africa in the recent years (Fraga *et al.*, 2013; Franzo *et al.*, 2015; Khataby *et al.*, 2016; Xu *et al.*, 2016).

Genetics and reverse genetics

Classical CoV genetic studies were mainly performed using two types of mutants, namely the naturally arising viral variants and temperature sensitive (*ts*) mutant isolates from MHV following chemical mutagenesis (Sawicki *et al.*, 2005). The naturally arising viral variants, especially the deletion mutants, can offer clues to the genetic changes accounting for the different pathogenic traits, as exemplified in the emergence of porcine respiratory coronavirus (PRCoV) from TGEV (Wesley *et al.*, 1991). On the other hand, *ts* mutants were classified into at least seven complementation groups, of which five cannot synthesize RNA at non-permissive temperature (Leibowitz *et al.*, 1982; Schaad *et al.*, 1990). Some of the *ts* mutants have proved to be useful in analyses of the functions of the structural proteins (Luytjes *et al.*, 1997; Narayanan, *et al.*, 2000; Shen and Liu, 2001; Shen *et al.*, 2004). However, usage of *ts* mutants was thwarted by caveats pertaining to the large *replicase* gene, which led to conditionally lethal, RNA-negative phenotypes in randomly generated mutants (Fischer *et al.*, 1998). Complementation analyses of these mutants have only yielded early insights into the multiplicity of functions entailed by the CoV RNA synthesis (Sawicki *et al.*, 2005). More recently, there has been a resurgence of interest in classical replicase *ts* mutants as they can now be fully examined by the tools of reverse genetics (Sawicki *et al.*, 2005).

The development of CoV reverse genetics proceeds in two phases (Deming and Baris, 2008). CoVs have a ss(+)RNA genome, the first phase requires the generation of a complementary DNA (cDNA) which can function as a template for the generation of an infectious RNA. This involves the conversion of the RNA genome into a manipulable cDNA using standard DNA technologies or homologous recombination. The final phase of the process is the generation of an infectious RNA from the modified cDNA using a DNA-dependent RNA polymerase. Having a ss(+)RNA genome, like the CoVs, provides the advantage that the infectious RNA derived from a cDNA copy, is similar to the genomic RNA that can be recognized by the host cell's transcriptional machinery as an mRNA. This can lead to the translation of the mRNA into proteins required for the replication of the RNA genome, which involves 15 proteins in IBV.

The reverse genetics system for IBV was first developed in 2001 using a vaccinia virus (VV) system (Casais *et al.*, 2001). In this study, a complete cDNA copy of the IBV Beaudette genome was generated and systematically ligated together *in vitro* before direct cloning into the VV vNotI/tk, via a NotI site introduced into the thymidine kinase (TK) gene of vNotI/tk (Merchlinksy and Moss, 1992). This resulted in a full-length cDNA under the control of a T7 promoter with a hepatitis δ ribozyme (HδR) sequence downstream of the IBV poly(A) tail followed by a T7 termination sequence. Infectious RNA can be generated *in vitro* from VV templates using T7 RNA polymerase and transfected into permissive cells for the recovery of the virus (Thiel *et al.*, 2001). Alternatively, infectious RNA generation can be performed *in situ* in which VV DNA is transfected into cells infected with a recombinant fowlpox virus, rFPV-T7 expressing T7 RNA polymerase (Britton *et al.*, 1996). The second approach was adapted from an *in vitro* ligation method originally developed by Yount *et al.* (2000) for TGEV and subsequently used for IBV (Youn *et al.*, 2005a; Fang *et al.*, 2007). This system relied on the *in vitro* assembly of a set of cloned cDNAs. Generally, the *in vitro* ligation method works by amplifying fragments of a viral genome through RT-PCR followed by amplicon ligation through unique restriction sites for the assembly of the entire genome. Later on, this strategy was further improved to construct an infectious cDNA clone with a 'seamless' feature, whereby restriction endonucleases sequences were eliminated prior to *in vitro* ligation (Yount *et al.*, 2002).

While N protein is an absolute requirement for IBV recovery in chick kidney cells, it is not an absolute requirement for recovery of other CoVs; although the recovery of CoVs can be significantly enhanced by the presence of N protein (Yount *et al.*, 2003; Almazán *et al.*, 2004; Coley *et al.*, 2005; Schelle *et al.*, 2006). A possible explanation for this observed enhancement comes from recent studies in which an interaction between MHV nsp 3 replicase protein and the N protein was found to be critical for replication (Hurst *et al.*, 2010).

Reverse genetics systems for several CoVs in all three genera have been developed and successfully used to recover infectious viruses (Table 5.4). The use of VV vector for a full-length CoV cDNA offers a highly stable system for producing and maintaining a cDNA, dispensing the need for repetitive cloning of cDNA fragments. Another major advantage of the VV-system is that homologous recombination can be used to modify or replace portions of the CoV cDNA, followed by transient dominant selection (TDS) system (Britton *et al.*, 2005). With the exception

Table 5.4 Reverse genetics system for recovery of infectious coronaviruses

System	Description	Developed for
BAC	Clone full-length genomic cDNA into a BAC vector and transfect into cells. Initiate infection by transcribing infectious gRNA from CMV promoter	*Alphacoronavirus* TGEV (Almázan *et al*., 2000) *Betacoronavirus* HCoV-OC43 (St-Jean *et al*., 2006); SARS-CoV (Almázan *et al*., 2006); MERS-CoV (Almázan *et al*., 2015)
In vitro ligation	Clone smaller parts of the genomic cDNA as a set of smaller stable clones; assemble full length cDNA by directed *in vitro* ligation	*Alphacoronavirus* PEDV (Beall *et al*., 2016); TGEV (Yount *et al*., 2000); HCoV-NL63 (Donaldson *et al*., 2008) *Betacoronavirus* MHV (Yount *et al*., 2002); SARS-CoV (Yount *et al*., 2003); MERS-CoV (Scobey *et al*., 2013); Bat-CoV (Becker *et al*., 2008) *Gammacoronavirus* IBV (Youn *et al*., 2005a; Fang *et al*., 2007)
Targeted recombination	Synthetic donor RNA bearing mutations of interest introduced into cells infected by the recipient parent virus possessing characteristics which can be selected against	*Alphacoronavirus* mFIPV (Haijema *et al*., 2003) *Betacoronavirus* MHV (Koetzner *et al*., 1992); fMHV (Kuo *et al*., 2000)
Vaccinia virus	Clone full-length genomic cDNA into Vaccinia virus genome; transcribe infectious gRNA and transfect into cells	*Alphacoronavirus* HCoV-229E (Thiel *et al*., 2001); FCoV (Tekes *et al*., 2008) *Betacoronavirus* MHV (Coley *et al*., 2005) *Gammacoronavirus* IBV (Casais *et al*., 2001)

BAC, Bacterial artificial chromosome; Bat-SCoV, severe acute respiratory syndrome-like coronavirus; fMHV, feline Mouse hepatitis virus; HCoV-229E, Human coronavirus 229E; HCoV-NL63, Human coronavirus Netherlands 63; HCoV-OC43, Human coronavirus organ culture 43; MERS-CoV, Middle East respiratory syndrome coronavirus; mFIPV, mutant Feline infectious peritonitis virus; MHV, Mouse hepatitis virus; PEDV, Porcine epidemic diarrhoea virus; SARS-CoV, Severe acute respiratory syndrome coronavirus; TGEV, Transmissible gastroenteritis coronavirus.

of the modification introduced, the resultant rIBVs are isogenic as they are derived from the same cDNA sequence.

Collectively, reverse genetics have been used to study the molecular biology of CoV interactions and functions of the replicase, structural and accessory proteins, providing a powerful means to unravel the complexities of the CoV genome.

Pathogenesis and clinical features

Domestic chickens have usually been regarded as the exclusive host of IBV, but respiratory disease and decreased egg production have also been reported in other avian species including pheasants, pigeons, peacock, partridge and mallard, indicating that the host range of IBV extends beyond chickens (Wickramasinghe *et al*., 2015).

Virulence factors influencing pathogenesis

Host and environment factors

Age, breed, nutrition and environment may affect the pathogenesis of IBV. All ages are susceptible to IBV, but clinical manifestations are pronounced in young chicks, and can often lead to permanent damages to the organs involved (Crinion and Hofstad, 1972; Smith *et al*., 1985). Chicks will become more resistant to IBV-induced clinical signs such as oviduct lesions, nephropathic effects and mortality as they grow older (Albassam *et al*., 1986; Crinion and Hofstad, 1972). Mortality rates induced by IBV vary among different inbred lines (Otsuki *et al*., 1990; Ignjatovic *et al*., 2003). Genetic difference in IBV susceptibility was noted, with the light breeds more susceptible than the heavy breeds (Cumming and Chubb, 1988; Jones, 2008). Nephropathogenic IBV (NIBV) has also been shown to induce a higher mortality in broilers than layers (Ignjatovic, 1988; Lambrechts *et al*., 1993), and male chicks were shown to be twice as susceptible as females to nephritis (Cumming, 1969). Nutrition and environment also appear to affect host susceptibility to IBV infection. Chickens on high protein diets, such as meat meals and poultry by-product meat-based diets are more prone to IBV-induced nephrosis and mortality (Cumming, 1969; Cumming and Chubb, 1988). Low temperature appears to have a significant impact on NIBV-induced mortality (Cumming, 1969) and IBV-induced tracheal lesions (Ratanasethakul and Cumming, 1983a). The associated mortality rate also increased to up to 50%. This has important implications for assessing vaccine protection, since cold exposure can be used to increase the severity of challenge imposed (Klieve and Cumming, 1990).

Viral virulence factors

IBV virulence is a crucial frontier of IB pathogenesis, as determined by successful entry, replication, and final release of the mature virion. S protein plays an essential role in the attachment and entry of host cells and therefore, contributes to virus infection. Amino acid substitutions in the S1 subunit of IBV can significantly alter the virulence and virus escape from host defences (Lee and Jackwood, 2001). In the cytoplasmic tail of IBV S protein, there exists a dilysine ER retrieval signal and a

tyrosine-based endocytosis signal which mediates virus infection (Lontok *et al.*, 2004). Mutations in these endocytosis signals of IBV S has shown to be essential for productive IBV infection, as mutant S protein can traffic through the secretory pathway faster than the wild-type S protein (Youn *et al.*, 2005b).

3a, 3b, 5a and 5b proteins of IBV are also thought to contribute to virus virulence (Shen *et al.*, 2003; Casais *et al.*, 2005). Accessory proteins 3a and 3b in IBV may modulate host immune response at transcriptional and translational levels (Kint *et al.*, 2015). Functional studies on the 5a-ns segment of IBV have established a possible link between ns-protein and virus virulence (Youn *et al.*, 2005a). Nsp1 is known to be a potential virulence factor due to increasing evidence supporting its role in the down-regulation of host innate immune response following infection (Narayanan *et al.*, 2015). Although IBV does not encode nsp1, it is suggested that IBV accessory proteins can perform the same function as nsp1 (Kint *et al.*, 2016). Several CoV proteins also encode functions related to IFN antagonist, such as nsp2 (Wang *et al.*, 2009), [96] nsp3 (Yang *et al.*, 2014), nsp5 (Zhu *et al.*, 2017) and N protein (Ye *et al.*, 2007).

Tissue tropism and associated clinical features

Respiratory system

IBV replication in the respiratory tissues can cause clinical signs such as gasping, coughing, tracheal rales and nasal discharge in birds (Bande *et al.*, 2016). Puffy, swollen eyes and inflamed eyes can sometimes be seen (Parsons *et al.*, 1992). In addition, infected chickens may appear depressed, resulting in a significant reduction in weight and feed intake within three days following infection (Otsuki *et al.*, 1990; Grgiæ *et al.*, 2008). Despite the symptoms presented in infected chicks, mortality rate is usually low in uncomplicated cases and these are usually triggered by asphyxiation due to bronchoconstriction by mucus plugs.

The main site of IBV replication is at the upper respiratory tract, following which a viraemia occurs and the virus gets disseminated to other tissues (Crinion and Hofstad, 1972; Dhinakar and Jones, 1997). Virus replication selectively occurs in epithelial and mucus-secreting cells (Nakamura *et al.*, 1991; Ferreira *et al.*, 2003; Shamsaddini-Bafti *et al.*, 2014). Apart from the upper respiratory tract, IBV can also replicate in the epithelial cells of lungs and air sacs (Otsuki *et al.*, 1990; Bezuidenhout *et al.*, 2011). Under these circumstances, infected chickens exhibit mucosal thickening in the nasal passages, trachea and sinuses. Areas of pneumonia may be observed in the lungs, and the air sac may appear cloudy or contain a yellow caseous exudate in histological tests (Feng *et al.*, 2012).

Reproductive system

IBV infection in young chicks less than 2 weeks of age can result in permanent damage of the oviduct, leading to the generation of 'false layers' that do not lay normally at sexual maturity (Crinion and Hofstad, 1972). In laying hens, IBV infection can cause a sharp decline in egg production, as well as a decrease in the external and internal quality of eggs (Bisgaard, 1976; Muhammad *et al.*, 2000), dependent on the virulence of the virus and the period of lay. While the effects of IBV on the male reproductive tract are rarely explored, two studies do not rule out the possibility of reduced fertility in the rooster following IBV infection (Boltz *et al.*, 2004; Villarreal *et al.*, 2007).

Among the IBV variants, strain YN has been demonstrated to cause damages to the reproductive organs of laying hens with a mortality rate of 40.5% upon infection (Zhong *et al.*, 2016). Studies of the differences in the virulence of QX-like, M41 and 793/B strains for the oviducts in day-old SPF chicks showed characteristic dilatation of the oviduct in all QX-like-infected chicks, while no changes were observed in M41- or 793/B-infected chicks (Benyeda *et al.*, 2009).

Renal system

Although most IBV strains target primarily the respiratory tract, some IBV strains are known to be nephropathogenic and may cause kidney damage, or nephritis (Winterfield and Albassam, 1984). The first report of IBV virulence for the kidneys came from Australia, followed by the reports of NIBV worldwide (Meir *et al.*, 2004; Bayry *et al.*, 2005). Some examples of NIBV strains include BJ1, BJ2, BJ3, M41, Holte, Grey, Italian and Australian T strain (Albassam *et al.*, 1986; Li and Yang, 2001).

During the initial stages of NIBV infection, typical respiratory symptoms are observed in infected birds, followed by signs of kidney damage, including wet droppings and increased water consumption (Reddy *et al.*, 2016). The first mortality usually occurs 6 days post infection, and mortality rates will increase rapidly around ten days post infection.

IBV replication has been demonstrated to occur in the proximal convoluted tubules (Goryo *et al.*, 1984), distal convoluted and collecting tubes (Chen and Itakura, 1996) and collecting ducts (Chen and Itakura, 1996; Tsukamoto *et al.*, 1996). Because of viral infection to these parts of the kidneys, acute renal failure may occur as a result of impaired fluid and electrolyte transport. Urinary water losses in infected birds appear to be associated with low urine osmolality and high electrolyte excretion (Afanador and Roberts, 1994). In a study which compared the nephropathogenicity of four NIBV, the Australian T strain proved to be the most pathogenic, followed by the Grey, Italian and Holte strains, but the younger birds are more susceptible to the nephritogenic effects following infection (Albassam *et al.*, 1986).

Post-mortem examinations reported swollen and pale-looking kidneys, with distended tubules and ureters (Feng *et al.*, 2012). The relative kidney weight and kidney asymmetry are also increased in infected birds (Afanador and Roberts, 1994). IBV can also cause granular degeneration, vacuolation and desquamation of the tubular epithelium, signs similar to ductotubular interstitial nephritis (Bayry *et al.*, 2005; Feng *et al.*, 2012).

Gastrointestinal system

IBV has been known to replicate well in the alimentary tract. Several gut tissues, including the oesophagus, duodenum, jejunum, bursa of Fabricius, caecal tonsils, rectum and cloaca, can support the growth of IBV (Cavanagh, 2003). The site of virus multiplication in these tissues was not confirmed, but it was postulated to be in the epithelial cells. In the lower gut, IBV replication has been

reported in the lymphoid and histocytes-resembling cells in the caecal tonsils (Gross, 1990), and in apical epithelial cells of the villi of the intestines as demonstrated by IF (Ambali and Jones, 1990).

Despite the enterotropic nature of some IBV strains, histological changes reported following IBV infection were limited. Recently, an IBV-like CoV isolated from the intestines of broiler chicks displayed clinical signs of runting stunting syndrome (Hauck *et al.*, 2016). This new IBV strain, which may have merged from the California 99 and Arkansas strains, causes pale and distended small intestines on post-mortem examination. Histopathology revealed changes on the epithelial surface of the intestines, including increased cellularity of the lamina propria, blunting of villi, and cystic changes in the crypts.

Muscular system

The presence of pectoral myopathy in birds has been associated with an IBV strain known as 793/B. It was first reported in England in the early 1990s, where affected chickens kept in the slaughterhouse were presented with both superficial and deep bilateral pectoral myopathy. The pectoral lesions are also marked by atrophy, occasional fascial haemorrhages and oedema over its surface (Gough *et al.*, 1992), but did not cause severe clinical issues in chickens (Bijanzad *et al.*, 2013). Several studies have been conducted to examine the relationship between this group of IBV with myopathy in chickens, but the findings have not been conclusive (Brentano *et al.*, 2005; Gomes and Brito, 2007; Trevisol *et al.*, 2009). It appears that the virus is involved in the formation and deposition of immune complexes in the capillary walls of the muscle, which may have contributed to the development of this strange lesion (Dhinakar and Jones, 1997).

Immune responses

Innate immunity

The innate and adaptive immunity to viral infections in chickens are interconnected, with the innate immunity response being more rapid. The innate immunity comprises of an assortment of factors which aim to protect the body against foreign pathogens. It includes physical barriers provided by the skin and mucous membranes, soluble factors such as lysozymes and complement proteins and immune cells such as phagocytic leucocytes, dendritic cells and natural killer (NK) cells. These immune cells, as well as cells on the mucosal surface, detect evolutionarily conserved structures on pathogens, termed pathogen associated molecular patterns (PAMPs). PAMPs are recognized upon binding to membrane associated or intra-cellular Toll-like receptors (TLRs) (Akira, 2001).

In chickens, TLR3 and TLR7 are most extensively studied in viral infection. TLR3 serves two roles in viral infection: first, to recognize and bind to double-stranded RNA (dsRNA) produced during viral replication (Alexopoulou *et al.*, 2001), and secondly, to activate TIR-domain-containing adapter-inducing-interferon-β (TRIF) adaptor protein-mediated pathway (Kawai and Akira, 2010). TLR7, on the other hand, responds to single-stranded RNA and activates the myeloid differentiation primary response gene 88 (MyD88) mediated-pathway (Watters *et al.*, 2007). In a study which compared the immune response genes in the tracheal samples following challenge with Brazilian field isolates, a suppressive effect on the activation of TLR7 was observed (Okino *et al.*, 2017). It may result in insufficient pro-inflammatory response and increased severity of renal lesions in chicken observed. Collectively, through the actions of the dual signalling pathways activated by TLR3 and TLR7, this would lead to the production of type I IFN-α and -β and pro-inflammatory cytokines (Guillot *et al.*, 2005). Among them, IL-1β plays an important role in chemotaxis to recruit immune cells, such as macrophages, to the site of infection (Babcock *et al.*, 2008; Amarasinghe *et al.*, 2018).

Besides TLRs, retinoic acid-inducible gene I (RIG-I) and melanoma differentiation-associated gene 5 (MDA5) are also pattern-recognition receptors (PRRs) that function as viral detectors in non-immune cells and contribute to type I IFN production (Barber, 2011). MDA5 is a functional compensate for RIG-I in chickens (Barber *et al.*, 2010). It is a cytoplasmic DExD/H-box helicase. Upon binding of dsRNA to the helicase domain, the signalling cascades in MDA5 are then initiated through homotypic caspase activation and recruitment domain (CARD) interactions with interferon promoter-stimulating factor 1 (IPS-1) adaptor proteins to activate downstream interferon-regulatory factors (IRFs) (Kawai *et al.*, 2005; Potter *et al.*, 2008). MDA5 can recognize CoV RNA products in virus-infected cells to induce IFN-α and -β signalling (Yoneyama and Fujita, 2007; Züst *et al.*, 2011). This process can be regulated by nsp16 methyltransferase (Yoneyama and Fujita, 2007; Züst *et al.*, 2011). MDA5-mediated innate immune responses are implicated in several CoV infections, including MHV (Zalinger *et al.*, 2015) and SARS-CoV (Yoshikawa *et al.*, 2010). In cells infected with IBV, MDA5 expression is up-regulated, as demonstrated in a number of studies (Cong *et al.*, 2013; Kint *et al.*, 2015; He *et al.*, 2016).

Macrophages and DCs are important cells of the immune system, facilitating the presentation of antigens to develop antigen-specific innate and adaptive immune response through PRRs (Akira *et al.*, 2006; Trinchieri and Sher, 2007). While IBV can infect the blood-derived monocytes/macrophages and induce apoptosis (Zhang and Whittaker, 2016), no studies have reported that IBV infection could impair the bactericidal or phagocytic activity of macrophages. NK cells are rapidly activated upon M41 infection (Vervelde *et al.*, 2013). On the other hand, CD59 is also reported to be down-regulated in IBV-infected cells and is found to be associated with IBV virions, protecting IBV from complement-mediated lysis (Wei *et al.*, 2017).

Adaptive immunity

Adaptive immunity involves the activation of antigen-specific B-cells (humoral), T-cells (cellular), macrophages and memory cells (Chaplin, 2010). The cross-neutralization test developed by Fabricant (1951) has enabled the detection and quantification of humoral antibodies following IBV infection. Chickens were reported to develop a good humoral response to IBV infections as measured by enzyme-linked immunosorbent assay (ELISA),

haemagglutination inhibition (HI) and VN tests (Gough and Alexander, 1977; Mockett and Darbyshire, 1981; Chhabra *et al.*, 2015). Upon receiving proper stimuli, B-cells differentiate into plasma cells to secrete antibodies, in either the presence or absence of T helper (T_h cells). Most HI and ELISA tests are developed to detect Immunoglobulin G (IgG), the most widely circulating antibody in the body (Mockett and Darbyshire, 1981). Generally, anti-IBV IgG can be detected as early as four days post infection and peaks around 21 days (Mockett and Darbyshire, 1981). On the other hand, IgM is only transiently present after infection and peaks around 8 days post infection, before it declines (Mockett and Cook, 1986). Antibody-capture ELISA for IBV-specific IgM has been developed to facilitate IB diagnosis (De Wit *et al.*, 1998).

The importance of B-cells in IBV infections was demonstrated by depletion experiments using hormone testosterone propionate (Chubb, 1974), chemical cyclophosphamide (Chubb, 1974) and surgical bursectomy (Cook *et al.*, 1991). Cyclophosphamide-treated chickens exhibited an increased clinical signs and more severe histopathological kidney lesions (Chandra, 1988) attributed to IBV persistence. IBV infection of a surgically bursectomised resistant chicken line also showed an increased severity and duration of clinical infection, albeit without mortality (Cook *et al.*, 1991). Humoral antibodies appeared to protect the tracheal epithelium following secondary challenge. This is evident in the positive correlation between high titres of humoral antibodies with no virus recovery in the organs studied, as well as protection against low egg production (Gough and Alexander, 1977; Box *et al.*, 1988; Mondal and Naqi, 2001). This may be partially explained by low viraemia induced by IBV-specific antibodies from the trachea to other susceptible organs. Nevertheless, there is no correlation between titres of circulating antibodies to IBV resistance (Raggi and Lee, 1965; Gough and Alexander, 1979; Gelb *et al.*, 1998). This suggests that while humoral antibodies may play a role in IBV infection recovery, other immunological mechanisms are involved.

Maternally derived antibodies can serve to provide some protection to progeny chicks from IBV, but these are often short-lived, with a half-life estimate of maternal IBV antibody titres of 3.8 days (Gharaibeh and Mahmoud, 2013). There is no report that these antibodies induce any adverse effect on the efficacy of IBV vaccines administered to day-old chicks (Davelaar and Kouwenhoven, 1977).

Local immunity

Local immunity in the respiratory tract of chicks is of fundamental importance in IBV protection, and can be aided by vaccines (Awad *et al.*, 2015; Chhabra *et al.*, 2015). This has been exemplified in the *in vitro* model using TOC of immunized chicken for cross-protection studies (Lohr *et al.*, 1991). IBV-specific IgA and IgG have been demonstrated in tracheal washes of infected chicks and antibody-secreting cells were shown in tracheal sections (Hawkes *et al.*, 1983; Nakamura *et al.*, 1991).

Local immunity in the oviduct has also been demonstrated in the oviduct washes of infected hens (Raj and Jones, 1996a). Additional to the local production of antibodies, antibodies were also transuded from the serum in the later course of infection. In young chicks, local antibodies in the oviduct do not appear to be more protective compared with those in the trachea using an *in vitro* challenge of TOC prepared from vaccinated chickens (Dhinakar Raj and Jones, 1996).

While IBV has been shown to multiply in the gut, no antibodies were detected following gut washings of vaccinated day-old chicks with H120 and H52 vaccines (Lutticken *et al.*, 1988). On the other hand, local antibody production was found in the duodenum and caecal tonsils of older hens infected with strain G of IBV (Dhinakar and Jones, 1997). The role of the antibodies in the gut limiting virus replication warrants further investigation.

Chicken Harderian gland is the primary source of immunoglobulins in the lachrymal fluid and plays important role in the development of vaccinal immunity as these vaccines are usually given by spray or eye-drop (Survashe *et al.*, 1979; Davelaar *et al.*, 1982; Raj and Jones, 1996a). Removal of the Harderian gland can result in decreased IBV protection (Davelaar and Kouwenhoven, 1980).

The source of IBV-specific antibodies is also different. While IgA is found in the lachrymal fluid and synthesized in the Harderian gland (Davelaar *et al.*, 1982; Toro *et al.*, 1997), IgG is mainly serum-derived (Davelaar *et al.*, 1982; Mockett *et al.*, 1987). IgA levels in tears were found to be better correlated with resisting IBV re-infection than serum antibodies (Toro and Fernandez, 1994), and this has since been recommended for antibody profiling of chicken flocks. The tear induction method used does not affect the levels of virus-specific IgG and IgA detected in SPF chickens (Ganapathy *et al.*, 2005).

Cell-mediated immunity

T-cells mediate cell-mediated immunity in the trachea following infection. $CD4^+$ and $CD8^+$ cells were demonstrated in tracheal sections (Kotani *et al.*, 2000). Despite the presence of T-cells, there is a debate on the prevalence of each of these cells, due to the different virus strain used in the study (Janse *et al.*, 1994; Raj and Jones, 1996b). Furthermore, T-cell suppression with cyclosporine resulted in higher virus titres in the kidneys compared with untreated birds, suggesting T-cells may play a role in kidney protection (Raj and Jones, 1997).

Memory T-cells can be detected in blood for no more than 10 weeks after infection, while virus-specific $CD8^+$ memory cells can protect syngeneic chicks from acute IBV infection (Pei *et al.*, 2003). *In vitro* stimulation of chicks with IBV antigen illustrated that B-cells can be activated to secrete antibody up to three weeks post infection (Pei and Collisson, 2005). Gene transcription profile of tracheal epithelial cells from three days post infection of chickens with an attenuated IBV Mass strain also confirmed that a diversity of innate immunity and helper type 1-T-cell-biased adaptive immunity are activated, which are responsible for the rapid virus clearance from local infection (Wang *et al.*, 2006).

In chickens experimentally challenged with IBV, the development of cell-meditated immune response has been correlated with effective virus clearance, reduction of clinical signs and resolution of lesions (Raggi and Lee, 1965; Collisson *et al.*, 2000). The $CD8^+$ cytotoxic T lymphocytes (CTLs) represent a good correlation for decreasing infection and correspond to a reduction of clinical

signs (Pei *et al.*, 2001). This was further illustrated by the transfer of CTLs obtained from the spleens of IBV-infected chickens to naive chicks, which protests chicks against a subsequent IBV challenge (Collisson *et al.*, 2000; Seo *et al.*, 2000). The clearance of IBV from the tracheal mucosa occurred at an early phase of infections and CTLs are thought to be involved in this clearance (Kotani *et al.*, 2000). To date, there are no reports pertaining to the tracheal mucosal leucocytes following live IBV vaccination. Nonetheless, analysis of tracheal samples of vaccinated and further challenged birds showed up-regulation of CTL genes in full-dose vaccinated birds at 24 hours post infection, indicating the development of cell-mediated immunity (Okino *et al.*, 2013). The cytotoxic mechanisms of these CTLs in cell-mediated immunity await further investigation.

Cytokines

Cytokines are secreted in response to T-cell mitogens such as concanavalin A (ConA) or specific antigens. Several studies have investigated the role of cytokines in IBV infections through alteration of cytokine profiles. Following *in ovo* administration of a potent TLR9 agonist CpG oligodeoxynucleotides (CpG ODN), significant differential up-regulation of IFN-γ, IL-8 and macrophage inflammatory protein (MIP)-1β genes and suppression of IL-6 expression were observed (Dar *et al.*, 2009). Furthermore, IBV can induce IFN-γ through polyclonal stimulation of chicken leucocytes (Ariaans *et al.*, 2009). A study on IBV T-strain infection of susceptible S-line and resistant HWL line showed that while IL-6 mRNA level was elevated in both lines at 4 hours post infection, it was 20 times higher in the S-line chickens than in the HWL-line (Asif *et al.*, 2007). Up-regulation of IL-6 and IL-8 was also observed in IBV-infected cells (Liao *et al.*, 2011).

Epizootiology

IBV on economic significance

Flock management and IBV variants involved play a major role in the economical outcome of the disease. In general, economical losses derived mainly from production efficiencies, such as poor feed conversion and reduced weight gain in broilers and sub-optimal egg production from layers and breeders. IBV can also exacerbate airsacculitis, leading to condemnation at processing plant (Martin *et al.*, 2007). For chicks which are infected by IBV at a young age, the infection can cause permanent damage to the oviduct (Crinion and Hofstad, 1972; Cavanagh and Naqi, 2003). While these future layers would mature like any other uninfected layers, they do not produce eggs. These 'false layers' may have consumed their full share in the food and housing without any return to the poultry grower.

Geographical distribution of IBV variants

The global distribution of IBV variants as of 2016 are grouped based on the continents to which they were discovered (Fig. 5.15). It is important to note that the incidence and distribution of IBV variants are complex and unpredictable. While some viruses, such as the Mass strain, are distributed worldwide, other IBV variants

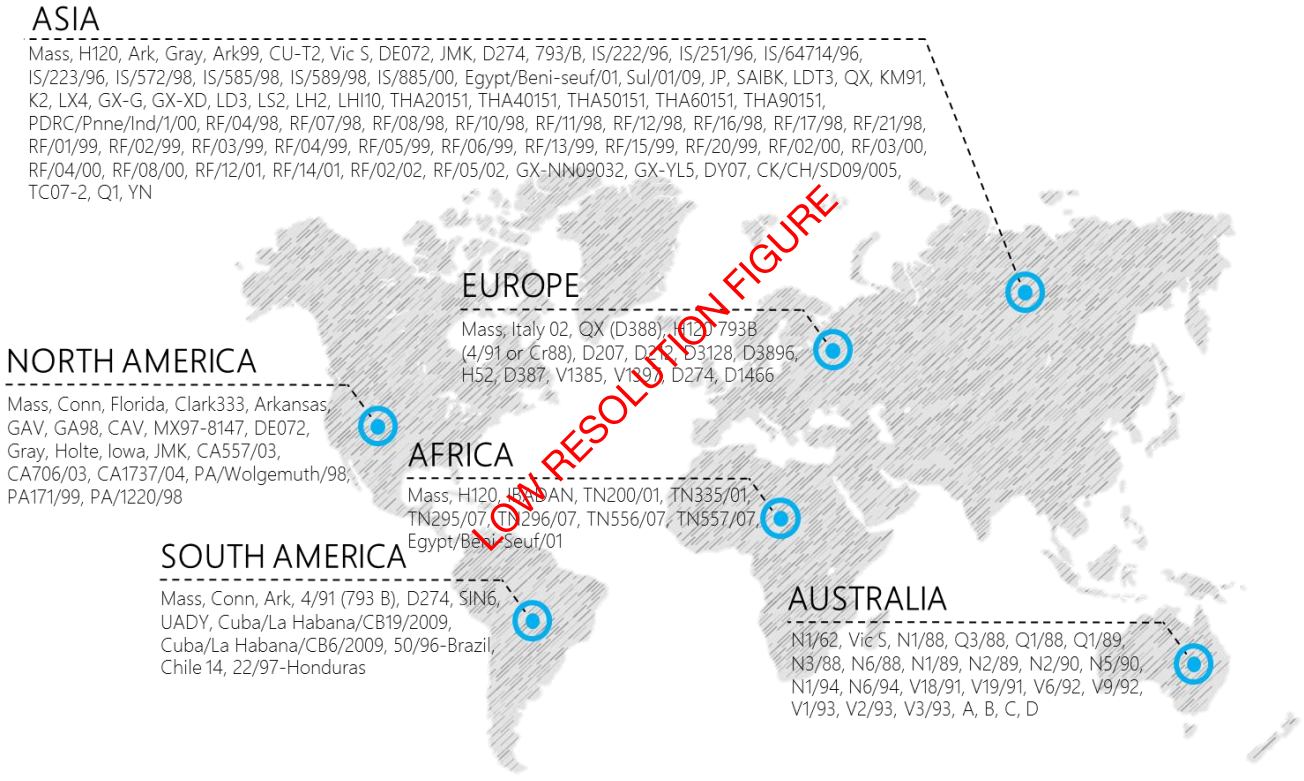

Figure 5.15 Global distribution of circulating infectious bronchitis virus (IBV) variants across continents.

are restricted to certain regions of the country (Arkansas) or unique to a continent (D274, Europe only). While many IBV variants have come and gone over the past four decades, some variants which have persisted for a long time still haunt the poultry industry, such as the Arkansas, California (cousin of Arkansas virus) and Delaware viruses (Jackwood, 2012).

Sources of infection, principal routes and duration of excretion

IBV is distributed worldwide, particularly in countries which have an intensive poultry industry. Being a highly infectious virus, the virus has a short incubation period of 36 hours and can spread rapidly in unvaccinated chickens within one to two days (Ignjatovic and Sapats, 2000). The major sources of IBV were from contaminated feed and drinking water, tracheal-bronchial exudate and faeces of chickens (ignjatovic and Sapats, 2000). Direct contact with these bodily fluids from infected chickens is the most likely source of infection. IBV can also spread horizontally via aerosol or ingestion.

While vertical transmission of the virus has been suspected in one study (McFerran *et al.*, 1971), it was recently demonstrated in two studies where viral RNA was detected in the allantoic fluid of viable embryos and infected eggs through natural infection and experimental inoculation, respectively (Cook, 1971; Pereira *et al.*, 2016). IBV was recovered from the semen of cockerels, and IBV RNA was detected in the trachea of hens artificially inseminated with semen of IBV infected roosters, providing experimental evidence for venereal transmission (Cook, 1971; Gallardo *et al.*, 2011).

For the respiratory forms of IBV, the virus is copiously shed from the respiratory tract of the birds and into the environment through coughing (Ignjatovic and Sapats, 2000). Thus, high titres of IBV can be recovered from the trachea and lungs of infected chickens from 1 to 7 days post infection. IBV can also be recovered from cloacal contents within 1 month post infection.

Methods of spread

Airborne transmission is the most common form of virus spread among chickens, houses and farms. Airborne transmission via aerosols can occur readily among birds kept within 1.5 m radius. Movement of live birds is another source of virus transmission, as it may introduce IBV to a different flock. Experimental evidence has also revealed IBV persistence and re-excretion as a potential risk factor for IB (Alexander and Gough, 1977).

Species susceptible to IBV infection

Apart from avian species, no other species are susceptible to natural IBV infection. However, IBV can be propagated in suckling mice, rabbits and guinea pigs when inoculated via the intracerebral route (McIntosh *et al.*, 1967). Even so, such virus passage only appears to result in the selection of a non-pathogenic strain for chicks (Yachida *et al.*, 1979).

Virus stability to environmental inactivation

IBV is temperature sensitive; most strains can be inactivated at temperatures of 56°C for a minimum 15 minutes to 45°C for 90 minutes (Cavanagh and Gelb, 2009). The virus will survive for only a few days at room temperature, at which their viral infectivity will exhibit a gradual decrease over time. On the other hand, virus residing in litter containing faeces can survive for a considerable amount of time (Animas *et al.*, 1994; de Wit *et al.*, 2010a). However, lyophilized virus can retain its infectivity for at least 21 months when stored at 4°C (Hofstad and Yoder, 1963). Commercially available common disinfectants can easily inactivate the virus (Bengtong *et al.*, 2013).

Risk and consequences of importing disease through poultry and associated products

IBV is listed as one of the avian diseases notifiable under the OIE list (World Organization for Animal Health, http://www.oie.int/en/animal-health-in-the-world/oie-listed-diseases-2017/), which implies that countries importing poultry should perform tests to minimize the risk of importing IBV into the country. While IBV is globally distributed, the introduction of an exotic strain can increase the genetic pool of viruses that circulate on site (Ignjatovic and Sapats, 2000; Toro *et al.*, 2015). This increases the likelihood of generating more and newer variants through spontaneous recombination (Toro *et al.*, 2015).

Diagnosis

Several laboratory tests are available to confirm diagnosis, and they can be divided into two broad categories – agent identification and detection of immune response.

Virus isolation and identification through antigen detection

Confirmation of IB is often based on serology-assisted virus isolation, and this is usually performed on 9- to 10-day-old embryonated SPF chicken eggs. Typical IBV clinical signs include lesions such as curling and dwarfing of the embryos, clubbing of the down or urate deposits in the kidneys 5 to 7 days post inoculation (Momayez *et al.*, 2002). Conversely, IBV can also be isolated from TOCs within 48 to 72 hours post inoculation, through the visualization of ciliostasis and damage to the tracheal epithelium under microscopy (Nicholas *et al.*, 1983). Immunofluorescence test containing fluorescein-conjugated antibodies that bind to IBV in tracheal smears is an alternative method of isolating the virus through detection of fluorescent signals (Yagyu and Ohta, 1990; Ahmed *et al.*, 2007).

Virus isolation and identification through genome detection

CAMs from infected eggs are first homogenized and subjected to tests such as immunodiffusion, immuno-histochemistry or RT-PCR (Hironao *et al.*, 1970; Jackwood *et al.*, 1992; Abdel-Moneim *et al.*, 2009). In addition to these methods, genetic based tests such as RT-PCR and RT-RFLP (reverse transcription restriction fragment length polymorphism) are commonly used to identify IBV isolates (Song *et al.*, 1998; Chousalkar *et al.*, 2009). Cells present in the allantoic fluid of infected eggs may also be tested for IBV using fluorescent antibody tests, RT-PCR and dot

hybridization assays (Clarke *et al.*, 1972; Jackwood *et al.*, 1992). For direct visualization of IBV in allantoic fluid or TOC fluid, direct negative-contrast electron microscopy and immunofluorescence staining can also be used to observe any viral particles displaying typical CoV morphology (Bhattacharjee *et al.*, 1994; Liu *et al.*, 2006).

Serotype identification and serological tests

Traditionally, serotyping of IBV field isolates were performed by HI and VN tests in embryonated chicks, TOCs and cell cultures (King and Hopkins, 1984; Villarreal, 2010). Using monoclonal antibodies (mABs) in ELISA has also been proven valuable in differentiating and grouping IBV strains (Koch *et al.*, 1990; Karaca *et al.*, 1992). The drawbacks in the adoption of mAbs for serotype definition are the availability of mAbs or hybridomas and the constant need to produce specific mAbs to keep pace with the ever-growing emergence of new IBV serotypes (Karaca *et al.*, 1992).

There are four serological tests available to test for IBV, that is, VN, HI, ELISA and agar gel immunodiffusion (AGID). Harvesting serum samples from blood at specific intervals, for instance one at the onset of disease and another weeks later provides the basis for serological diagnosis (De Wit, 2010b). Each serological test has its own merits and demerits in terms of practicality, specificity, sensitivity and cost (de Wit, 2000).

Virus neutralization

VN is the serological method of choice for differentiating different IBV serotypes as well as identifying new serotypes due to its high accuracy and sensitivity (de Wit, 2000). To perform VN, a culture of each IBV of interest and its corresponding monospecific antiserum are required, especially if accurate differentiation of serotypes is desired. The VN test begins by inoculating intranasally to a group of SPF chickens with one of the IBV serotypes of interest and the chicken blood is collected approximately three to four weeks later. The serum from the blood would contain the serotype specific antibodies to the IB serotypes inoculated.

Two methods, by either testing one dilution of each antiserum against varying dilutions of virus or testing one dilution of virus against varying dilutions of antiserum, have been adopted to estimate neutralizing antibodies (Hesselink, 1991). The second one is more widely used neutralization test for chicken embryos and TOCs. By estimating the titre of each IBV against the serum of the homologous and heterologous IBV serotype, it is possible to designate a field isolate to be a new variant or it is related to a known IBV serotype since the higher the titre indicates greater relationship between the IBVs (Hesselink, 1991).

Haemagglutination inhibition

The HI test is a much simpler and quicker alternative to the VN test, and strong correlation between VN and HI tests has been demonstrated in vaccinated SPF chickens following M41 challenge (Park *et al.*, 2016). A standard protocol for HI test for IBV has been described (Villarreal, 2010). As IBV does not spontaneously agglutinate chicken red blood cells (RBCs), it needs to be pre-treated with neuraminidase prior to the HI test. The antigen for the HI test is prepared mainly from IBV-laden allantoic fluids (Ruano *et al.*, 2000).

Enzyme-linked immunosorbent assay

ELISA is a more sensitive serological diagnostic method in comparison to other tests, attributing to its fast reaction time and high antibody titres (Monreal *et al.*, 1985; Thayer *et al.*, 1987). Although this assay lacks serotype or strain specificity, it is valuable as a flock test for monitoring vaccination responses under field conditions, or to give an indication of a recent or recurrent IB infection. Many commercial ELISA kits are available based on different detection strategies of IBV antibodies. In ELISA, virus antigens are attached to the bottom of a 96-well plate, specific antibodies in serum from suspected chickens are then applied over the surface to allow it to bind to the antigen. Since the antibody is often linked to an enzyme, a detectable signal can be measured following addition of an enzyme substrate.

Agar gel immunodiffusion

For this test, two holes are punched in an agar gel and incubated with known IBV antigen and sera from suspected chickens. Should the antigen react with the IBV-specific antibodies, antigen precipitation will occur as they migrate through the gel, displaying a visible line in the gel. While this test is quick and easy to perform, it is not serotype specific and appears to lack sensitivity since the presence and duration required for detection of precipitating antibodies may vary between individual chickens (de Wit, 2000).

Genotype identification

IBV molecular typing is now routinely conducted by RT-PCR, followed by sequence analysis of the S glycoprotein or the S1 subunit of the S glycoprotein, where the HVRs that correlate with the IBV serotype can be found. Basic Local Alignment Search Tool, or BLAST, can be utilized to search for similar sequence in GenBank (http://www.ncbi.nlm.nih.gov/) and phylogenetic trees of the virus can be constructed to see how closely the IBV strains are related to each other (Valastro *et al.*, 2016).

An alternative to multiple IBV genotype identification is the S1 genotype-specific RT-PCR. S1 gene primers specific for several genotypes such as Mass, Ark, Conn, De and JMK have been developed and described (Meir *et al.*, 2010; Maier *et al.*, 2013; Roh *et al.*, 2014) and may be used in conjunction with a universal primer that amplifies all IBV genotypes (Adzhar *et al.*, 1996). Other primer sets may be used, depending on the circulating IBV serotypes in the region. By far, nucleotide sequencing of the S1 gene is the most useful technique in differentiating IBV strains and is routinely utilized in many laboratories. Through RT-PCR product cycle sequencing of the

S1 HVR, recognized field isolates and variants can now be identified and referenced to previously unknown field isolates and variants in establishing potential relatedness (Kingham *et al.*, 2000). Sequencing of a conserved region of the 3′UTR of the IBV genome revealed that CoVs isolated from turkey and pheasants are 90% genetically similar to IBV (Cavanagh *et al.*, 2001, 2002).

Prevention and control

Exclusion and eradication

Given the highly infectious nature of the virus, basic management practices such as ensuring personal hygiene, limited site access and separate footwear and equipment for each site/house can all minimize IBV and disease spread. However, it is important to note even with the strictest preventative measures in place, it is impossible to fully eradicate IB in countries which have an intensive poultry industry. Flock management also plays a major role in preventing IBV from being passed on from the older flocks to the younger replacements. With an 'all-in/all-out' system, poultry grower can clean and disinfect sites/houses between batches and limit the level of infection to a minimum. This system also provides at least two economic benefits, which include an increase in egg production and simplification of vaccination schedule, since each batch of chickens are of the same age and can be on the same vaccination schedule (Dhama *et al.*, 2014).

Breeding to increase resistance

It is possible to protect chickens against IBV by 'controlled exposure' – exposing chickens to attenuated IBV and letting it spread naturally though the rest of the flock (Cook *et al.*, 2012). Albeit a crude method, breeding to increase resistance to IBV is effective as it provides maternal antibodies to progeny chicks (Cook *et al.*, 2012). However, the outcome of infection may differ among different lines, and therefore it is not practised in the poultry industry.

Vaccination

IBV vaccines are produced by virus passage in embryonated eggs, and they come in two types, namely the live-attenuated and inactivated vaccines. Each has an intended use for broilers (live attenuated) and layers and breeders (inactivated), respectively (Ladman *et al.*, 2002; Jackwood *et al.*, 2009). More recently, molecular vaccines are emerging as the third type of IBV vaccines.

Live-attenuated vaccines

Live vaccines have been widely used against IBV from as early as the 1970s, with the live attenuated M41 most widely used worldwide (Gelb *et al.*, 1991; Cook *et al.*, 1999). Live vaccines work by reducing the virulence through passage in chicken embryonated eggs. They are administered in masses either through coarse spray, aerosol or drinking water, depending on the live vaccine used (Gough and Alexander, 1979; Ratanasethakul and Cumming, 1983b; Martin *et al.*, 2007), although the oculonasal route is deemed to be the ideal route of vaccination (De Wit, 2010b). To boost the immunity of chicks through live vaccines, vaccination programs at the site/house usually comprises of two vaccinations, the first dose with a low-virulence, or mild vaccine in day-old chicks, followed by a more virulent vaccine approximately seven to ten days after as a booster dose given in drinking water (Ignjatovic and Sapats, 2000).

Inactivated vaccines

Inactivated vaccines, unlike live vaccines, can deliver high and uniform doses of antibody in pullets that persists for an extended period, resulting in long-lasting immunity (Dhama *et al.*, 2014). To harness the full potential of inactivated vaccines, the only prerequisite is that layers and breeders between 13 and 18 weeks of age must be previously primed properly with live vaccines. In addition, the interval between the live and inactivated vaccines should be between four to six weeks to obtain the highest titre of antibodies.

The benefit of inactivated vaccines lies particularly in the absence of vaccinal reactions and the ability in providing protection for the internal organs by preventing virus spread. Practically, they could also provide protection against egg reduction which might not always be afforded by the live vaccines (Box *et al.*, 1980). The only disadvantage of inactivated vaccines is the cost and the need to administer each fowl individually via subcutaneous route.

Molecular vaccines

In recent years, biotechnology research aimed at developing new IBV vaccines has produced a new class of vaccine, known as molecular vaccines (Kapczynski *et al.*, 2003; Cook *et al.*, 2012). Including subunit- and DNA-vaccines, virus-like particles and recombinant vaccine vectors, these molecular vaccines have each been tested for its efficacy against IBV and had displayed remarkable potential for their use in the future (Cook *et al.*, 2012). In one case, a recombinant vaccine developed by replacing the ectodomain of the S1 gene of IBV Beaudette provided 80% of immune protection against M41 challenge in young chicks (Wei *et al.*, 2014).

Perspectives

Despite major breakthroughs in IBV research, many fundamental problems remain to be resolved by future studies. One critical question would be to understand the viral determinants that control virulence and immunogenicity of IBV. More systematic comparison and swapping of sequences between IBV Beaudette strain and a virulent strain using the available reverse genetics tools would be a useful approach to address this issue. However, this effort has been partially hampered by the lack of a robust cell culture system for most IBV isolates. The second issue would be then to establish a reliable cell culture system for IBV field isolates. While most laboratory-based molecular biology studies are conducted in cells or chicken embryos infected with the Beaudette strain, this chicken embryo- and cultured cell-adapted IBV is highly attenuated in terms of both pathogenicity and immunogenicity and has lost infectivity to young chicks. It would be ideal if comparative studies would be readily carried out with a virulent strain in parallel experiments in cells and in embryonated eggs. Such a cell culture system would be used to replace or complement the current practice of relying on embryonated eggs for vaccine production, a technology that has been used for over half a century. A third area of importance would lie in

the development of vaccines against emerging IBV variants. Rapid development of a specific, reliable, tailored vaccine against each new variant of importance would be achievable with the advances of molecular genetics approaches over the past decades and further identification and characterization of viral virulence and antigenicity determinants. Another question is concerned with the evolution and geographical distribution of IBV variants: how do some IBV variants have a worldwide distribution, while others are localized? Are there wild bird reservoirs which could enable the virus to transmit over a long distance? Finally, there is no standardized nomenclature in naming new IBV variants, which has caused confusion within the community. As an effort to define and develop a standardized nomenclature and classification of avian coronaviruses (AvCoV), the European Union COST Action FA1207 has recommended the following nomenclature for AvCoV specimens and isolates: CoV/Genus/AvCoV/host/country/specimen id/year (Ducatez and European Union COST Action FA1207, 2016).

In the past 30 or so years, we have witnessed the emergence and extensive use of molecular cell biology tools to study the mechanisms behind the replication and pathogenesis of IBV, IBV–host interactions and host cell responses to IBV infection. Future research on IBV remains crucial to decipher many aspects of viral replication mechanisms and pathogenesis. Currently, many nsps and accessory proteins encoded by IBV remain uncharacterized. Solving the crystal structures of these proteins could aid in defining their functional roles in viral replication, which may lead to the identification of novel therapeutic targets. Knowledge derived from such studies will be important for future understanding and control of the disease caused by existing and emerging IBV variants.

Acknowledgements

This work was partially supported by an Academic Research Fund (AcRF) Tier 2 grant (ACR47/14), Ministry of Education, Singapore, and by Guangdong Province Key Laboratory of Microbial Signals and Disease Control grant MSDC-2017-05 and MSDC-2017-06, Guangdong, People's Republic of China.

References

Abdel-Moneim, A.S., Zlotowski, P., Veits, J., Keil, G.M., and Teifke, J.P. (2009). Immunohistochemistry for detection of avian infectious bronchitis virus strain M41 in the proventriculus and nervous system of experimentally infected chicken embryos. Virol. J. *6*, 15. https://doi.org/10.1186/1743-422X-6-15

Abd El Rahman, S., El-Kenawy, A.A., Neumann, U., Herrler, G., and Winter, C. (2009). Comparative analysis of the sialic acid binding activity and the tropism for the respiratory epithelium of four different strains of avian infectious bronchitis virus. Avian Pathol. *38*, 41–45. https://doi.org/10.1080/03079450802632049

Abraham, S.M., and Clark, A.R. (2006). Dual-specificity phosphatase 1: a critical regulator of innate immune responses. Biochem. Soc. Trans. *34*, 1018–1023.

Abro, S.H., Renström, L.H., Ullman, K., Belák, S., and Baule, C. (2012). Characterization and analysis of the full-length genome of a strain of the European QX-like genotype of infectious bronchitis virus. Arch. Virol. *157*, 1211–1215. https://doi.org/10.1007/s00705-012-1284-0

Adams, N.R., and Hofstad, M.S. (1971). Isolation of transmissible enteritis agent of turkeys in avian embryos. Avian Dis. *15*, 426–433.

Adzhar, A., Shaw, K., Britton, P., and Cavanagh, D. (1996). Universal oligonucleotides for the detection of infectious bronchitis virus by the polymerase chain reaction. Avian Pathol. *25*, 817–836.

Afanador, G., and Roberts, J.R. (1994). Effect of nephropathogenic infectious bronchitis viruses on renal function in young male broiler chickens. Br. Poult. Sci. *35*, 445–456. https://doi.org/10.1080/00071669408417709

Ahmed, H.N. (1954). Incidence and treatment of some infectious viral respiratory diseases of poultry in Egypt. PhD Thesis. Faculty of Veterinary Medicine, Cairo University, Egypt.

Ahmed, Z., Naeem, K., and Hameed, A. (2007). Detection and seroprevalence of infectious bronchitis virus strains in commercial poultry in Pakistan. Poult. Sci. *86*, 1329–1335.

Akira, S. (2001). Toll-like receptors and innate immunity. Adv. Immunol. *78*, 1–56.

Akira, S., Uematsu, S., and Takeuchi, O. (2006). Pathogen recognition and innate immunity. Cell *124*, 783–801.

Albassam, M.A., Winterfield, R.W., and Thacker, H.L. (1986). Comparison of the nephropathogenicity of four strains of infectious bronchitis virus. Avian Dis. *30*, 468–476.

Alexander, D.J., and Collins, M.S. (1975). Effect of pH on the growth and cytopathogenicity of avian infectious bronchitis virus in chick kidney cells. Arch. Virol. *49*, 339–348.

Alexander, D.J., and Gough, R.E. (1977). Isolation of avian infectious bronchitis virus from experimentally infected chickens. Res. Vet. Sci. *23*, 344–347.

Alexopoulou, L., Holt, A.C., Medzhitov, R., and Flavell, R.A. (2001). Recognition of double-stranded RNA and activation of NF-kappaB by Toll-like receptor 3. Nature *413*, 732–738. https://doi.org/10.1038/35099560

Almazán, F., González, J.M., Pénzes, Z., Izeta, A., Calvo, E., Plana-Durán, J., and Enjuanes, L. (2000). Engineering the largest RNA virus genome as an infectious bacterial artificial chromosome. Proc. Natl. Acad. Sci. U.S.A. *97*, 5516–5521.

Almazán, F., Galán, C., and Enjuanes, L. (2004). The nucleoprotein is required for efficient coronavirus genome replication. J. Virol. *78*, 12683–12688.

Almazán, F., Dediego, M.L., Galán, C., Escors, D., Alvarez, E., Ortego, J., Sola, I., Zuñiga, S., Alonso, S., Moreno, J.L., *et al.* (2006). Construction of a severe acute respiratory syndrome coronavirus infectious cDNA clone and a replicon to study coronavirus RNA synthesis. J. Virol. *80*, 10900–10906.

Almazán, F., Márquez-Jurado, S., Nogales, A., and Enjuanes, L. (2015). Engineering infectious cDNAs of coronavirus as bacterial artificial chromosomes. Methods Mol. Biol. *1282*, 135–152. https://doi.org/10.1007/978-1-4939-2438-7_13

Almeida, M.S., Johnson, M.A., Herrmann, T., Geralt, M., and Wüthrich, K. (2007). Novel beta-barrel fold in the nuclear magnetic resonance structure of the replicase nonstructural protein 1 from the severe acute respiratory syndrome coronavirus. J. Virol. *81*, 3151–3161.

Alonso-Caplen, F.V., Matsuoka, Y., Wilcox, G.E., and Compans, R.W. (1984). Replication and morphogenesis of avian coronavirus in Vero cells and their inhibition by monensin. Virus Res. *1*, 153–167.

Alvarado, I.R., Villegas, P., Mossos, N., and Jackwood, M.W. (2005). Molecular characterization of avian infectious bronchitis virus strains isolated in Colombia during 2003. Avian Dis. *49*, 494–499. https://doi.org/10.1637/7202-050304R.1

Amarasinghe, A., Abdul-Cader, M.S., Almatrouk, Z., van der Meer, F., Cork, S.C., Gomis, S., and Abdul-Careem, M.F. (2018). Induction of innate host responses characterized by production of interleukin (IL)-1β and recruitment of macrophages to the respiratory tract of chickens following infection with infectious bronchitis virus (IBV). Vet. Microbiol. *215*, 1–10.

Ambali, A.G., and Jones, R.C. (1990). Early pathogenesis in chicks of infection with an enterotropic strain of infectious bronchitis virus. Avian Dis. *34*, 809–817.

Ammayappan, A., and Vakharia, V.N. (2009). Complete nucleotide analysis of the structural genome of the infectious bronchitis virus strain md27 reveals its mosaic nature. Viruses *1*, 1166–1177. https://doi.org/10.3390/v1031166

Anand, K., Palm, G.J., Mesters, J.R., Siddell, S.G., Ziebuhr, J., and Hilgenfeld, R. (2002). Structure of coronavirus main proteinase reveals combination

of a chymotrypsin fold with an extra alpha-helical domain. EMBO J. *21*, 3213–3224. https://doi.org/10.1093/emboj/cdf327

Angelini, M.M., Akhlaghpour, M., Neuman, B.W., and Buchmeier, M.J. (2013). Severe acute respiratory syndrome coronavirus nonstructural proteins 3, *4*, and 6 induce double-membrane vesicles. MBio *4*, e00524–13. https://doi.org/10.1128/mBio.00524-13

Animas, S.B., Otsuki, K., Hanayama, M., Sanekata, T., and Tsubokura, M. (1994). Experimental infection with avian infectious bronchitis virus (Kagoshima-34 strain) in chicks at different ages. J. Vet. Med. Sci. *56*, 443–447.

Ariaans, M.P., van de Haar, P.M., Hensen, E.J., and Vervelde, L. (2009). Infectious bronchitis virus induces acute interferon-gamma production through polyclonal stimulation of chicken leukocytes. Virology *385*, 68–73. https://doi.org/10.1016/j.virol.2008.11.021

Armesto, M., Cavanagh, D., and Britton, P. (2009). The replicase gene of avian coronavirus infectious bronchitis virus is a determinant of pathogenicity. PLOS ONE *4*, e7384. https://doi.org/10.1371/journal.pone.0007384

Armstrong, J., Niemann, H., Smeekens, S., Rottier, P., and Warren, G. (1984). Sequence and topology of a model intracellular membrane protein, E1 glycoprotein, from a coronavirus. Nature *308*, 751–752.

Asif, M., Lowenthal, J.W., Ford, M.E., Schat, K.A., Kimpton, W.G., and Bean, A.G. (2007). Interleukin-6 expression after infectious bronchitis virus infection in chickens. Viral Immunol. *20*, 479–486. https://doi.org/10.1089/vim.2006.0109

Awad, F., Baylis, M., and Ganapathy, K. (2014). Detection of variant infectious bronchitis viruses in broiler flocks in Libya. Int. J. Vet. Sci. Med. *2*, 78–82.

Awad, F., Forrester, A., Baylis, M., Lemiere, S., Ganapathy, K., Hussien, H.A., and Capua, I. (2015). Protection conferred by live infectious bronchitis vaccine viruses against variant Middle East IS/885/00-like and IS/1494/06-like isolates in commercial broiler chicks. Vet. Rec. Open *2*, e000111. https://doi.org/10.1136/vetreco-2014-000111

Babcock, A.A., Toft-Hansen, H., and Owens, T. (2008). Signalling through MyD88 regulates leukocyte recruitment after brain injury. J. Immunol. *181*, 6481–6490.

Baliji, S., Cammer, S.A., Sobral, B., and Baker, S.C. (2009). Detection of nonstructural protein 6 in murine coronavirus-infected cells and analysis of the transmembrane topology by using bioinformatics and molecular approaches. J. Virol. *83*, 6957–6962. https://doi.org/10.1128/JVI.00254-09

Bande, F., Arshad, S.S., Omar, A.R., Bejo, M.H., Abubakar, M.S., and Abba, Y. (2016). Pathogenesis and diagnostic approaches of avian infectious bronchitis. Adv. Virol. *2016*, 4621659. https://doi.org/10.1155/2016/4621659

Baranov, P.V., Henderson, C.M., Anderson, C.B., Gesteland, R.F., Atkins, J.F., and Howard, M.T. (2005). Programmed ribosomal frameshifting in decoding the SARS-CoV genome. Virology *332*, 498–510.

Barber, G.N. (2011). Innate immune DNA sensing pathways: STING, AIMII and the regulation of interferon production and inflammatory responses. Curr. Opin. Immunol. *23*, 10–20. https://doi.org/10.1016/j.coi.2010.12.015

Barber, M.R., Aldridge, J.R., Webster, R.G., and Magor, K.E. (2010). Association of RIG-I with innate immunity of ducks to influenza. Proc. Natl. Acad. Sci. U.S.A. *107*, 5913–5918. https://doi.org/10.1073/pnas.1001755107

Barrette-Ng, I.H., Ng, K.K., Mark, B.L., Van Aken, D., Cherney, M.M., Garen, C., Kolodenko, Y., Gorbalenya, A.E., Snijder, E.J., and James, M.N. (2002). Structure of arterivirus nsp4. The smallest chymotrypsin-like proteinase with an alpha/beta C-terminal extension and alternate conformations of the oxyanion hole. J. Biol. Chem. *277*, 39960–39966. https://doi.org/10.1074/jbc.M206978200

Bayry, J., Goudar, M.S., Nighot, P.K., Kshirsagar, S.G., Ladman, B.S., Gelb, J., Ghalsasi, G.R., and Kolte, G.N. (2005). Emergence of a nephropathogenic avian infectious bronchitis virus with a novel genotype in India. J. Clin. Microbiol. *43*, 916–918.

Beall, A., Yount, B., Lin, C.M., Hou, Y., Wang, Q., Saif, L., and Baric, R. (2016). Characterization of a pathogenic full-length cDNA clone and transmission model for porcine epidemic diarrhea virus strain PC22A. MBio *7*, e01451–15. https://doi.org/10.1128/mBio.01451-15

Bechill, J., Chen, Z., Brewer, J.W., and Baker, S.C. (2008). Coronavirus infection modulates the unfolded protein response and mediates sustained translational repression. J. Virol. *82*, 4492–4501. https://doi.org/10.1128/JVI.00017-08

Becker, M.M., Graham, R.L., Donaldson, E.F., Rockx, B., Sims, A.C., Sheahan, T., Pickles, R.J., Corti, D., Johnston, R.E., Baric, R.S., *et al.* (2008). Synthetic recombinant bat SARS-like coronavirus is infectious in cultured cells and in mice. Proc. Natl. Acad. Sci. U.S.A. *105*, 19944–19949. https://doi.org/10.1073/pnas.0808116105

Becker, W.B., McIntosh, K., Dees, J.H., and Chanock, R.M. (1967). Morphogenesis of avian infectious bronchitis virus and a related human virus (strain 229E). J. Virol. *1*, 1019–1027.

Beese, L.S., and Steitz, T.A. (1991). Structural basis for the 3'-5' exonuclease activity of escherichia coli DNA polymerase I: a two metal ion mechanism. EMBO J. *10*, 25–33.

Belouzard, S., Chu, V.C., and Whittaker, G.R. (2009). Activation of the SARS coronavirus spike protein via sequential proteolytic cleavage at two distinct sites. Proc. Natl. Acad. Sci. U.S.A. *106*, 5871–5876. https://doi.org/10.1073/pnas.0809524106

Belouzard, S., Millet, J.K., Licitra, B.N., and Whittaker, G.R. (2012). Mechanisms of coronavirus cell entry mediated by the viral spike protein. Viruses *4*, 1011–1033. https://doi.org/10.3390/v4061011

Benedict, C.A., Norris, P.S., and Ware, C.F. (2002). To kill or be killed: viral evasion of apoptosis. Nat. Immunol. *3*, 1013–1018. https://doi.org/10.1038/ni1102-1013

Bengtong, P., Thomrongsuwannakij, T., and Chansiripornchai, N. (2013). Inactivation of infectious bronchitis virus with various kinds of disinfectants. Thai J. Vet. Med. *43*, 405–409.

Bentley, K., Keep, S.M., Armesto, M., and Britton, P. (2013). Identification of a noncanonically transcribed subgenomic mRNA of infectious bronchitis virus and other gammacoronaviruses. J. Virol. *87*, 2128–2136. https://doi.org/10.1128/JVI.02967-12

Benyeda, Z., Mató, T., Süveges, T., Szabó, E., Kardi, V., Abonyi-Tóth, Z., Rusvai, M., and Palya, V. (2009). Comparison of the pathogenicity of QX-like, M41 and 793/B infectious bronchitis strains from different pathological conditions. Avian Pathol. *38*, 449–456. https://doi.org/10.1080/03079450903349196

Bezuidenhout, A., Mondal, S.P., and Buckles, E.L. (2011). Histopathological and immunohistochemical study of air sac lesions induced by two strains of infectious bronchitis virus. J. Comp. Pathol. *145*, 319–326. https://doi.org/10.1016/j.jcpa.2011.01.011

Bhardwaj, K., Sun, J., Holzenburg, A., Guarino, L.A., and Kao, C.C. (2006). RNA recognition and cleavage by the SARS coronavirus endoribonuclease. J. Mol. Biol. *361*, 243–256.

Bhattacharjee, P.S., Naylor, C.J., and Jones, R.C. (1994). A simple method for immunofluorescence staining of tracheal organ cultures for the rapid identification of infectious bronchitis virus. Avian Pathol. *23*, 471–480.

Bickerton, E., Maier, H.J., Stevenson-Leggett, P., Armesto, M., and Britton, P. (2018). The S2 Subunit of Infectious Bronchitis Virus Beaudette Is a Determinant of Cellular Tropism. J. Virol. *92*, e01044–18.

Bijanzad, P., Momayez, R., Mohammad, H.B.F., Mohammad, H.H., Mahmoodzadeh, M., Moghaddam, A.R.J., Kaboli, K., Azizpour, A., and Esharatabadi, F. (2013). Clinical evaluation of SPF chickens infected with 793/B serotype of Infectious Bronchitis virus. Eur. J. Exp. Biol. *3*, 226-230.

Bisgaard, M. (1976). [The influence of infectious bronchitis virus on egg production, fertility, hatchability and mortality rate in chickens (author's transl).] Nord. Vet. Med. *28*, 368–376. [99]

Boltz, D.A., Nakai, M., and Bahra, J.M. (2004). Avian infectious bronchitis virus: a possible cause of reduced fertility in the rooster. Avian Dis. *48*, 909–915. https://doi.org/10.1637/7192-040808R1

Bos, E.C., Luytjes, W., van der Meulen, H.V., Koerten, H.K., and Spaan, W.J. (1996). The production of recombinant infectious DI-particles of a murine coronavirus in the absence of helper virus. Virology *218*, 52–60.

Boscarino, J.A., Logan, H.L., Lacny, J.J., and Gallagher, T.M. (2008). Envelope protein palmitoylations are crucial for murine coronavirus assembly. J. Virol. *82*, 2989–2999. https://doi.org/10.1128/JVI.01906-07

Bosch, B.J., van der Zee, R., de Haan, C.A., and Rottier, P.J. (2003). The coronavirus spike protein is a class I virus fusion protein: structural and functional characterization of the fusion core complex. J. Virol. *77*, 8801–8811.

Bosch, B.J., de Haan, C.A., and Rottier, P.J. (2004). Coronavirus spike glycoprotein, extended at the carboxy terminus with green fluorescent protein, is assembly competent. J. Virol. *78*, 7369–7378. https://doi.org/10.1128/JVI.78.14.7369-7378.2004

Bosch, B.J., Bartelink, W., and Rottier, P.J. (2008). Cathepsin L functionally cleaves the severe acute respiratory syndrome coronavirus class I fusion protein upstream of rather than adjacent to the fusion peptide. J. Virol. *82*, 8887–8890. https://doi.org/10.1128/JVI.00415-08

Bouvet, M., Lugari, A., Posthuma, C.C., Zevenhoven, J.C., Bernard, S., Betzi, S., Imbert, I., Canard, B., Guillemot, J.C., Lécine, P., *et al.* (2014). Coronavirus Nsp10, a critical co-factor for activation of multiple replicative enzymes. J. Biol. Chem. *289*, 25783–25796. https://doi.org/10.1074/jbc.M114.577353

Box, P.G., Beresford, A.V., and Roberts, B. (1980). Protection of laying hens against infectious bronchitis with inactivated emulsion vaccines. Vet. Rec. *106*, 264–268.

Box, P.G., Holmes, H.C., Finney, P.M., and Froymann, R. (1988). Infectious bronchitis in laying hens: the relationship between haemagglutination inhibition antibody levels and resistance to experimental challenge. Avian Pathol. *17*, 349–361.

Brentano, L., Klein, T.A.P., Jaenisch, F.R., Back, A., and Castro, A.G.M. (2005). Isolamento do vírus de bronquite infecciosa das aves de surtos da doença associada a lesões atípicas de miopatia de músculo peitoral. Braz. J. Poult. Sci. *7*, 232.

Brierley, I., Boursnell, M.E., Binns, M.M., Bilimoria, B., Blok, V.C., Brown, T.D., and Inglis, S.C. (1987). An efficient ribosomal frame-shifting signal in the polymerase-encoding region of the coronavirus IBV. EMBO J. *6*, 3779–3785.

Brierley, I., Digard, P., and Inglis, S.C. (1989). Characterization of an efficient coronavirus ribosomal frameshifting signal: requirement for an RNA pseudoknot. Cell *57*, 537–547.

Britton, P., Green, P., Kottier, S., Mawditt, K.L., Penzes, Z., Cavanagh, D., and Skinner, M.A. (1996). Expression of bacteriophage T7 RNA polymerase in avian and mammalian cells by a recombinant fowlpox virus. J. Gen. Virol. *77*, 963–967. https://doi.org/10.1099/0022-1317-77-5-963

Britton, P., Evans, S., Dove, B., Davies, M., Casais, R., and Cavanagh, D. (2005). Generation of a recombinant avian coronavirus infectious bronchitis virus using transient dominant selection. J. Virol. Methods *123*, 203–211.

Britton, P., Armesto, M., Cavanagh, D., and Keep, S. (2012). Modification of the avian coronavirus infectious bronchitis virus for vaccine development. Bioeng. Bugs *3*, 114–119. https://doi.org/10.4161/bbug.18983

Broadfoot, D.I., Pomeroy, B.S., and Smith, W.M. Jr. (1956). Effects of infectious bronchitis in baby chicks. Poult. Sci. *35*, 757–762.

Brown, C.G., Nixon, K.S., Senanayake, S.D., and Brian, D.A. (2007). An RNA stem-loop within the bovine coronavirus nsp1 coding region is a cis-acting element in defective interfering RNA replication. J. Virol. *81*, 7716–7724.

Brown, T.D., Boursnell, M.E., and Binns, M.M. (1984). A leader sequence is present on mRNA A of avian infectious bronchitis virus. J. Gen. Virol. *65*, 1437–1442. https://doi.org/10.1099/0022-1317-65-8-1437

Callison, S.A., Jackwood, M.W., and Hilt, D.A. (2001). Molecular characterization of infectious bronchitis virus isolates foreign to the United States and comparison with United States isolates. Avian Dis. *45*, 492–499.

Casais, R., Thiel, V., Siddell, S.G., Cavanagh, D., and Britton, P. (2001). Reverse genetics system for the avian coronavirus infectious bronchitis virus. J. Virol. *75*, 12359–12369.

Casais, R., Dove, B., Cavanagh, D., and Britton, P. (2003). Recombinant avian infectious bronchitis virus expressing a heterologous spike gene demonstrates that the spike protein is a determinant of cell tropism. J. Virol. *77*, 9084–9089.

Casais, R., Davies, M., Cavanagh, D., and Britton, P. (2005). Gene 5 of the avian coronavirus infectious bronchitis virus is not essential for replication. J. Virol. *79*, 8065–8078.

Cavanagh, D. (1983). Coronavirus IBV glycopolypeptides: size of their polypeptide moieties and nature of their oligosaccharides. J. Gen. Virol. *64*, 1187–1191.

Cavanagh, D. (1995). The coronavirus surface glycoprotein. In The Coronaviridae, S.G. Siddell, ed. (Plenum Press, New York, NY).

Cavanagh, D. (2003). Severe acute respiratory syndrome vaccine development: experiences of vaccination against avian infectious bronchitis coronavirus. Avian Pathol. *32*, 567–582. https://doi.org/10.1080/0307945031000162119 8

Cavanagh, D. (2007). Coronavirus avian infectious bronchitis virus. Vet. Res. *38*, 281–297.

Cavanagh, D., and Gelb, J. Jr. (2009). Infectious Bronchitis. In Diseases of Poultry 12th edn, Y.M. Saif, A.M. Fadly, J.R. Glisson, L.R. McDougald, L.K. Nolan and D.E. Swayne, eds. (John Wiley & Sons, New York, NY), pp. 117–136.

Cavanagh, D., and Naqi, S.A. (2003). Infectious bronchitis. In Diseases of Poultry, 11th edn, Y.M. Saif, H.J. Barnes, A. Fadly, J.R. Glisson, L.R. McDougald and D.E. Swayne, eds (Iowa State University Pressm Ames, IA), pp. 101–120.

Cavanagh, D., Davis, P.J., Pappin, D.J., Binns, M.M., Boursnell, M.E., and Brown, T.D. (1986). Coronavirus IBV: partial amino terminal sequencing of spike polypeptide S2 identifies the sequence Arg-Arg-Phe-Arg-Arg at the cleavage site of the spike precursor propolypeptide of IBV strains Beaudette and M41. Virus Res. *4*, 133–143.

Cavanagh, D., Davis, P.J., and Cook, J.K. (1992). Infectious bronchitis virus: evidence for recombination within the Massachusetts serotype. Avian Pathol. *21*, 401–408.

Cavanagh, D., Mawditt, K., Sharma, M., Drury, S.E., Ainsworth, H.L., Britton, P., and Gough, R.E. (2001). Detection of a coronavirus from turkey poults in Europe genetically related to infectious bronchitis virus of chickens. Avian Pathol. *30*, 355–368. https://doi.org/10.1080/03079450120066368

Cavanagh, D., Mawditt, K., Welchman, D.d.e.B., Britton, P., and Gough, R.E. (2002). Coronaviruses from pheasants (Phasianus colchicus) are genetically closely related to coronaviruses of domestic fowl (infectious bronchitis virus) and turkeys. Avian Pathol. *31*, 81–93. https://doi.org/10.1080/03079450120106651

Cavanagh, D., Picault, J.P., Gough, R., Hess, M., Mawditt, K., and Britton, P. (2005). Variation in the spike protein of the 793/B type of infectious bronchitis virus, in the field and during alternate passage in chickens and embryonated eggs. Avian Pathol. *34*, 20–25.

Chandra, M. (1988). Comparative nephropathogenicity of infectious bronchitis virus in bursectomized and nonbursectomized chickens. Am. J. Vet. Res. *49*, 831–834.

Chang, C.K., Sue, S.C., Yu, T.H., Hsieh, C.M., Tsai, C.K., Chiang, Y.C., Lee, S.J., Hsiao, H.H., Wu, W.J., Chang, W.L., *et al.* (2006). Modular organization of SARS coronavirus nucleocapsid protein. J. Biomed. Sci. *13*, 59–72. https://doi.org/10.1007/s11373-005-9035-9

Chaplin, D.D. (2010). Overview of the immune response. J. Allergy Clin. Immunol. 125 (Suppl. 2), S3–23. https://doi.org/10.1016/j.jaci.2009.12.980

Chen, B., Fang, S., Tam, J.P., and Liu, D.X. (2009). Formation of stable homodimer via the Cterminal alpha-helical domain of coronavirus nonstructural protein 9 is critical for its function in viral replication. Virology *383*, 328–337.

Chen, B.Y., and Itakura, C. (1996). Cytopathology of chick renal epithelial cells experimentally infected with avian infectious bronchitis virus. Avian Pathol. *25*, 675–690.

Chen, H., Gill, A., Dove, B.K., Emmett, S.R., Kemp, C.F., Ritchie, M.A., Dee, M., and Hiscox, J.A. (2005). Mass spectroscopic characterization of the coronavirus infectious bronchitis virus nucleoprotein and elucidation of the role of phosphorylation in RNA binding by using surface plasmon resonance. J. Virol. *79*, 1164–1179.

Chen, P., Jiang, M., Hu, T., Liu, Q., Chen, X.S., and Guo, D. (2007). Biochemical characterization of exoribonuclease encoded by SARS coronavirus. J. Biochem. Mol. Biol. *40*, 649–655.

Cheng, A., Zhang, W., Xie, Y., Jiang, W., Arnold, E., Sarafianos, S.G., and Ding, J. (2005). Expression, purification, and characterization of SARS coronavirus RNA polymerase. Virology *335*, 165–176.

Cherry, J.D., and Taylor-Robinson, D. (1970). Large quantity production of chicken embryo organ culture and use in virus and mycoplasma studies. Appl. Microbiol. *19*, 658–662.

Chhabra, R., Forrester, A., Lemiere, S., Awad, F., Chantrey, J., and Ganapathy, K. (2015). Mucosal, cellular, and humoral immune responses induced by different live infectious bronchitis virus vaccination regimes and protection conferred against infectious bronchitis virus Q1 strain.

Clin. Vaccine Immunol. *22*, 1050–1059. https://doi.org/10.1128/CVI.00368-15

Chhabra, R., Kuchipudi, S.V., Chantrey, J., and Ganapathy, K. (2016). Pathogenicity and tissue tropism of infectious bronchitis virus is associated with elevated apoptosis and innate immune responses. Virology *488*, 232–241. https://doi.org/10.1016/j.virol.2015.11.011

Chiramel, A.I., Brady, N.R., and Bartenschlager, R. (2013). Divergent roles of autophagy in virus infection. Cells *2*, 83–104. https://doi.org/10.3390/cells2010083

Choi, K.S., Lee, E.K., Jeon, W.J., Park, M.J., Kim, J.W., and Kwon, J.H. (2009). Pathogenicity and antigenicity of a new variant of Korean nephropathogenic infectious bronchitis virus. J. Vet. Sci. *10*, 357–359.

Chousalkar, K.K., Cheetham, B.F., and Roberts, J.R. (2009). LNA probe-based real-time RT-PCR for the detection of infectious bronchitis virus from the oviduct of unvaccinated and vaccinated laying hens. J. Virol. Methods *155*, 67–71. https://doi.org/10.1016/j.jviromet.2008.09.028

Chu, V.C., McElroy, L.J., Chu, V., Bauman, B.E., and Whittaker, G.R. (2006a). The avian coronavirus infectious bronchitis virus undergoes direct low-pH-dependent fusion activation during entry into host cells. J. Virol. *80*, 3180–3188.

Chu, V.C., McElroy, L.J., Ferguson, A.D., Bauman, B.E., and Whittaker, G.R. (2006b). Avian infectious bronchitis virus enters cells via the endocytic pathway. Adv. Exp. Med. Biol. *581*, 309–312. https://doi.org/10.1007/978-0-387-33012-9_54

Chubb, R.C. (1974). The effect of the suppression of circulating antibody on resistance to the Australian avian infectious bronchitis virus. Res. Vet. Sci. *17*, 169–173.

Churchill, A.E. (1965). The use of chicken kidney tissue culture in the study of the avian viruses of Newcastle disease, infectious laryngo tracheitis and infectious bronchitis. Res. Vet. Sci. *6*, 162–169.

Clarke, J.K., McFerran, J.B., and Gay, F.W. (1972). Use of allantoic cells for the detection of avian infectious bronchitis virus. Arch. Gesamte Virusforsch. *36*, 62–70.

Coley, S.E., Lavi, E., Sawicki, S.G., Fu, L., Schelle, B., Karl, N., Siddell, S.G., and Thiel, V. (2005). Recombinant mouse hepatitis virus strain A59 from cloned, full-length cDNA replicates to high titers *in vitro* and is fully pathogenic *in vivo*. J. Virol. *79*, 3097–3106.

Collisson, E.W., Pei, J., Dzielawa, J., and Seo, S.H. (2000). Cytotoxic T lymphocytes are critical in the control of infectious bronchitis virus in poultry. Dev. Comp. Immunol. *24*, 187–200.

Cong, F., Liu, X., Han, Z., Shao, Y., Kong, X., and Liu, S. (2013). Transcriptome analysis of chicken kidney tissues following coronavirus avian infectious bronchitis virus infection. BMC Genomics *14*, 743. https://doi.org/10.1186/1471-2164-14-743

Cook, J.K. (1971). Recovery of infectious bronchitis virus from eggs and chicks produced by experimentally inoculated hens. J. Comp. Pathol. *81*, 203–211.

Cook, J.K., Darbyshire, J.H., and Peters, R.W. (1976). The use of chicken tracheal organ cultures for the isolation and assay of avian infectious bronchitis virus. Arch. Virol. *50*, 109–118.

Cook, J.K., Davison, T.F., Huggins, M.B., and McLaughlan, P. (1991). Effect of *in ovo* bursectomy on the course of an infectious bronchitis virus infection *in* line C White Leghorn chickens. Arch. Virol. *118*, 225–234.

Cook, J.K., Orbell, S.J., Woods, M.A., and Huggins, M.B. (1999). Breadth of protection of the respiratory tract provided by different live-attenuated infectious bronchitis vaccines against challenge with infectious bronchitis viruses of heterologous serotypes. Avian Pathol. *28*, 477–485. https://doi.org/10.1080/03079459994506

Cook, J.K., Jackwood, M., and Jones, R.C. (2012). The long view: 40 years of infectious bronchitis research. Avian Pathol. *41*, 239–250. https://doi.org/10.1080/03079457.2012.680432

Corse, E., and Machamer, C.E. (2003). The cytoplasmic tails of infectious bronchitis virus E and M proteins mediate their interaction. Virology *312*, 25–34.

Cottam, E.M., Maier, H.J., Manifava, M., Vaux, L.C., Chandra-Schoenfelder, P., Gerner, W., Britton, P., Ktistakis, N.T., and Wileman, T. (2011). Coronavirus nsp6 proteins generate autophagosomes from the endoplasmic reticulum via an omegasome intermediate. Autophagy *7*, 1335–1347. https://doi.org/10.4161/auto.7.11.16642

Cowen, B.S., and Hitchner, S.B. (1975a). Serotyping of avian infectious bronchitis viruses by the virus-neutralization test. Avian Dis. *19*, 583–595.

Cowen, B.S., and Hitchner, S.B. (1975b). pH stability studies with avian infectious bronchitis virus (coronavirus) strains. J. Virol. *15*, 430–432.

Crinion, R.A., and Hofstad, M.S. (1972). Pathogenicity of four serotypes of avian infectious bronchitis virus for the oviduct of young chickens of various ages. Avian Dis. *16*, 351–363.

Cumming, R.B. (1969). The control of avian infectious bronchitis/nephrosis in Australia. Aust. Vet. J. *45*, 200–203.

Cumming, R.B., and Chubb, R.C. (1988). The pathogenesis of nephritis evoked by Australian IB viruses. Proceedings of the 1st International Symposium on Infectious Bronchitis (Rauischholzhausen, Germany) pp. 129–132.

Cummiskey, J.F., Hallum, J.V., Skinner, M.S., and Leslie, G.A. (1973). Persistent Newcastle disease virus infection in embryonic chicken tracheal organ cultures. Infect. Immun. *8*, 657–664.

Cunningham, C.H. (1970). Avian infectious bronchitis. Adv. Vet. Sci. Comp. Med. *14*, 105–148.

Cunningham, C.H., Spring, M.P., and Nazerian, K. (1972). Replication of avian infectious bronchitis virus in African green monkey kidney cell line VERO. J. Gen. Virol. *16*, 423–427. https://doi.org/10.1099/0022-1317-16-3-423

Dar, A., Potter, A., Tikoo, S., Gerdts, V., Lai, K., Babiuk, L.A., and Mutwiri, G. (2009). CpG oligodeoxynucleotides activate innate immune response that suppresses infectious bronchitis virus replication in chicken embryos. Avian Dis. *53*, 261–267. https://doi.org/10.1637/8560-121808-Reg.1

Darbyshire, J.H., Cook, J.K., and Peters, R.W. (1975). Comparative growth kinetic studies on avian infectious bronchitis virus in different systems. J. Comp. Pathol. *85*, 623–630.

Davelaar, F.G., and Kouwenhoven, B. (1977). Influence of maternal antibodies on vaccination of chicks of different ages against infectious bronchitis. Avian Pathol. *6*, 41–50.

Davelaar, F.G., and Kouwenhoven, B. (1980). Effect of the removal of the Harderian gland in 1-day-old chicks on immunity following IB vaccination. Avian Pathol. *9*, 489–497.

Davelaar, F.G., Noordzij, A., and Vanderdonk, J.A. (1982). A study on the synthesis and secretion of immunoglobulins by the Jarderian gland of the fowl after eyedrop vaccination against infectious bronchitis at 1-day-old. Avian Pathol. *11*, 63–79.

Dawson, P.S., and Gough, R.E. (1971). Antigenic variation in strains of avian infectious bronchitis virus. Arch. Gesamte Virusforsch. *34*, 32–39.

de Haan, C.A., and Rottier, P.J. (2005). Molecular interactions in the assembly of coronaviruses. Adv. Virus Res. *64*, 165–230.

de Wit, J.J. (2000). Detection of infectious bronchitis virus. Avian Pathol. *29*, 71–93.

De Wit, J.J., Mekkes, D.R., Koch, G., and Westenbrink, F. (1998). [100] Detection of specific IgM antibodies to infectious bronchitis virus by an antibody-capture ELISA. Avian Pathol. *27*, 155–160. https://doi.org/10.1080/03079459808419317

de Wit, J.J., Cook, J.K.A., and van der Heijden, H.M.J.F. (2010a). Infectious bronchitis virus in Asia, Africa, Australia and Latin America – history, current situation and control measures. Rev. Bras. Cienc. Avic. *12*, 97–106.

De Wit, J.J., Swart, W.A., and Fabri, T.H. (2010b). [101] Efficacy of infectious bronchitis virus vaccinations in the field: association between the alpha-IBV IgM response, protection and vaccine application parameters. Avian Pathol. *39*, 123–131. https://doi.org/10.1080/03079451003604639

Decroly, E., Imbert, I., Coutard, B., Bouvet, M., Selisko, B., Alvarez, K., Gorbalenya, A.E., Snijder, E.J., and Canard, B. (2008). Coronavirus nonstructural protein 16 is a cap-0 binding enzyme possessing (nucleoside-2'O)-methyltransferase activity. J. Virol. *82*, 8071–8084.

Decroly, E., Debarnot, C., Ferron, F., Bouvet, M., Coutard, B., Imbert, I., Gluais, L., Papageorgiou, N., Sharff, A., Bricogne, G., *et al.* (2011). Crystal structure and functional analysis of the SARS-coronavirus RNA cap 2'-O-methyltransferase nsp10/nsp16 complex. PLOS Pathog. *7*, e1002059. https://doi.org/10.1371/journal.ppat.1002059

DeDiego, M.L., Alvarez, E., Almazán, F., Rejas, M.T., Lamirande, E., Roberts, A., Shieh, W.J., Zaki, S.R., Subbarao, K., and Enjuanes, L. (2007). A

severe acute respiratory syndrome coronavirus that lacks the E gene is attenuated *in vitro* and *in vivo*. J. Virol. *81*, 1701–1713.

Deming, D.J., and Baris, R.S. (2008). Genetics and reverse genetics of Nidovirales. In Nidovirales, S. Perlman, T Gallagher, E.J. Snijder, eds (Asm Press, Washington DC), pp. 47–64.

Denison, M.R., Hughes, S.A., and Weiss, S.R. (1995). Identification and characterization of a 65-kDa protein processed from the gene 1 polyprotein of the murine coronavirus MHV-A59. Virology *207*, 316–320.

Dent, S.D., Xia, D., Wastling, J.M., Neuman, B.W., Britton, P., and Maier, H.J. [104] (2015). The proteome of the infectious bronchitis virus Beau-R virion. J. Gen. Virol. *96*, 3499–3506.

Deschesnes, R.G., Huot, J., Valerie, K., and Landry, J. (2001). Involvement of p38 in apoptosis-associated membrane blebbing and nuclear condensation. Mol. Cell. Biol. *12*, 1569–1582.

Dever, T.E., Sripriya, R., McLachlin, J.R., Lu, J., Fabian, J.R., Kimball, S.R., and Miller, L.K. (1998). Disruption of cellular translational control by a viral truncated eukaryotic translation initiation factor 2alpha kinase homolog. Proc. Natl. Acad. Sci. U.S.A. *95*, 4164–4169.

Dhama, K., Singh, S.D., Barathidasan, R., Desingu, P.A., Chakraborty, S., Tiwari, R., and Kumar, M.A. (2014). Emergence of avian infectious bronchitis virus and its variants need better diagnosis, prevention and control strategies: a global perspective. Pak. J. Biol. Sci. *17*, 751–767.

Dhillon, A.S., Hagan, S., Rath, O., and Kolch, W. (2007). MAP kinase signalling pathways in cancer. Oncogene *26*, 3279–3290.

Dhinakar R.G., and Jones R.C. (1997). Infectious bronchitis virus: Immuno-pathogenesis of infection in the chicken. Avian Pathol. *26*, 677–706.

[102] Dhinakar Raj, G., and Jones, R.C. (1996). Protectotypic differentiation of avian infectious bronchitis viruses using an *in vitro* challenge model. Vet. Microbiol. *53*, 239–252.

Diemer, C., Schneider, M., Seebach, J., Quaas, J., Frösner, G., Schätzl, H.M., and Gilch, S. (2008). Cell type-specific cleavage of nucleocapsid protein by effector caspases during SARS coronavirus infection. J. Mol. Biol. *376*, 23–34.

Donaldson, E.F., Graham, R.L., Sims, A.C., Denison, M.R., and Baric, R.S. (2007). Analysis of murine hepatitis virus strain A59 temperature-sensitive mutant TS-LA6 suggests that nsp10 plays a critical role in polyprotein processing. J. Virol. *81*, 7086–7098.

Donaldson, E.F., Yount, B., Sims, A.C., Burkett, S., Pickles, R.J., and Baric, R.S. (2008). Systematic assembly of a full-length infectious clone of human coronavirus NL63. J. Virol. *82*, 11948–11957. https://doi.org/10.1128/JVI.01804-08

[103] Ducatez, M.F., European Union COST Action FA1207. (2016). Recommendations for a standardized avian coronavirus (AvCoV) nomenclature: outcome from discussions within the framework of the European Union COST Action FA1207: 'towards control of avian coronaviruses: strategies for vaccination, diagnosis and surveillance'. Avian Pathol. *45*, 602–603. https://doi.org/10.1080/03079457.2016.1211834

Dulbecco, R., and Vogt, M. (1954). Plaque formation and isolation of pure lines with poliomyelitis viruses. J. Exp. Med. *99*, 167–182.

Eckerle, L.D., Lu, X., Sperry, S.M., Choi, L., and Denison, M.R. (2007). High fidelity of murine hepatitis virus replication is decreased in nsp14 exoribonuclease mutants. J. Virol. *81*, 12135–12144.

Eckerle, L.D., Becker, M.M., Halpin, R.A., Li, K., Venter, E., Lu, X., Scherbakova, S., Graham, R.L., Baric, R.S., Stockwell, T.B., *et al.* (2010). Infidelity of SARS-CoV Nsp14-exonuclease mutant virus replication is revealed by complete genome sequencing. PLOS Pathog. *6*, e1000896. https://doi.org/10.1371/journal.ppat.1000896

Egloff, M.P., Ferron, F., Campanacci, V., Longhi, S., Rancurel, C., Dutartre, H., Snijder, E.J., Gorbalenya, A.E., Cambillau, C., and Canard, B. (2004). The severe acute respiratory syndrome-coronavirus replicative protein nsp9 is a single-stranded RNA-binding subunit unique in the RNA virus world. Proc. Natl. Acad. Sci. U.S.A. *101*, 3792–3796. https://doi.org/10.1073/pnas.0307877101

Eléouët, J.F., Slee, E.A., Saurini, F., Castagné, N., Poncet, D., Garrido, C., Solary, E., and Martin, S.J. (2000). The viral nucleocapsid protein of transmissible gastroenteritis coronavirus (TGEV) is cleaved by caspase-6 and -7 during TGEV-induced apoptosis. J. Virol. *74*, 3975–3983.

Elmore, S. (2007). Apoptosis: a review of programmed cell death. Toxicol. Pathol. *35*, 495–516.

Emmott, E., Munday, D., Bickerton, E., Britton, P., Rodgers, M.A., Whitehouse, A., Zhou, E.M., and Hiscox, J.A. (2013). The cellular interactome of the coronavirus infectious bronchitis virus nucleocapsid protein and functional implications for virus biology. J. Virol. *87*, 9486–9500. https://doi.org/10.1128/JVI.00321-13

Escorcia, M., Jackwood, M.W., Lucio, B., Petrone, V.M., López, C., Fehervari, T., and Téllez, G. (2000). Characterization of Mexican strains of avian infectious bronchitis isolated during 1997. Avian Dis. *44*, 944–947.

Fabricant, J. (1951). Studies on the diagnosis of Newcastle disease and infectious bronchitis. IV. The use of the serum neutralization test in the diagnosis of infectious bronchitis. Cornell Vet. *41*, 68–80.

Fabricant, J. (1998). The early history of infectious bronchitis. Avian Dis. *42*, 648–650.

Fan, H., Ooi, A., Tan, Y.W., Wang, S., Fang, S., Liu, D.X., and Lescar, J. (2005). The nucleocapsid protein of coronavirus infectious bronchitis virus: crystal structure of its N-terminal domain and multimerization properties. Structure *13*, 1859–1868.

Fang, S., Chen, B., Tay, F.P., Ng, B.S., and Liu, D.X. (2007). An arginine-to-proline mutation in a domain with undefined functions within the helicase protein (Nsp13) is lethal to the coronavirus infectious bronchitis virus in cultured cells. Virology *358*, 136–147.

Fang, S., Shen, H., Wang, J., Tay, F.P., and Liu, D.X. (2010). Functional and genetic studies of the substrate specificity of coronavirus infectious bronchitis virus 3C-like proteinase. J. Virol. *84*, 7325–7336. https://doi.org/10.1128/JVI.02490-09

Fang, S., Xu, L., Huang, M., Qisheng Li, F., and Liu, D.X. (2013). Identification of two ATR-dependent phosphorylation sites on coronavirus nucleocapsid protein with nonessential functions in viral replication and infectivity in cultured cells. Virology *444*, 225–232. https://doi.org/10.1016/j.virol.2013.06.014

Fang, S.G., Shen, S., Tay, F.P., and Liu, D.X. (2005). Selection of and recombination between minor variants lead to the adaptation of an avian coronavirus to primate cells. Biochem. Biophys. Res. Commun. *336*, 417–423.

Fang, S.G., Shen, H., Wang, J., Tay, F.P., and Liu, D.X. (2008). Proteolytic processing of polyproteins 1a and 1ab between non-structural proteins 10 and 11/12 of Coronavirus infectious bronchitis virus is dispensable for viral replication in cultured cells. Virology *379*, 175–180. https://doi.org/10.1016/j.virol.2008.06.038

Fehr, A.R., and Perlman, S. (2015). Coronaviruses: an overview of their replication and pathogenesis. Methods Mol. Biol. *1282*, 1–23. https://doi.org/10.1007/978-1-4939-2438-7_1

Feng, J., Hu, Y., Ma, Z., Yu, Q., Zhao, J., Liu, X., and Zhang, G. (2012). Virulent avian infectious bronchitis virus, People's Republic of China. Emerging Infect. Dis. *18*, 1994–2001. https://doi.org/10.3201/eid1812.120552

Ferreira, H.L., Pilz, D., Mesquita, L.G., and Cardoso, T. (2003). Infectious bronchitis virus replication in the chicken embryo related cell line. Avian Pathol. *32*, 413–417. https://doi.org/10.1080/0307945031000121167

Fischer, F., Stegen, C.F., Masters, P.S., and Samsonoff, W.A. (1998). Analysis of constructed E gene mutants of mouse hepatitis virus confirms a pivotal role for E protein in coronavirus assembly. J. Virol. *72*, 7885–7894.

Fraga, A.P., Balestrin, E., Ikuta, N., Fonseca, A.S., Spilki, F.R., Canal, C.W., and Lunge, V.R. (2013). Emergence of a new genotype of avian infectious bronchitis virus in Brazil. Avian Dis. *57*, 225–232. https://doi.org/10.1637/10346-090412-Reg.1

Franklin, C.C., and Kraft, A.S. (1997). Conditional expression of the mitogen-activated protein kinase (MAPK) phosphatase MKP-1 preferentially inhibits p38 MAPK and stress-activated protein kinase in U937 cells. J. Biol. Chem. *272*, 16917–16923.

Franzo, G., Listorti, V., Naylor, C.J., Lupini, C., Laconi, A., Felice, V., Drigo, M., Catelli, E., and Cecchinato, M. (2015). Molecular investigation of a full-length genome of a Q1-like IBV strain isolated in Italy in 2013. Virus Res. *210*, 77–80. https://doi.org/10.1016/j.virusres.2015.07.008

Fung, T.S., and Liu, D.X. (2017). Activation of the c-Jun NH2-terminal kinase pathway by coronavirus infectious bronchitis virus promotes apoptosis independently of c-Jun. Cell Death Dis. *8*, 3215. https://doi.org/10.1038/s41419-017-0053-0

Fung, T.S., and Liu, D.X. (2018). Post-translational modifications of coronavirus proteins: roles and function. Future Virology *13*, 405–430.

Fung, T.S., Liao, Y., and Liu, D.X. (2014a). The endoplasmic reticulum stress sensor IRE1α protects cells from apoptosis induced by the coronavirus infectious bronchitis virus. J. Virol. *88*, 12752–12764. https://doi.org/10.1128/JVI.02138-14

Fung, T.S., Huang, M., and Liu, D.X. (2014b). Coronavirus-induced ER stress response and its involvement in regulation of coronavirus-host interactions. Virus Res. *194*, 110–123. https://doi.org/10.1016/j.virusres.2014.09.016

Gallardo, R.A., Hoerr, F.J., Berry, W.D., van Santen, V.L., and Toro, H. (2011). Infectious bronchitis virus in testicles and venereal transmission. Avian Dis. *55*, 255–258. https://doi.org/10.1637/9592-102910-Reg.1

Ganapathy, K., Cargill, P.W., and Jones, R.C. (2005). A comparison of methods of inducing lachrymation and tear collection in chickens for detection of virus-specific immuoglobulins after infection with infectious bronchitis virus. Avian Pathol. *34*, 248–251.

Gelb, J., and Cloud, S.S. (1983). Effect of serial embryo passage of an Arkansas-type avian infectious bronchitis virus isolate on clinical response, virus recovery, and immunity. Avian Dis. *27*, 679–687.

Gelb, J., Wolff, J.B., and Moran, C.A. (1991). Variant serotypes of infectious bronchitis virus isolated from commercial layer and broiler chickens. Avian Dis. *35*, 82–87.

Gelb, J., Nix, W.A., and Gellman, S.D. (1998). Infectious bronchitis virus antibodies in tears and their relationship to immunity. Avian Dis. *42*, 364–374.

Gelb, J., Ladman, B.S., Tamayo, M., Gonzalez, M., and Sivanandan, V. (2001). Novel infectious bronchitis virus S1 genotypes in Mexico 1998-1999. Avian Dis. *45*, 1060–1063.

Gharaibeh, S., and Mahmoud, K. (2013). Decay of maternal antibodies in broiler chickens. Poult. Sci. *92*, 2333–2336. https://doi.org/10.3382/ps.2013-03249

Godeke, G.J., de Haan, C.A., Rossen, J.W., Vennema, H., and Rottier, P.J. (2000). Assembly of spikes into coronavirus particles is mediated by the carboxy-terminal domain of the spike protein. J. Virol. *74*, 1566–1571.

Gomes, L.M., and Brito, B.G. (2007). Genotipagem do vírus de bronquite infecciosa relacionado com quadro de miopatia do músculo peitoral em frangos de corte. Braz. J. Poult. Sci. *9*, 243.

Gorbalenya, A.E., Koonin, E.V., Donchenko, A.P., and Blinov, V.M. (1989). Coronavirus genome: prediction of putative functional domains in the non-structural polyprotein by comparative amino acid sequence analysis. Nucleic Acids Res. *17*, 4847–4861.

Gorbalenya, A.E., Pringle, F.M., Zeddam, J.L., Luke, B.T., Cameron, C.E., Kalmakoff, J., Hanzlik, T.N., Gordon, K.H., and Ward, V.K. (2002). The palm subdomain-based active site is internally permuted in viral RNA-dependent RNA polymerases of an ancient lineage. J. Mol. Biol. *324*, 47–62.

Goryo, M., Umemura, T., and Itakura, C. (1984). Concurrence of nephrosis-nephritis due to infectious bronchitis virus and infectious bursal disease in broiler chickens. Avian Pathol. *13*, 191–200.

Gough, R.E., and Alexander, D.J. (1977). Comparison of serological tests for the measurement of the primary immune response to avian infectious bronchitis virus vaccines. Vet. Microbiol. *2*, 289–301.

Gough, R.E., and Alexander, D.J. (1979). Comparison of duration of immunity in chickens infected with a live infectious bronchitis vaccine by three different routes. Res. Vet. Sci. *26*, 329–332.

Gough, R.E., Randall, C.J., Dagless, M., Alexander, D.J., Cox, W.J., and Pearson, D. (1992). A 'new' strain of infectious bronchitis virus infecting domestic fowl in Great Britain. Vet. Rec. *130*, 493–494.

Gough, R.E., Cox, W.J., Winkler, C.E., Sharp, M.W., and Spackman, D. (1996). Isolation and identification of infectious bronchitis virus from pheasants. Vet. Rec. *138*, 208–209.

Graham, R.L., Sims, A.C., Brockway, S.M., Baric, R.S., and Denison, M.R. (2005). The nsp2 replicase proteins of murine hepatitis virus and severe acute respiratory syndrome coronavirus are dispensable for viral replication. J. Virol. *79*, 13399–13411.

Grgiæ, H., Hunter, D.B., Hunton, P., and Nagy, E. (2008). Pathogenicity of infectious bronchitis virus isolates from Ontario chickens. Can. J. Vet. Res. *72*, 403–410.

Gross, W.B. (1990). Factors affecting the development of respiratory disease complex in chickens. Avian Dis. *34*, 607–610.

Guarino, L.A., Bhardwaj, K., Dong, W., Sun, J., Holzenburg, A., and Kao, C. (2005). Mutational analysis of the SARS virus Nsp15 endoribonuclease: identification of residues affecting hexamer formation. J. Mol. Biol. *353*, 1106–1117.

Guillot, L., Le Goffic, R., Bloch, S., Escriou, N., Akira, S., Chignard, M., and Si-Tahar, M. (2005). Involvement of toll-like receptor 3 in the immune response of lung epithelial cells to double-stranded RNA and influenza A virus. J. Biol. Chem. *280*, 5571–5580.

Guo, H., Huang, M., Yuan, Q., Wei, Y., Gao, Y., Mao, L., Gu, L., Tan, Y.W., Zhong, Y., Liu, D., *et al.* (2017). The important role of lipid raft-mediated attachment in the infection of cultured cells by coronavirus infectious bronchitis virus beaudette strain. PLOS ONE *12*, e0170123. https://doi.org/10.1371/journal.pone.0170123

Guy, J.S. (2013). Turkey coronavirus enteritis. In Diseases of Poultry, 13th edn, D.E. Swayne, J.R. Glisson and L.R. McDougald, eds. (Wiley-Blackwell, Ames, IA), pp. 376–381.

Hagemeijer, M.C., Ulasli, M., Vonk, A.M., Reggiori, F., Rottier, P.J., and de Haan, C.A. (2011). Mobility and interactions of coronavirus nonstructural protein 4. J. Virol. *85*, 4572–4577. https://doi.org/10.1128/JVI.00042-11

Haijema, B.J., Volders, H., and Rottier, P.J. (2003). Switching species tropism: an effective way to manipulate the feline coronavirus genome. J. Virol. *77*, 4528–4538.

Hammer, M., Mages, J., Dietrich, H., Servatius, A., Howells, N., Cato, A.C., and Lang, R. (2006). Dual specificity phosphatase 1 (DUSP1) regulates a subset of LPS-induced genes and protects mice from lethal endotoxin shock. J. Exp. Med. *203*, 15–20.

Harding, H.P., Zhang, Y., Bertolotti, A., Zeng, H., and Ron, D. (2000a). Perk is essential for translational regulation and cell survival during the unfolded protein response. Mol. Cell *5*, 897–904.

Harding, H.P., Novoa, I., Zhang, Y., Zeng, H., Wek, R., Schapira, M., and Ron, D. (2000b). Regulated translation initiation controls stress-induced gene expression in mammalian cells. Mol. Cell *6*, 1099–1108.

Hauck, R., Gallardo, R.A., Woolcock, P.R., and Shivaprasad, H.L. (2016). A coronavirus associated with runting stunting syndrome in broiler chickens. Avian Dis. *60*, 528–534. https://doi.org/10.1637/11353-122215-Case

Hawkes, R.A. (1979). General principals underlying laboratory diagnosis of viral infections. In Diagnostic Procedures for Viral, Rickettsial and Chlamydial Infections, 5th edn, E.H. Lennette and N. J. Schmidt, eds (American Public Health Association, Washington DC), pp. 1–48.

Hawkes, R.A., Darbyshire, J.H., Peters, R.W., Mockett, A.P., and Cavanagh, D. (1983). Presence of viral antigens and antibody in the trachea of chickens infected with avian infectious bronchitis virus. Avian Pathol. *12*, 331–340.

He, Y., Xie, Z., Dai, J., Cao, Y., Hou, J., Zheng, Y., Wei, T., Mo, M., and Wei, P. (2016). Responses of the toll-like receptor and melanoma differentiation-associated protein 5 signaling pathways to avian infectious bronchitis virus infection in chicks. Virol. Sin. *31*, 57–68. https://doi.org/10.1007/s12250-015-3696-y

Hesselink, W.G. (1991). Serotyping avian infectious bronchitis virus: selection of a unified method. In Proceedings of the II International Symposium on Infectious Bronchitis, E.F. Kaleta and U. Heffels-Redmann, eds (Rauischholzhausen, Germany), pp. 87–97.

Higgins, P.G., and Ellis, E.M. (1972). The isolation of influenza viruses. J. Clin. Pathol. *25*, 521–524.

Hipólito, O. (1957). Isolamento e identificacão do virus da bronquite infecciosa das galinhas no Brasil. Arquivo Escuela Veterinaria Universidade de Minas Gerais *10*, 131–151.

Hironao, T., Masui, T., and Bito, Y. (1970). A soluble antigen of infectious bronchitis virus. Jpn. J. Microbiol. *14*, 495–500.

Hitchner, S.B., Winterfield, R.W., and Appleton, G.S. (1966). Infectious bronchitis virus types – incidence in the United States. Avian Dis. *10*, 98–102.

Hodgson, T., Casais, R., Dove, B., Britton, P., and Cavanagh, D. (2004). Recombinant infectious bronchitis coronavirus Beaudette with the spike protein gene of the pathogenic M41 strain remains attenuated but induces protective immunity. J. Virol. *78*, 13804–13811.

Hofstad, M.S. (1958). Antigenic differences among isolates of avian infectious bronchitis virus. Am. J. Vet. Res. *19*, 740–743.

Hofstad, M.S., and Yoder, H.W. (1963). Inactivation rates of some lyophilized poultry viruses at 37 and 3 degrees C. Avian Dis. *7*, 170–177.

Holmes, E.C. (2009). The Evolution and Emergence of RNA Viruses, 1st edn (Oxford University Press Inc., New York, NY).

Hon, C.C., Lam, T.Y., Shi, Z.L., Drummond, A.J., Yip, C.W., Zeng, F., Lam, P.Y., and Leung, F.C. (2008). Evidence of the recombinant origin of a bat severe acute respiratory syndrome (SARS)-like coronavirus and its implications on the direct ancestor of SARS coronavirus. J. Virol. *82*, 1819–1826.

Hopkins, S.R. (1974). Serological comparisons of strains of infectious bronchitis virus using plaque-purified isolants. Avian Dis. *18*, 231–239.

Hosokawa, N., Hara, T., Kaizuka, T., Kishi, C., Takamura, A., Miura, Y., Iemura, S., Natsume, T., Takehana, K., Yamada, N., *et al.* (2009). Nutrient-dependent mTORC1 association with the ULK1-Atg13-FIP200 complex required for autophagy. Mol. Biol. Cell *20*, 1981–1991. https://doi.org/10.1091/mbc.E08-12-1248

Hu, T., Chen, C., Li, H., Dou, Y., Zhou, M., Lu, D., Zong, Q., Li, Y., Yang, C., Zhong, Z., *et al.* (2017). Structural basis for dimerization and RNA binding of avian infectious bronchitis virus nsp9. Protein Sci. *26*, 1037–1048. https://doi.org/10.1002/pro.3150

Huang, I.C., Bosch, B.J., Li, W., Farzan, M., Rottier, P.M., and Choe, H. (2006). SARS-CoV, but not HCoV-NL63, utilizes cathepsins to infect cells: viral entry. Adv. Exp. Med. Biol. *581*, 335–338.

Hurst, K.R., Koetzner, C.A., and Masters, P.S. (2009). Identification of in *vivo*-interacting domains of the murine coronavirus nucleocapsid protein. J. Virol. *83*, 7221–7234. https://doi.org/10.1128/JVI.00440-09

Hurst, K.R., Ye, R., Goebel, S.J., Jayaraman, P., and Masters, P.S. (2010). An interaction between the nucleocapsid protein and a component of the replicase-transcriptase complex is crucial for the infectivity of coronavirus genomic RNA. J. Virol. *84*, 10276–10288. https://doi.org/10.1128/JVI.01287-10

Hurst, K.R., Koetzner, C.A., and Masters, P.S. (2013). Characterization of a critical interaction between the coronavirus nucleocapsid protein and nonstructural protein 3 of the viral replicase-transcriptase complex. J. Virol. *87*, 9159–9172. https://doi.org/10.1128/JVI.01275-13

Igney, F.H., and Krammer, P.H. (2002). Death and anti-death: tumour resistance to apoptosis. Nat. Rev. Cancer *2*, 277–288. https://doi.org/10.1038/nrc776

Ignjatovic, J. (1988). Epidemiology of Infectious Bronchitis in Australia. Proceedings of the 1st International Symposium on Infectious Bronchitis (Rauischholzhausen, Germany), pp. 84–88.

Ignjatovic, J., and Sapats, S. (2000). Avian infectious bronchitis virus. Rev. Sci. Tech. *19*, 493–508.

Ignjatovic, J., Reece, R., and Ashton, F. (2003). Susceptibility of three genetic lines of chicks to infection with a nephropathogenic T strain of avian infectious bronchitis virus. J. Comp. Pathol. *128*, 92–98.

Imbert, I., Guillemot, J.C., Bourhis, J.M., Bussetta, C., Coutard, B., Egloff, M.P., Ferron, F., Gorbalenya, A.E., and Canard, B. (2006). A second, non-canonical RNA-dependent RNA polymerase in SARS coronavirus. EMBO J. *25*, 4933–4942.

Inberg, A., and Linial, M. (2004). Evolutional insights on uncharacterized SARS coronavirus genes. FEBS Lett. *577*, 159–164.

Ivanov, K.A., and Ziebuhr, J. (2004). Human coronavirus 229E nonstructural protein 13: characterization of duplex-unwinding, nucleoside triphosphatase, and RNA 5′-triphosphatase activities. J. Virol. *78*, 7833–7838. https://doi.org/10.1128/JVI.78.14.7833-7838.2004

Ivanov, K.A., Hertzig, T., Rozanov, M., Bayer, S., Thiel, V., Gorbalenya, A.E., and Ziebuhr, J. (2004b). Major genetic marker of nidoviruses encodes a replicative endoribonuclease. Proc. Natl. Acad. Sci. U.S.A. *101*, 12694–12699. https://doi.org/10.1073/pnas.0403127101

Ivanov, K.A., Thiel, V., Dobbe, J.C., van der Meer, Y., Snijder, E.J., and Ziebuhr, J. (2004a). Multiple enzymatic activities associated with severe acute respiratory syndrome coronavirus helicase. J. Virol. *78*, 5619–5632. https://doi.org/10.1128/JVI.78.11.5619-5632.2004

Jackwood, M.W. (2012). Review of infectious bronchitis virus around the world. Avian Dis. *56*, 634–641. https://doi.org/10.1637/10227-043012-Review.1

Jackwood, M.W., Kwon, H.M., and Hilt, D.A. (1992). Infectious bronchitis virus detection in allantoic fluid using the polymerase chain reaction and a DNA probe. Avian Dis. *36*, 403–409.

Jackwood, M.W., Hilt, D.A., Lee, C.W., Kwon, H.M., Callison, S.A., Moore, K.M., Moscoso, H., Sellers, H., and Thayer, S. (2005). Data from 11 years of molecular typing infectious bronchitis virus field isolates. Avian Dis. *49*, 614–618. https://doi.org/10.1637/7389-052905R.1

Jackwood, M.W., Hilt, D.A., McCall, A.W., Polizzi, C.N., McKinley, E.T., and Williams, S.M. (2009). Infectious bronchitis virus field vaccination coverage and persistence of Arkansas-type viruses in commercial broilers. Avian Dis. *53*, 175–183. https://doi.org/10.1637/8465-090308-Reg.1

Jackwood, M.W., Hall, D., and Handel, A. (2012). Molecular evolution and emergence of avian gammacoronaviruses. Infect. Genet. Evol. *12*, 1305–1311. https://doi.org/10.1016/j.meegid.2012.05.003

Janse, E.M., van Roozelaar, D., and Koch, G. (1994). Leukocyte subpopulations in kidney and trachea of chickens infected with infectious bronchitis virus. Avian Pathol. *23*, 513–523.

Jia, W., and Naqi, S.A. (1997). Sequence analysis of gene 3, gene 4 and gene 5 of avian infectious bronchitis virus strain CU-T2. Gene *189*, 189–193.

Johnson, M.A., Jaudzems, K., and Wüthrich, K. (2010). NMR Structure of the SARS-CoV Nonstructural Protein 7 in Solution at pH 6.5. J. Mol. Biol. *402*, 619–628. https://doi.org/10.1016/j.jmb.2010.07.043

Johnson, R.B., and Marquardt, W.W. (1976). Strains of infectious bronchitis virus on the Delmarva peninsula and in Arkansas. Avian Dis. *20*, 382–386.

Jones, R.C. (1974). Nephrosis in laying chickens caused by Massachusetts-type infectious bronchitis virus. Vet. Rec. *95*, 319.

Jones, R.C. (2008). Infectious laryngotracheitis. In Poultry Diseases, 6th edn, M. Pattison, P. McMullin, J.M. Bradbury, and D. Alexander, eds (Elsevier, Edinburgh), pp. 267–271.

Jones, R.C., and Jordan, F.T. (1972). Persistence of virus in the tissues and development of the oviduct in the fowl following infection at day old with infectious bronchitis virus. Res. Vet. Sci. *13*, 52–60.

Jordan, F.T.W., and Nassar, T.J. (1973). The combined influence of age of embryo, temperature and duration of incubation on the replication and yield of avian infectious bronchitis virus in the developing chicken embryo. Avian Pathol. *2*, 279–294.

Joseph, J.S., Saikatendu, K.S., Subramanian, V., Neuman, B.W., Brooun, A., Griffith, M., Moy, K., Yadav, M.K., Velasquez, J., Buchmeier, M.J., *et al.* (2006). Crystal structure of nonstructural protein 10 from the severe acute respiratory syndrome coronavirus reveals a novel fold with two zinc-binding motifs. J. Virol. *80*, 7894–7901.

Jungherr, E.L., Chomiak, T.W., and Luginbuhl, R.E. (1956). Immunologic differences in strains of infectious bronchitis virus. In Proceedings of 60th Annual Meeting of the United States Livestock Sanitary Association (Chicago, IL), pp. 203–209.

Kamitani, W., Narayanan, K., Huang, C., Lokugamage, K., Ikegami, T., Ito, N., Kubo, H., and Makino, S. (2006). Severe acute respiratory syndrome coronavirus nsp1 protein suppresses host gene expression by promoting host mRNA degradation. Proc. Natl. Acad. Sci. U.S.A. *103*, 12885–12890.

Kanjanahaluethai, A., Chen, Z., Jukneliene, D., and Baker, S.C. (2007). Membrane topology of murine coronavirus replicase nonstructural protein 3. Virology *361*, 391–401.

Kapczynski, D.R., Hilt, D.A., Shapiro, D., Sellers, H.S., and Jackwood, M.W. (2003). Protection of chickens from infectious bronchitis by *in ovo* and intramuscular vaccination with a DNA vaccine expressing the S1 glycoprotein. Avian Dis. *47*, 272–285. https://doi.org/10.1637/0005-2086(2003)047[0272:POCFIB]2.0.CO;2

Kapke, P.A., Tung, F.Y., Hogue, B.G., Brian, D.A., Woods, R.D., and Wesley, R. (1988). The amino-terminal signal peptide on the porcine transmissible gastroenteritis coronavirus matrix protein is not an absolute requirement for membrane translocation and glycosylation. Virology *165*, 367–376.

Karaca, K., Naqi, S., and Gelb, J. (1992). Production and characterization of monoclonal antibodies to three infectious bronchitis virus serotypes. Avian Dis. *36*, 903–915.

Kawai, T., and Akira, S. (2010). The role of pattern-recognition receptors in innate immunity: update on Toll-like receptors. Nat. Immunol. *11*, 373–384. https://doi.org/10.1038/ni.1863

Kawai, T., Takahashi, K., Sato, S., Coban, C., Kumar, H., Kato, H., Ishii, K.J., Takeuchi, O., and Akira, S. (2005). IPS-1, an adaptor triggering RIG-I- and Mda5-mediated type I interferon induction. Nat. Immunol. *6*, 981–988.

Keshet, Y., and Seger, R. (2010). The MAP kinase signaling cascades: a system of hundreds of components regulates a diverse array of physiological functions. Methods Mol. Biol. *661*, 3–38. https://doi.org/10.1007/978-1-60761-795-2_1

Khataby, K., Souiri, A., Kasmi, Y., Loutfi, C., and Ennaji, M.M. (2016). Current situation, genetic relationship and control measures of infectious bronchitis virus variants circulating in African regions. J. Basic. Appl. Zool. *76*, 20–30.

Kimura, S., Noda, T., and Yoshimori, T. (2007). Dissection of the autophagosome maturation process by a novel reporter protein, tandem fluorescent-tagged LC3. Autophagy *3*, 452–460.

King, D.J., and Hopkins, S.R. (1984). Rapid serotyping of infectious bronchitis virus isolates with the hemagglutination-inhibition test. Avian Dis. *28*, 727–733.

Kingham, B.F., Keeler, C.L., Nix, W.A., Ladman, B.S., and Gelb, J. (2000). Identification of avian infectious bronchitis virus by direct automated cycle sequencing of the S-1 gene. Avian Dis. *44*, 325–335.

Kint, J., Fernandez-Gutierrez, M., Maier, H.J., Britton, P., Langereis, M.A., Koumans, J., Wiegertjes, G.F., and Forlenza, M. (2015). Activation of the chicken type I interferon response by infectious bronchitis coronavirus. J. Virol. *89*, 1156–1167. https://doi.org/10.1128/JVI.02671-14

Kint, J., Langereis, M.A., Maier, H.J., Britton, P., van Kuppeveld, F.J., Koumans, J., Wiegertjes, G.F., and Forlenza, M. (2016). Infectious bronchitis coronavirus limits interferon production by inducing a host shutoff that requires accessory protein 5b. J. Virol. *90*, 7519–7528. https://doi.org/10.1128/JVI.00627-16

Klieve, A.V., and Cumming, R.B. (1990). Respiratory disease and immunity to challenge produced by Australian strains of infectious bronchitis virus. Avian Pathol. *19*, 305–312.

Klionsky, D.J., Abdelmohsen, K., Abe, A., Abedin, M.J., Abeliovich, H., Acevedo Arozena, A., Adachi, H., Adams, C.M., Adams, P.D., Adeli, K., *et al.* (2016). Guidelines for the use and interpretation of assays for monitoring autophagy (3rd edition). Autophagy *12*, 1–222. https://doi.org/10.1080/15548627.2015.1100356

Knoops, K., Kikkert, M., Worm, S.H., Zevenhoven-Dobbe, J.C., van der Meer, Y., Koster, A.J., Mommaas, A.M., and Snijder, E.J. (2008). SARS-coronavirus replication is supported by a reticulovesicular network of modified endoplasmic reticulum. PLOS Biol. *6*, e226. https://doi.org/10.1371/journal.pbio.0060226

Koch, G., Hartog, L., Kant, A., and van Roozelaar, D.J. (1990). Antigenic domains on the peplomer protein of avian infectious bronchitis virus: correlation with biological functions. J. Gen. Virol. *71*, 1929–1935. https://doi.org/10.1099/0022-1317-71-9-1929

Koetzner, C.A., Parker, M.M., Ricard, C.S., Sturman, L.S., and Masters, P.S. (1992). Repair and mutagenesis of the genome of a deletion mutant of the coronavirus mouse hepatitis virus by targeted RNA recombination. J. Virol. *66*, 1841–1848.

Kokame, K., Kato, H., and Miyata, T. (2001). Identification of ERSE-II, a new cis-acting element responsible for the ATF6-dependent mammalian unfolded protein response. J. Biol. Chem. *276*, 9199–9205. https://doi.org/10.1074/jbc.M010486200

Kong, Q., Xue, C., Ren, X., Zhang, C., Li, L., Shu, D., Bi, Y., and Cao, Y. (2010). Proteomic analysis of purified coronavirus infectious bronchitis virus particles. Proteome Sci. *8*, 29. https://doi.org/10.1186/1477-5956-8-29

Koonin, E.V. (1991). The phylogeny of RNA-dependent RNA polymerases of positive-strand RNA viruses. J. Gen. Virol. *72*, 2197–2206. https://doi.org/10.1099/0022-1317-72-9-2197

Korennykh, A.V., Egea, P.F., Korostelev, A.A., Finer-Moore, J., Zhang, C., Shokat, K.M., Stroud, R.M., and Walter, P. (2009). The unfolded protein response signals through high-order assembly of Ire1. Nature *457*, 687–693. https://doi.org/10.1038/nature07661

Kotani, T., Wada, S., Tsukamoto, Y., Kuwamura, M., Yamate, J., and Sakuma, S. (2000). Kinetics of lymphocytic subsets in chicken tracheal lesions infected with infectious bronchitis virus. J. Vet. Med. Sci. *62*, 397–401.

Kroemer, G., Mariño, G., and Levine, B. (2010). Autophagy and the integrated stress response. Mol. Cell *40*, 280–293. https://doi.org/10.1016/j.molcel.2010.09.023

Kubo, H., Yamada, Y.K., and Taguchi, F. (1994). Localization of neutralizing epitopes and the receptor-binding site within the amino-terminal 330 amino acids of the murine coronavirus spike protein. J. Virol. *68*, 5403–5410.

Kuo, L., and Masters, P.S. (2003). The small envelope protein E is not essential for murine coronavirus replication. J. Virol. *77*, 4597–4608.

Kuo, L., Godeke, G.J., Raamsman, M.J., Masters, P.S., and Rottier, P.J. (2000). Retargeting of coronavirus by substitution of the spike glycoprotein ectodomain: crossing the host cell species barrier. J. Virol. *74*, 1393–1406.

Kvansakul, M., and Hinds, M.G. (2013). Structural biology of the Bcl-2 family and its mimicry by viral proteins. Cell Death Dis. *4*, e909. https://doi.org/10.1038/cddis.2013.436

Laconi, A., van Beurden, S.J., Berends, A.J., Krämer-Kühl, A., Jansen, C.A., Spekreijse, D., Chénard, G., Philipp, H.C., Mundt, E., Rottier, P.J.M., *et al.* (2018). Deletion of accessory genes 3a, 3b, 5a or 5b from avian coronavirus infectious bronchitis virus induces an attenuated phenotype both *in vitro* and *in vivo*. J. Gen. Virol. [Epub ahead of print]. https://doi.org/10.1099/jgv.0.001130

Ladman, B.S., Pope, C.R., Ziegler, A.F., Swieczkowski, T., Callahan, C.J., Davison, S., and Gelb, J. (2002). Protection of chickens after live and inactivated virus vaccination against challenge with nephropathogenic infectious bronchitis virus PA/Wolgemuth/98. Avian Dis. *46*, 938–944. https://doi.org/10.1637/0005-2086(2002)046[0938:POCALA]2.0.CO;2

Lambrechts, C., Pensaert, M., and Ducatelle, R. (1993). Challenge experiments to evaluate cross-protection induced at the trachea and kidney level by vaccine strains and Belgian nephropathogenic isolates of avian infectious bronchitis virus. Avian Pathol. *22*, 577–590.

Lang, R., Hammer, M., and Mages, J. (2006). DUSP meet immunology: dual specificity MAPK phosphatases in control of the inflammatory response. J. Immunol. *177*, 7497–7504.

Lee, A.H., Iwakoshi, N.N., and Glimcher, L.H. (2003). XBP-1 regulates a subset of endoplasmic reticulum resident chaperone genes in the unfolded protein response. Mol. Cell. Biol. *23*, 7448–7459.

Lee, C.W., and Jackwood, M.W. (2000). Evidence of genetic diversity generated by recombination among avian coronavirus IBV. Arch. Virol. *145*, 2135–2148.

Lee, C.W., and Jackwood, M.W. (2001). Origin and evolution of Georgia 98 (GA98), a new serotype of avian infectious bronchitis virus. Virus Res. *80*, 33–39.

Leibowitz, J.L., DeVries, J.R., and Haspel, M.V. (1982). Genetic analysis of murine hepatitis virus strain JHM. J. Virol. *42*, 1080–1087.

Levine, B., and Deretic, V. (2007). Unveiling the roles of autophagy in innate and adaptive immunity. Nat. Rev. Immunol. *7*, 767–777.

Lewerenz, J., and Maher, P. (2009). Basal levels of eIF2alpha phosphorylation determine cellular antioxidant status by regulating ATF4 and xCT expression. J. Biol. Chem. *284*, 1106–1115. https://doi.org/10.1074/jbc.M807325200

Leyson, C.L.M., Jordan, B.J., and Jackwood, M.W. (2016). Insights from molecular structure predictions of the infectious bronchitis virus S1 spike glycoprotein. Infect. Genet. Evol. *46*, 124–129.

Li, F.Q., Tam, J.P., and Liu, D.X. (2007). Cell cycle arrest and apoptosis induced by the coronavirus infectious bronchitis virus in the absence of p53. Virology *365*, 435–445.

Li, H., and Yang, H. (2001). Sequence analysis of nephropathogenic infectious bronchitis virus strains of the Massachusetts genotype in Beijing. Avian Pathol. *30*, 535–541. https://doi.org/10.1080/03079450120078734

Liao, Y., Lescar, J., Tam, J.P., and Liu, D.X. (2004). Expression of SARS-coronavirus envelope protein in Escherichia coli cells alters membrane permeability. Biochem. Biophys. Res. Commun. *325*, 374–380.

Liao, Y., Yuan, Q., Torres, J., Tam, J.P., and Liu, D.X. (2006). Biochemical and functional characterization of the membrane association and membrane permeabilizing activity of the severe acute respiratory syndrome coronavirus envelope protein. Virology *349*, 264–275.

Liao, Y., Wang, X., Huang, M., Tam, J.P., and Liu, D.X. (2011). Regulation of the p38 mitogenactivated protein kinase and dual-specificity phosphatase 1 feedback loop modulates the induction of interleukin 6 and 8 in cells infected with coronavirus infectious bronchitis virus. Virology *420*, 106–116.

Liao, Y., Fung, T.S., Huang, M., Fang, S.G., Zhong, Y., and Liu, D.X. (2013). Upregulation of CHOP/GADD153 during coronavirus infectious bronchitis virus infection modulates apoptosis by restricting activation of the extracellular signal-regulated kinase pathway. J. Virol. *87*, 8124–8134. https://doi.org/10.1128/JVI.00626-13

Lim, K.P., and Liu, D.X. (1998a). Characterization of the two overlapping papain-like proteinase domains encoded in gene 1 of the coronavirus

infectious bronchitis virus and determination of the C-terminal cleavage site of an 87-kDa protein. Virology *245*, 303–312.

Lim, K.P., and Liu, D.X. (1998b). Characterisation of a papain-like proteinase domain encoded by ORF1a of the coronavirus IBV and determination of the C-terminal cleavage site of an 87 kDa protein. Adv. Exp. Med. Biol. *440*, 173–184.

Lim, K.P., and Liu, D.X. (2001). The missing link in coronavirus assembly. Retention of the avian coronavirus infectious bronchitis virus envelope protein in the pre-Golgi compartments and physical interaction between the envelope and membrane proteins. J. Biol. Chem. *276*, 17515–17523. https://doi.org/10.1074/jbc.M009731200

Lim, K.P., Ng, L.F., and Liu, D.X. (2000). Identification of a novel cleavage activity of the first papain-like proteinase domain encoded by open reading frame 1a of the coronavirus Avian infectious bronchitis virus and characterization of the cleavage products. J. Virol. *74*, 1674–1685.

Lim, K.P., Xu, H.Y., and Liu, D.X. (2001). Physical interaction between the membrane (M) and envelope (E) proteins of the coronavirus avian infectious bronchitis virus (IBV). Adv. Exp. Med. Biol. *494*, 595–602.

Lim, T.H., Lee, H.J., Lee, D.H., Lee, Y.N., Park, J.K., Youn, H.N., Kim, M.S., Lee, J.B., Park, S.Y., Choi, I.S., *et al.* (2011). An emerging recombinant cluster of nephropathogenic strains of avian infectious bronchitis virus in Korea. Infect. Genet. Evol. *11*, 678–685. https://doi.org/10.1016/j.meegid.2011.01.007

Lin, S.Y., Li, Y.T., Chen, Y.T., Chen, T.C., Hu, C.J., and Chen, H.W. (2016). Identification of an infectious bronchitis coronavirus strain exhibiting a classical genotype but altered antigenicity, pathogenicity, and innate immunity profile. Sci. Rep. *6*, 37725. https://doi.org/10.1038/srep37725

Liu, C., Xu, H.Y., and Liu, D.X. (2001). Induction of caspase-dependent apoptosis in cultured cells by the avian coronavirus infectious bronchitis virus. J. Virol. *75*, 6402–6409. https://doi.org/10.1128/JVI.75.14.6402-6409.2001

Liu, D.X., and Inglis, S.C. (1991). Association of the infectious bronchitis virus 3c protein with the virion envelope. Virology *185*, 911–917.

Liu, D.X., and Inglis, S.C. (1992). Internal entry of ribosomes on a tricistronic mRNA encoded by infectious bronchitis virus. J. Virol. *66*, 6143–6154.

Liu, D.X., Cavanagh, D., Green, P., and Inglis, S.C. (1991). A polycistronic mRNA specified by the coronavirus infectious bronchitis virus. Virology *184*, 531–544.

Liu, D.X., Brierley, I., Tibbles, K.W., and Brown, T.D. (1994). A 100-kilodalton polypeptide encoded by open reading frame (ORF) 1b of the coronavirus infectious bronchitis virus is processed by ORF 1a products. J. Virol. *68*, 5772–5780.

Liu, D.X., Tibbles, K.W., Cavanagh, D, Brown, T.D.K., and Brierley, I. (1995a). Identification, expression and processing of an 87K polypeptide encoded by ORF1a of the coronavirus infectious bronchitis virus. Virology *208*, 48–57.

Liu, D.X., Brierley, I., and Brown, T.D. (1995b). Identification of a trypsin-like serine proteinase domain encoded by ORF 1a of the coronavirus IBV. Adv. Exp. Med. Biol. *380*, 405–411.

Liu, D.X., Tibbles, K.W., Cavanagh, D., Brown, T.D., and Brierley, I. (1995c). Involvement of viral and cellular factors in processing of polyprotein encoded by ORF1a of the coronavirus IBV. Adv. Exp. Med. Biol. *380*, 413–421.

Liu, D.X., Xu, H.Y., and Brown, T.D. (1997). Proteolytic processing of the coronavirus infectious bronchitis virus 1a polyprotein: identification of a 10-kilodalton polypeptide and determination of its cleavage sites. J. Virol. *71*, 1814–1820.

Liu, D.X., Shen, S., Xu, H.Y., and Wang, S.F. (1998a). Proteolytic mapping of the coronavirus infectious bronchitis virus 1b polyprotein: evidence for the presence of four cleavage sites of the 3C-like proteinase and identification of two novel cleavage products. Virology *246*, 288–297.

Liu, D.X., Shen, S., Xu, H.Y., and Brown, T.D. (1998b). Proteolytic processing of the polyprotein encoded by ORF1b of the coronavirus infectious bronchitis virus (IBV). Adv. Exp. Med. Biol. *440*, 149–159.

Liu, D.X., Xu, H.Y., and Lim, K.P. (1998c). Regulation of mRNA1 expression by the 5′untranslated region (5′-UTR) of the coronavirus infectious bronchitis virus (IBV). Adv. Exp. Med. Biol. *440*, 303–311.

Liu, D.X., Yuan, Q., and Liao, Y. (2007). Coronavirus envelope protein: a small membrane protein with multiple functions. Cell. Mol. Life Sci. *64*, 2043–2048. https://doi.org/10.1007/s00018-007-7103-1

Liu, S., Chen, J., Han, Z., Zhang, Q., Shao, Y., Kong, X., and Tong, G. (2006). Infectious bronchitis virus: S1 gene characteristics of vaccines used in China and efficacy of vaccination against heterologous strains from China. Avian Pathol. *35*, 394–399.

Liu, X., Shao, Y., Ma, H., Sun, C., Zhang, X., Li, C., Han, Z., Yan, B., Kong, X., and Liu, S. (2013). Comparative analysis of four Massachusetts type infectious bronchitis coronavirus genomes reveals a novel Massachusetts type strain and evidence of natural recombination in the genome. Infect. Genet. Evol. *14*, 29–38. https://doi.org/10.1016/j.meegid.2012.09.016

Liu, Y., Shepherd, E.G., and Nelin, L.D. (2007). MAPK phosphatases – regulating the immune response. Nat. Rev. Immunol. *7*, 202–212.

Lohr, J.E., Hinze, V., and Kaleta, E.F. (1991). Immunological relationship between the New Zealand A and the Australian T strains of infectious bronchitis virus as measured by cross-immunisation tests in tracheal organ cultures from immunised birds. N. Z. Vet. J. *39*, 113–114. https://doi.org/10.1080/00480169.1991.35674

Lokugamage, K.G., Narayanan, K., Huang, C., and Makino, S. (2012). Severe acute respiratory syndrome coronavirus protein nsp1 is a novel eukaryotic translation inhibitor that represses multiple steps of translation initiation. J. Virol. *86*, 13598–13608. https://doi.org/10.1128/JVI.01958-12

Lontok, E., Corse, E., and Machamer, C.E. (2004). Intracellular targeting signals contribute to localization of coronavirus spike proteins near the virus assembly site. J. Virol. *78*, 5913–5922. https://doi.org/10.1128/JVI.78.11.5913-5922.2004

Lu, Y., Liu, D.X., and Tam, J.P. (2008). Lipid rafts are involved in SARS-CoV entry into Vero E6 cells. Biochem. Biophys. Res. Commun. *369*, 344–349. https://doi.org/10.1016/j.bbrc.2008.02.023

Lutticken, D., Rijke, E.O., Loeffen, T., and Hesselink, W.G. (1988). Aspects of local immune response to IBV. In Proceedings of the 1st International Symposium on Infectious Bronchitis (Rauischholzhausen, Germany), pp. 173–181.

Luytjes, W., Gerritsma, H., Bos, E., and Spaan, W. (1997). Characterization of two temperature-sensitive mutants of coronavirus mouse hepatitis virus strain A59 with maturation defects in the spike protein. J. Virol. *71*, 949–955.

Ma, Y., Wu, L., Shaw, N., Gao, Y., Wang, J., Sun, Y., Lou, Z., Yan, L., Zhang, R., and Rao, Z. (2015). Structural basis and functional analysis of the SARS coronavirus nsp14-nsp10 complex. Proc. Natl. Acad. Sci. U.S.A. *112*, 9436–9441. https://doi.org/10.1073/pnas.1508686112

Maassab, H.F. (1959). The propagation of multiple viruses in chick kidney cultures. Proc. Natl. Acad. Sci. U.S.A. *45*, 1035–1039.

Machamer, C.E., and Rose, J.K. (1987). A specific transmembrane domain of a coronavirus E1 glycoprotein is required for its retention in the Golgi region. J. Cell Biol. *105*, 1205–1214.

Machamer, C.E., and Youn, S. (2006). The transmembrane domain of the infectious bronchitis virus E protein is required for efficient virus release. Adv. Exp. Med. Biol. *581*, 193–198. https://doi.org/10.1007/978-0-387-33012-9_33

Maier, H.J., Hawes, P.C., Cottam, E.M., Mantell, J., Verkade, P., Monaghan, P., Wileman, T., and Britton, P. (2013). Infectious bronchitis virus generates spherules from zippered endoplasmic reticulum membranes. MBio *4*, e00801–13. https://doi.org/10.1128/mBio.00801-13

Maiuri, M.C., Zalckvar, E., Kimchi, A., and Kroemer, G. (2007). Self-eating and self-killing: crosstalk between autophagy and apoptosis. Nat. Rev. Mol. Cell Biol. *8*, 741–752.

Marandino, A., Pereda, A., Tomás, G., Hernández, M., Iraola, G., Craig, M.I., Hernández, D., Banda, A., Villegas, P., Panzera, Y., *et al.* (2015). Phylodynamic analysis of avian infectious bronchitis virus in South America. J. Gen. Virol. *96*, 1340–1346.

Martin, M.P., Wakenell, P.S., Woolcock, P., and O'Connor, B. (2007). Evaluation of the effectiveness of two infectious bronchitis virus vaccine programs for preventing disease caused by a California IBV field isolate. Avian Dis. *51*, 584–589. https://doi.org/10.1637/0005-2086(2007)51[584:EOTEOT]2.0.CO;2

Martinvalet, D., Zhu, P., and Lieberman, J. (2005). Granzyme A induces caspase-independent mitochondrial damage, a required first step for apoptosis. Immunity *22*, 355–370.

McFerran, J.B., Cahill, H.T., Young, J.A., and Wright, C.L. (1971). Isolation of infectious bronchitis virus from newborn chicks and dead-in-shell embryos. Vet. Rec. *89*, 560–561.

McGee, Z.A., and Woods, M.L. (1987). Use of organ cultures in microbiological research. Annu. Rev. Microbiol. *41*, 291–300. https://doi.org/10.1146/annurev.mi.41.100187.001451

McIntosh, K., Becker, W.B., and Chanock, R.M. (1967). Growth in suckling-mouse brain of 'IBV-like' viruses from patients with upper respiratory tract disease. Proc. Natl. Acad. Sci. U.S.A. *58*, 2268–2273.

Mehrpour, M., Esclatine, A., Beau, I., and Codogno, P. (2010). Overview of macroautophagy regulation in mammalian cells. Cell Res. *20*, 748–762. https://doi.org/10.1038/cr.2010.82

Meir, R., Rosenblut, E., Perl, S., Kass, N., Ayali, G., Perk, S., and Hemsani, E. (2004). Identification of a novel nephropathogenic infectious bronchitis virus in Israel. Avian Dis. *48*, 635–641. https://doi.org/10.1637/7107

Meir, R., Maharat, O., Farnushi, Y., and Simanov, L. (2010). Development of a real-time TaqMan RT-PCR assay for the detection of infectious bronchitis virus in chickens, and comparison of RT-PCR and virus isolation. J. Virol. Methods *163*, 190–194. https://doi.org/10.1016/j.jviromet.2009.09.014

Merchlinsky, M., and Moss, B. (1992). Introduction of foreign DNA into the vaccinia virus genome by *in vitro* ligation: recombination-independent selectable cloning vectors. Virology *190*, 522–526.

Minakshi, R., Padhan, K., Rani, M., Khan, N., Ahmad, F., and Jameel, S. (2009). The SARS Coronavirus 3a protein causes endoplasmic reticulum stress and induces ligand-independent downregulation of the type 1 interferon receptor. PLOS ONE *4*, e8342. https://doi.org/10.1371/journal.pone.0008342

Minskaia, E., Hertzig, T., Gorbalenya, A.E., Campanacci, V., Cambillau, C., Canard, B., and Ziebuhr, J. (2006). Discovery of an RNA virus 3'->5' exoribonuclease that is critically involved in coronavirus RNA synthesis. Proc. Natl. Acad. Sci. U.S.A. *103*, 5108–5113.

Mizushima, N., Levine, B., Cuervo, A.M., and Klionsky, D.J. (2008). Autophagy fights disease through cellular self-digestion. Nature *451*, 1069–1075. https://doi.org/10.1038/nature06639

Mockett, A.P., and Cook, J.K. (1986). The detection of specific IgM to infectious bronchitis virus in chicken serum using an ELISA. Avian Pathol. *15*, 437–446.

Mockett, A.P., and Darbyshire, J.H. (1981). Comparative studies with an enzyme-linked immunosorbent assay (ELISA) for antibodies to avian infectious bronchitis virus. Avian Pathol. *10*, 1–10.

Mockett, A.P., Cook, J.K., and Huggins, M.B. (1987). Maternally-derived antibody to infectious bronchitis virus: Its detection in chick trachea and serum and its role in protection. Avian Pathol. *16*, 407–416.

Molenkamp, R., and Spaan, W.J. (1997). Identification of a specific interaction between the coronavirus mouse hepatitis virus A59 nucleocapsid protein and packaging signal. Virology *239*, 78–86.

Momayez, R., Pourbakhsh, S.A., Khodashenas, M., and Banani, M. (2002). Isolation and Identification of Infectious Bronchitis Virus from Commercial Chickens. Arch. Razi Inst. *53*, 1–10.

Mondal, S.P., and Naqi, S.A. (2001). Maternal antibody to infectious bronchitis virus: its role in protection against infection and development of active immunity to vaccine. Vet. Immunol. Immunopathol. *79*, 31–40.

Monreal, G., Bauer, H.J., and Wiegmann, J. (1985). Comparison of the enzyme-linked immunosorbent assay (ELISA), haemagglutination inhibition test and agar gel precipitation test for detection of antibodies to avian infectious bronchitis virus. Avian Pathol. *14*, 421–434.

Montassier, H.J. (2010). Molecular epidemiology and evolution of avian infectious bronchitis virus. Rev. Bras. Cienc. Avic. *12*, 87–96.

Morishima, N., Nakanishi, K., and Nakano, A. (2011). Activating transcription factor-6 (ATF6) mediates apoptosis with reduction of myeloid cell leukemia sequence 1 (Mcl-1) protein via induction of WW domain binding protein 1. J. Biol. Chem. *286*, 35227–35235. https://doi.org/10.1074/jbc.M111.233502

Moser, M.J., Holley, W.R., Chatterjee, A., and Mian, I.S. (1997). The proofreading domain of Escherichia coli DNA polymerase I and other DNA and/or RNA exonuclease domains. Nucleic Acids Res. *25*, 5110–5118.

Muhammad A.M., Chaudhry, K.M., and Khawaja, K.N. (2000). Losses due to infectious bronchitis virus infection in laying and breeding hens. Pak. Vet. J. *20*, 64–70.

Nakamura, K., Cook, J.K., Otsuki, K., Huggins, M.B., and Frazier, J.A. (1991). Comparative study of respiratory lesions in two chicken lines of different susceptibility infected with infectious bronchitis virus: histology, ultrastructure and immunohistochemistry. Avian Pathol. *20*, 241–257.

Narayanan, K., Maeda, A., Maeda, J., and Makino, S. (2000). Characterization of the coronavirus M protein and nucleocapsid interaction in infected cells. J. Virol. *74*, 8127–8134.

Narayanan, K., Ramirez, S.I., Lokugamage, K.G., and Makino, S. (2015). Coronavirus nonstructural protein 1: Common and distinct functions in the regulation of host and viral gene expression. Virus Res. *202*, 89–100. https://doi.org/10.1016/j.virusres.2014.11.019

Neuman, B.W., Kiss, G., Kunding, A.H., Bhella, D., Baksh, M.F., Connelly, S., Droese, B., Klaus, J.P., Makino, S., Sawicki, S.G., *et al.* (2011). A structural analysis of M protein in coronavirus assembly and morphology. J. Struct. Biol. *174*, 11–22. https://doi.org/10.1016/j.jsb.2010.11.021

Ng, L.F., and Liu, D.X. (2000). Further characterization of the coronavirus infectious bronchitis virus 3C-like proteinase and determination of a new cleavage site. Virology *272*, 27–39. https://doi.org/10.1006/viro.2000.0330

Ng, L.F.P., and Liu, D.X. (1998). Further characterization of the coronavirus IBV ORF1a products encoded by the 3C-like proteinase domain and the flanking regions. Adv. Exp. Med. Biol. *440*, 161–171.

Ng, L.F.P., and Liu, D.X. (2002). Membrane association and dimerization of a cysteine-rich, 16kDa polypeptide released from the C-terminal region of the coronavirus infectious bronchitis virus 1a polyprotein. J. Virol. *76*, 6257–6267.

Nicholas, R.A., Wood, G.W., and Thornton, D.H. (1983). Comparison of techniques for the detection of avian infectious bronchitis virus as a contaminant of vaccines. J. Biol. Stand. *11*, 75–81.

Nomura, R., Kiyota, A., Suzaki, E., Kataoka, K., Ohe, Y., Miyamoto, K., Senda, T., and Fujimoto, T. (2004). Human coronavirus 229E binds to CD13 in rafts and enters the cell through caveolae. J. Virol. *78*, 8701–8708. https://doi.org/10.1128/JVI.78.16.8701-8708.2004

Ogata, M., Hino, S., Saito, A., Morikawa, K., Kondo, S., Kanemoto, S., Murakami, T., Taniguchi, M., Tanii, I., Yoshinaga, K., *et al.* (2006). Autophagy is activated for cell survival after endoplasmic reticulum stress. Mol. Cell. Biol. *26*, 9220–9231.

Okada, T., Yoshida, H., Akazawa, R., Negishi, M., and Mori, K. (2002). Distinct roles of activating transcription factor 6 (ATF6) and double-stranded RNA-activated protein kinase-like endoplasmic reticulum kinase (PERK) in transcription during the mammalian unfolded protein response. Biochem. J. *336*, 585–594.

Okino, C.H., Alessi, A.C., Montassier, M. de F., Rosa, A.J., Wang, X., and Montassier, H.J. (2013). Humoral and cell-mediated immune responses to different doses of attenuated vaccine against avian infectious bronchitis virus. Viral Immunol. *26*, 259–267. https://doi.org/10.1089/vim.2013.0015

Okino, C.H., Mores, M.A., Trevisol, I.M., Coldebella, A., Montassier, H.J., and Brentano, L. (2017). Early immune responses and development of pathogenesis of avian infectious bronchitis viruses with different virulence profiles. PLOS ONE *12*, e0172275. https://doi.org/10.1371/journal.pone.0172275

Oostra, M., te Lintelo, E.G., Deijs, M., Verheije, M.H., Rottier, P.J., and de Haan, C.A. (2007). Localization and membrane topology of coronavirus nonstructural protein 4: involvement of the early secretory pathway in replication. J. Virol. *81*, 12323–12336.

Otsuki, K., Noro, K., Yamamoto, H., and Tsubokura, M. (1979). Studies on avian infectious bronchitis virus (IBV). II. Propagation of IBV in several cultured cells. Arch. Virol. *60*, 115–122.

Otsuki, K., Huggins, M.B., and Cook, J.K. (1990). Comparison of the susceptibility to avian infectious bronchitis virus infection of two inbred lines of white leghorn chickens. Avian Pathol. *19*, 467–475.

Park, M., Joh, S., Choi, K., Kim, A., Seo, M., Song, J., and Yun, S. (2016). Correlations in the results of virus neutralization test, hemagglutination inhibition test, and enzyme-linked immunosorbent assay to determine infectious bronchitis virus vaccine potency. Korean J. Vet. Res. *56*, 189–192.

Parsons, D., Ellis, M.M., Cavanagh, D., and Cook, J.K. (1992). Characterisation of an infectious bronchitis virus isolated from vaccinated broiler breeder flocks. Vet. Rec. *131*, 408–411.

Pei, J., and Collisson, E.W. (2005). Specific antibody secreting cells from chickens can be detected by three days and memory B cells by three

weeks post-infection with the avian respiratory coronavirus. Dev. Comp. Immunol. *29*, 153–160. https://doi.org/10.1016/j.dci.2004.06.009

Pei, J., Sekellick, M.J., Marcus, P.I., Choi, I.S., and Collisson, E.W. (2001). Chicken interferon type I inhibits infectious bronchitis virus replication and associated respiratory illness. J. Interferon Cytokine Res. *21*, 1071–1077. https://doi.org/10.1089/107999001317205204

Pei, J., Briles, W.E., and Collisson, E.W. (2003). Memory T-cells protect chicks from acute infectious bronchitis virus infection. Virology *306*, 376–384.

Pendleton, A.R., and Machamer, C.E. (2005). Infectious bronchitis virus 3a protein localizes to a novel domain of the smooth endoplasmic reticulum. J. Virol. *79*, 6142–6151.

Pensaert, M., and Lambrechts, C. (1994). Vaccination of chickens against a Belgian nephropathogenic strain of infectious bronchitis virus B1648 using attenuated homologous and heterologous strains. Avian Pathol. *23*, 631–641.

Pereira, C.G., Saraiva, G.L., Vidigal, P.M., Fietto, J.L., Bressan, G.C., Moreira, M.A., de Almeida, M.R., and Júnior, A.S. (2016). Distribution of infectious bronchitis virus strains in different organs and evidence of vertical transmission in natural infection. Arch. Virol. *161*, 3355–3363. https://doi.org/10.1007/s00705-016-3030-5

Pettersson, R.F., Ambros, V., and Baltimore, D. (1978). Identification of a protein linked to nascent poliovirus RNA and to the polyuridylic acid of negative-strand RNA. J. Virol. *27*, 357–365.

Plant, E.P., Pérez-Alvarado, G.C., Jacobs, J.L., Mukhopadhyay, B., Hennig, M., and Dinman, J.D. (2005). A three-stemmed mRNA pseudoknot in the SARS coronavirus frameshift signal. PLOS Biol. *3*, e172.

Ponnusamy, R., Moll, R., Weimar, T., Mesters, J.R., and Hilgenfeld, R. (2008). Variable oligomerization modes in coronavirus non-structural protein 9. J. Mol. Biol. *383*, 1081–1096. https://doi.org/10.1016/j.jmb.2008.07.071

Potter, J.A., Randall, R.E., and Taylor, G.L. (2008). Crystal structure of human IPS1/MAVS/VISA/Cardif caspase activation recruitment domain. BMC Struct. Biol. *8*, 11.

Prentice, E., Jerome, W.G., Yoshimori, T., Mizushima, N., and Denison, M.R. (2004a). Coronavirus replication complex formation utilizes components of cellular autophagy. J. Biol. Chem. *279*, 10136–10141. https://doi.org/10.1074/jbc.M306124200

Prentice, E., McAuliffe, J., Lu, X., Subbarao, K., and Denison, M.R. (2004b). Identification and characterization of severe acute respiratory syndrome coronavirus replicase proteins. J. Virol. *78*, 9977–9986. https://doi.org/10.1128/JVI.78.18.9977-9986.2004

Promkuntod, N., Wickramasinghe, I.N., de Vrieze, G., Gröne, A., and Verheije, M.H. (2013). Contributions of the S2 spike ectodomain to attachment and host range of infectious bronchitis virus. Virus Res. *177*, 127–137. https://doi.org/10.1016/j.virusres.2013.09.006

Promkuntod, N., van Eijndhoven, R.E., de Vrieze, G., Gröne, A., and Verheije, M.H. (2014). Mapping of the receptor-binding domain and amino acids critical for attachment in the spike protein of avian coronavirus infectious bronchitis virus. Virology *448*, 26–32. https://doi.org/10.1016/j.virol.2013.09.018

Raggi, L.G., and Lee, G.G. (1965). Lack of correlation between infectivity, serologic response and challenge results in immunization with an avian infectious bronchitis vaccine. J. Immunol. *94*, 538–543.

Raj, G.D., and Jones, R.C. (1996a). Local antibody production in the oviduct and gut of hens infected with a variant strain of infectious bronchitis virus. Vet. Immunol. Immunopathol. *53*, 147–161.

Raj, G.D., and Jones, R.C. (1996b). Immunopathogenesis of infection in SPF chicks and commercial broiler chickens of a variant infectious bronchitis virus of economic importance. Avian Pathol. *25*, 481–501.

Raj, G.D., and Jones, R.C. (1997). Effect of T-cell suppression by cyclosporin on primary and persistent infections of infectious bronchitis virus in chickens. Avian Pathol. *26*, 257–276.

Raman, S., Bouma, P., Williams, G.D., and Brian, D.A. (2003). Stem-loop III in the 5′ untranslated region is a cis-acting element in bovine coronavirus defective interfering RNA replication. J. Virol. *77*, 6720–6730.

Ratanasethakul, C., and Cumming, R.B. (1983a). Effect of environmental temperature on the mortality in vaccinated chickens after challenge with Australian infectious bronchitis virus. Aust. Vet. J. *60*, 255–256.

Ratanasethakul, C., and Cumming, R.B. (1983b). Immune response of chickens to various routes of administration of Australian infectious bronchitis vaccine. Aust. Vet. J. *60*, 214–216.

Ratia, K., Saikatendu, K.S., Santarsiero, B.D., Barretto, N., Baker, S.C., Stevens, R.C., and Mesecar, A.D. (2006). Severe acute respiratory syndrome coronavirus papain-like protease: structure of a viral deubiquitinating enzyme. Proc. Natl. Acad. Sci. U.S.A. *103*, 5717–5722.

Reddy, V.R., Trus, I., Desmarets, L.M., Li, Y., Theuns, S., and Nauwynck, H.J. (2016). Productive replication of nephropathogenic infectious bronchitis virus in peripheral blood monocytic cells, a strategy for viral dissemination and kidney infection in chickens. Vet. Res. *47*, 70. https://doi.org/10.1186/s13567-016-0354-9

Reggiori, F., Monastyrska, I., Verheije, M.H., Calì, T., Ulasli, M., Bianchi, S., Bernasconi, R., de Haan, C.A., and Molinari, M. (2010). Coronaviruses Hijack the LC3-I-positive EDEMosomes, ER-derived vesicles exporting short-lived ERAD regulators, for replication. Cell Host Microbe *7*, 500–508. https://doi.org/10.1016/j.chom.2010.05.013

Ricagno, S., Egloff, M.P., Ulferts, R., Coutard, B., Nurizzo, D., Campanacci, V., Cambillau, C., Ziebuhr, J., and Canard, B. (2006). Crystal structure and mechanistic determinants of SARS coronavirus nonstructural protein 15 define an endoribonuclease family. Proc. Natl. Acad. Sci. U.S.A. *103*, 11892–11897.

Roh, H.J., Hilt, D.A., and Jackwood, M.W. (2014). Detection of infectious bronchitis virus with the use of real-time quantitative reverse transcriptase-PCR and correlation with virus detection in embryonated eggs. Avian Dis. *58*, 398–403. https://doi.org/10.1637/10764-010914-Reg.1

Ron, D., and Walter, P. (2007). Signal integration in the endoplasmic reticulum unfolded protein response. Nat. Rev. Mol. Cell Biol. *8*, 519–529.

Ruano, M., El-Attrache, J., and Villegas, P. (2000). A rapid-plate hemagglutination assay for the detection of infectious bronchitis virus. Avian Dis. *44*, 99–104.

Ruch, T.R., and Machamer, C.E. (2012). A single polar residue and distinct membrane topologies impact the function of the infectious bronchitis coronavirus E protein. PLOS Pathog. *8*, e1002674. https://doi.org/10.1371/journal.ppat.1002674

Salojin, K.V., Owusu, I.B., Millerchip, K.A., Potter, M., Platt, K.A., and Oravecz, T. (2006). Essential role of MAPK phosphatase-1 in the negative control of innate immune responses. J. Immunol. *176*, 1899–1907.

Sapats, S.I., Ashton, F., Wright, P.J., and Ignjatovic, J. (1996). Novel variation in the N protein of avian infectious bronchitis virus. Virology *226*, 412–417.

Sawicki, S.G., and Sawicki, D.L. (1995). Coronaviruses use discontinuous extension for synthesis of subgenome-length negative strands. Adv. Exp. Med. Biol. *380*, 499–506.

Sawicki, S.G., Sawicki, D.L., Younker, D., Meyer, Y., Thiel, V., Stokes, H., and Siddell, S.G. (2005). Functional and genetic analysis of coronavirus replicase-transcriptase proteins. PLOS Pathog. *1*, e39. https://doi.org/10.1371/journal.ppat.0010039

Schaad, M.C., Stohlman, S.A., Egbert, J., Lum, K., Fu, K., Wei, T., and Baric, R.S. (1990). Genetics of mouse hepatitis virus transcription: identification of cistrons which may function in positive and negative strand RNA synthesis. Virology *177*, 634–645.

Schalk, A.F., and Hawn, M.C. (1931). An apparently new respiratory disease of baby chicks. J. AVMA *78*, 413–422.

Schelle, B., Karl, N., Ludewig, B., Siddell, S.G., and Thiel, V. (2006). Nucleocapsid protein expression facilitates coronavirus replication. Adv. Exp. Med. Biol. *581*, 43–48. https://doi.org/10.1007/978-0-387-33012-9_6

Schröder, M. (2008). Endoplasmic reticulum stress responses. Cell Mol. Life Sci. *65*, 862–894.

Schwegmann-Wessels, C., Al-Falah, M., Escors, D., Wang, Z., Zimmer, G., Deng, H., Enjuanes, L., Naim, H.Y., and Herrler, G. (2004). A novel sorting signal for intracellular localization is present in the S protein of a porcine coronavirus but absent from severe acute respiratory syndrome-associated coronavirus. J. Biol. Chem. *279*, 43661–43666. https://doi.org/10.1074/jbc.M407233200

Scobey, T., Yount, B.L., Sims, A.C., Donaldson, E.F., Agnihothram, S.S., Menachery, V.D., Graham, R.L., Swanstrom, J., Bove, P.F., Kim, J.D., *et al.* (2013). Reverse genetics with a full-length infectious cDNA of the

Middle East respiratory syndrome coronavirus. Proc. Natl. Acad. Sci. U.S.A. *110*, 16157–16162. https://doi.org/10.1073/pnas.1311542110

Senne, D.A. (2008). Virus propagation in embryonating eggs. In A Laboratory Manual for Isolation and Identification of Avian Pathogens, 5th edn, L. Dufour-Zavala, D.E. Swayne, J.R. Glisson, J.E. Pearson, W.M. Reed, M.W. Jackwood and P.R. Woocock, eds (American Association of Avian Pathologists, Jacksonville, FL), pp. 204–208.

Seo, S.H., Pei, J., Briles, W.E., Dzielawa, J., and Collisson, E.W. (2000). Adoptive transfer of infectious bronchitis virus primed alphabeta T-cells bearing CD8 antigen protects chicks from acute infection. Virology *269*, 183–189. https://doi.org/10.1006/viro.2000.0211

Sethna, P.B., Hofmann, M.A., and Brian, D.A. (1991). Minus-strand copies of replicating coronavirus mRNAs contain antileaders. J. Virol. *65*, 320–325.

Seybert, A., Posthuma, C.C., van Dinten, L.C., Snijder, E.J., Gorbalenya, A.E., and Ziebuhr, J. (2005). A complex zinc finger controls the enzymatic activities of nidovirus helicases. J. Virol. *79*, 696–704.

Shamsaddini-Bafti, M., Vasfi-Marandi, M., Momayez, R., Toroghi, R., Pourbakhsh, S.A., Salari, R., and Tabrizchi, H. (2014). Detection of 793/B serotype of infectious bronchitis virus in tissue sample by indirect immunoperoxidase assay. Comp. Clin. Pathol. *23*, 347–352.

Shang, J., Zheng, Y., Yang, Y., Liu, C., Geng, Q., Luo, C., Zhang, W., and Li, F. (2018). Cryo-EM structure of infectious bronchitis coronavirus spike protein reveals structural and functional evolution of coronavirus spike proteins. PLOS Pathog. *14*, e1007009. https://doi.org/10.1371/journal.ppat.1007009

Shen, S., and Liu, D.X. (2001). Characterization of temperature-sensitive (ts) mutants of coronavirus infectious bronchitis virus (IBV). Adv. Exp. Med. Biol. *494*, 557–562.

Shen, S., Wen, Z.L., and Liu, D.X. (2003). Emergence of a coronavirus infectious bronchitis virus mutant with a truncated 3b gene: functional characterization of the 3b protein in pathogenesis and replication. Virology *311*, 16–27.

Shen, S., Law, Y.C., and Liu, D.X. (2004). A single amino acid mutation in the spike protein of coronavirus infectious bronchitis virus hampers its maturation and incorporation into virions at the nonpermissive temperature. Virology *326*, 288–298. https://doi.org/10.1016/j.virol.2004.06.016

Shi, D., Shi, H., Sun, D., Chen, J., Zhang, X., Wang, X., Zhang, J., Ji, Z., Liu, J., Cao, L., *et al.* (2017). Nucleocapsid interacts with npm1 and protects it from proteolytic cleavage, enhancing cell survival, and is involved in PEDV growth. Sci. Rep. *7*, 39700. https://doi.org/10.1038/srep39700

Shi, J., Sivaraman, J., and Song, J. (2008). Mechanism for controlling the dimer-monomer switch and coupling dimerization to catalysis of the severe acute respiratory syndrome coronavirus 3C-like protease. J. Virol. *82*, 4620–4629. https://doi.org/10.1128/JVI.02680-07

Shirato, K., Kawase, M., and Matsuyama, S. (2013). Middle East respiratory syndrome coronavirus infection mediated by the transmembrane serine protease TMPRSS2. J. Virol. *87*, 12552–12561. https://doi.org/10.1128/JVI.01890-13

Siu, Y.L., Teoh, K.T., Lo, J., Chan, C.M., Kien, F., Escriou, N., Tsao, S.W., Nicholls, J.M., Altmeyer, R., Peiris, J.S., *et al.* (2008). The M, E, and N structural proteins of the severe acute respiratory syndrome coronavirus are required for efficient assembly, trafficking, and release of virus-like particles. J. Virol. *82*, 11318–11330. https://doi.org/10.1128/JVI.01052-08

Smith, H.W., Cook, J.K., and Parsell, Z.E. (1985). The experimental infection of chickens with mixtures of infectious bronchitis virus and Escherichia coli. J. Gen. Virol. *66*, 777–786. https://doi.org/10.1099/0022-1317-66-4-777

Snijder, E.J., Bredenbeek, P.J., Dobbe, J.C., Thiel, V., Ziebuhr, J., Poon, L.L., Guan, Y., Rozanov, M., Spaan, W.J., and Gorbalenya, A.E. (2003). Unique and conserved features of genome and proteome of SARS-coronavirus, an early split-off from the coronavirus group 2 lineage. J. Mol. Biol. *331*, 991–1004.

Snijder, E.J., van der Meer, Y., Zevenhoven-Dobbe, J., Onderwater, J.J., van der Meulen, J., Koerten, H.K., and Mommaas, A.M. (2006). Ultrastructure and origin of membrane vesicles associated with the severe acute respiratory syndrome coronavirus replication complex. J. Virol. *80*, 5927–5940.

Song, C.S., Lee, Y.J., Kim, J.H., Sung, H.W., Lee, C.W., Izumiya, Y., Miyazawa, T., Jang, H.K., and Mikami, T. (1998). Epidemiological classification of infectious bronchitis virus isolated in Korea between 1986 and 1997. Avian Pathol. *27*, 409–416. https://doi.org/10.1080/03079459808419360

Spencer, K.A., Dee, M., Britton, P., and Hiscox, J.A. (2008). Role of phosphorylation clusters in the biology of the coronavirus infectious bronchitis virus nucleocapsid protein. Virology *370*, 373–381.

Steil, B.P., Kempf, B.J., and Barton, D.J. (2010). Poly(A) at the 3' end of positive-strand RNA and VPg-linked poly(U) at the 5' end of negative-strand RNA are reciprocal templates during replication of poliovirus RNA. J. Virol. *84*, 2843–2858. https://doi.org/10.1128/JVI.02620-08

Stennicke, H.R., Ryan, C.A., and Salvesen, G.S. (2002). Reprieval from execution: the molecular basis of caspase inhibition. Trends Biochem. Sci. *27*, 94–101.

Stern, D.F., Burgess, L., and Sefton, B.M. (1982). Structural analysis of virion proteins of the avian coronavirus infectious bronchitis virus. J. Virol. *42*, 208–219.

St-Jean, J.R., Desforges, M., Almazán, F., Jacomy, H., Enjuanes, L., and Talbot, P.J. (2006). Recovery of a neurovirulent human coronavirus OC43 from an infectious cDNA clone. J. Virol. *80*, 3670–3674.

Stohlman, S.A., Baric, R.S., Nelson, G.N., Soe, L.H., Welter, L.M., and Deans, R.J. (1988). Specific interaction between coronavirus leader RNA and nucleocapsid protein. J. Virol. *62*, 4288–4295.

Stokes, H.L., Baliji, S., Hui, C.G., Sawicki, S.G., Baker, S.C., and Siddell, S.G. (2010). A new cistron in the murine hepatitis virus replicase gene. J. Virol. *84*, 10148–10158. https://doi.org/10.1128/JVI.00901-10

Sturman, L.S., Holmes, K.V., and Behnke, J. (1980). Isolation of coronavirus envelope glycoproteins and interaction with the viral nucleocapsid. J. Virol. *33*, 449–462.

Su, D., Lou, Z., Sun, F., Zhai, Y., Yang, H., Zhang, R., Joachimiak, A., Zhang, X.C., Bartlam, M., and Rao, Z. (2006). Dodecamer structure of severe acute respiratory syndrome coronavirus nonstructural protein nsp10. J. Virol. *80*, 7902–7908.

Su, M.C., Chang, C.T., Chu, C.H., Tsai, C.H., and Chang, K.Y. (2005). An atypical RNA pseudoknot stimulator and an upstream attenuation signal for -1 ribosomal frameshifting of SARS coronavirus. Nucleic Acids Res. *33*, 4265–4275.

Sumi, V., Singh, S.D., Dhama, K., Gowthaman, V., Barathidasan, R., and Sukumar, K. (2012). Isolation and molecular characterization of infectious bronchitis virus from recent outbreaks in broiler flocks reveals emergence of novel strain in India. Trop. Anim. Health Prod. *44*, 1791–1795. https://doi.org/10.1007/s11250-012-0140-2.

Survashe, B.D., Aitken, I.D., and Powell, J.R. (1979). The response of the Harderian gland of the fowl to antigen given by the ocular route. I. Histological changes. Avian Pathol. *8*, 77–93.

Sutton, G., Fry, E., Carter, L., Sainsbury, S., Walter, T., Nettleship, J., Berrow, N., Owens, R., Gilbert, R., Davidson, A., *et al.* (2004). The nsp9 replicase protein of SARS-coronavirus, structure and functional insights. Structure *12*, 341–353. https://doi.org/10.1016/j.str.2004.01.016.

Tabas, I., and Ron, D. (2011). Integrating the mechanisms of apoptosis induced by endoplasmic reticulum stress. Nat. Cell Biol. *13*, 184–190. https://doi.org/10.1038/ncb0311-184.

Tait, S.W., and Green, D.R. (2010). Mitochondria and cell death: outer membrane permeabilization and beyond. Nat. Rev. Mol. Cell Biol. *11*, 621–632. https://doi.org/10.1038/nrm2952.

Tamura, R., Kanda, T., Imazeki, F., Wu, S., Nakamoto, S., Tanaka, T., Arai, M., Fujiwara, K., Saito, K., Roger, T., *et al.* (2011). Hepatitis C Virus nonstructural 5A protein inhibits lipopolysaccharide-mediated apoptosis of hepatocytes by decreasing expression of Toll-like receptor 4. J. Infect. Dis. *204*, 793–801. https://doi.org/10.1093/infdis/jir381.

Tan, J., Verschueren, K.H., Anand, K., Shen, J., Yang, M., Xu, Y., Rao, Z., Bigalke, J., Heisen, B., Mesters, J.R., *et al.* (2005). pH-dependent conformational flexibility of the SARS-CoV main proteinase (M(pro)) dimer: molecular dynamics simulations and multiple X-ray structure analyses. J. Mol. Biol. *354*, 25–40.

Tan, Y.W., Fang, S., Fan, H., Lescar, J., and Liu, D.X. (2006). Amino acid residues critical for RNA-binding in the N-terminal domain of the nucleocapsid protein are essential determinants for the infectivity of coronavirus in cultured cells. Nucleic Acids Res. *34*, 4816–4825.

Tan, Y.W., Hong, W., and Liu, D.X. (2012). Binding of the 5′-untranslated region of coronavirus RNA to zinc finger CCHC-type and RNA-binding motif 1 enhances viral replication and transcription. Nucleic Acids Res. *40*, 5065–5077. https://doi.org/10.1093/nar/gks165.

Tan, Y.W., Fung, T.S., Shen, H., Huang, M., and Liu, D.X. (2018). Coronavirus infectious bronchitis virus non-structural proteins 8 and 12 form stable complex independent of the non-translated regions of viral RNA and other viral proteins. Virology *513*, 75–84.

Tay, F.P., Huang, M., Wang, L., Yamada, Y., and Liu, D.X. (2012). Characterization of cellular furin content as a potential factor determining the susceptibility of cultured human and animal cells to coronavirus infectious bronchitis virus infection. Virology *433*, 421–430. https://doi.org/10.1016/j.virol.2012.08.037.

Tekes, G., Hofmann-Lehmann, R., Stallkamp, I., Thiel, V., and Thiel, H.J. (2008). Genome organization and reverse genetic analysis of a type I feline coronavirus. J. Virol. *82*, 1851–1859.

Teske, B.F., Wek, S.A., Bunpo, P., Cundiff, J.K., McClintick, J.N., Anthony, T.G., and Wek, R.C. (2011). The eIF2 kinase PERK and the integrated stress response facilitate activation of ATF6 during endoplasmic reticulum stress. Mol. Biol. Cell *22*, 4390–4405. https://doi.org/10.1091/mbc.E11-06-0510.

Thayer, S.G., Nersessian, B.N., Rivetz, B., and Fletcher, O.J. (1987). Comparison of serological tests for antibodies against Newcastle disease virus and infectious bronchitis virus using ImmunoComb solid-phase immunoassay, a commercial enzyme-linked immunosorbent assay, and the hemagglutination-inhibition assay. Avian Dis. *31*, 459–463.

Thiel, V., Herold, J., Schelle, B., and Siddell, S.G. (2001). Infectious RNA transcribed *in vitro* from a cDNA copy of the human coronavirus genome cloned in vaccinia virus. J. Gen. Virol. *82*, 1273–1281.

Thompson, A.A., and Peersen, O.B. (2004). Structural basis for proteolysis-dependent activation of the poliovirus RNA-dependent RNA polymerase. EMBO J. *23*, 3462–3471. https://doi.org/10.1038/sj.emboj.7600357.

Thor, S.W., Hilt, D.A., Kissinger, J.C., Paterson, A.H., and Jackwood, M.W. (2011). Recombination in avian gamma-coronavirus infectious bronchitis virus. Viruses *3*, 1777–1799. https://doi.org/10.3390/v3091777.

To, J., Surya, W., Fung, T.S., Li, Y., Verdià-Bàguena, C., Queralt-Martin, M., Aguilella, V.M., Liu, D.X., and Torres, J. (2017). Channel-inactivating mutations and their revertant mutants in the envelope protein of infectious bronchitis virus. J. Virol. *91*, e02158–16.

Toro, H., and Fernandez, I. (1994). Avian infectious bronchitis: specific lachrymal IgA level and resistance against challenge. Zentralblatt Veterinarmedizin Reihe B *41*, 467–472.

Toro, H., Espinoza, C., Ponce, V., Rojas, V., Morales, M.A., and Kaleta, E.F. (1997). Infectious bronchitis: effect of viral doses and routes on specific lacrimal and serum antibody responses in chickens. Avian Dis. *41*, 379–387.

Toro, H., van Santen, V.L., and Jackwood, M.W. (2012). Genetic diversity and selection regulates evolution of infectious bronchitis virus. Avian Dis. *56*, 449–455. https://doi.org/10.1637/10072-020212-Review.1.

Toro, H., van Santen, V.L., Ghetas, A.M., and Joiner, K.S. (2015). Cross-protection by infectious bronchitis viruses under controlled experimental conditions. Avian Dis. *59*, 532–536. https://doi.org/10.1637/11231-070615-Reg.1.

Torres, J., Parthasarathy, K., Lin, X., Saravanan, R., Kukol, A., and Liu, D.X. (2006). Model of a putative pore: the pentameric alpha-helical bundle of SARS coronavirus E protein in lipid bilayers. Biophys. J. *91*, 938–947.

Trevisol, I.M., Esteves, P.A., Schaefer, R., Jaenisch, F.R.F., Di Fabio, J., and Brentano, L. (2009). Associação entre o vírus da bronquite infecciosa das galinhas e alterações da musculatura peitoral. Rev. Bras. Cienc. Avic. *11*.

Trinchieri, G., and Sher, A. (2007). Cooperation of toll-like receptor signals in innate immune defence. Nat. Rev. Immunol. *7*, 179–190.

Tsukamoto, Y., Kotani, T., Shiraishi, Y., Kawamura, H., and Sakuma, S. (1996). Epithelial cell proliferation of collecting ducts and ureters in the regenerating process of interstitial nephritis caused by infectious bronchitis virus. Avian Pathol. *25*, 95–102.

[105] Tyrrell, D.A., and Bynoe, M.L. (1965). Cultivation of a novel type of common-cold virus in organ cultures. Br. Med. J. *1*, 1467–1470.

Umar, S., Shah, M.A.A., Munir, M.T., Ahsan, U., and Kaboudi, K. (2016). Infectious bronchitis virus: evolution and vaccination. World Poult. Sci. *72*, 49–60.

Valastro, V., Holmes, E.C., Britton, P., Fusaro, A., Jackwood, M.W., Cattoli, G., and Monne, I. (2016). S1 gene-based phylogeny of infectious bronchitis virus: An attempt to harmonize virus classification. Infect. Genet. Evol. *39*, 349–364.

van Beurden, S.J., Berends, A.J., Krämer-Kühl, A., Spekreijse, D., Chenard, G., Philipp, H.C., Mundt, E., Rottier, P.J.M., and Verheije, M.H. (2018). Recombinant live attenuated avian coronavirus vaccines with deletions in the accessory genes 3ab and/or 5ab protect against infectious bronchitis in chickens. Vaccine *36*, 1085–1092.

van der Meer, Y., van Tol, H., Locker, J.K., and Snijder, E.J. (1998). ORF1a-encoded replicase subunits are involved in the membrane association of the arterivirus replication complex. J. Virol. *72*, 6689–6698.

van Hamme, E., Dewerchin, H.L., Cornelissen, E., Verhasselt, B., and Nauwynck, H.J. (2008). Clathrin- and caveolae-independent entry of feline infectious peritonitis virus in monocytes depends on dynamin. J. Gen. Virol. *89*, 2147–2156.

van Vliet, A.L., Smits, S.L., Rottier, P.J., and de Groot, R.J. (2002). Discontinuous and non-discontinuous subgenomic RNA transcription [106] in a nidovirus. EMBO J. *21*, 6571–6580.

Vennema, H., Godeke, G.J., Rossen, J.W., Voorhout, W.F., Horzinek, M.C., Opstelten, D.J., and Rottier, P.J. (1996). Nucleocapsid-independent assembly of coronavirus-like particles by coexpression of viral envelope protein genes. EMBO J. *15*, 2020–2028.

Verdiá-Báguena, C., Nieto-Torres, J.L., Alcaraz, A., DeDiego, M.L., Torres, J., Aguilella, V.M., and Enjuanes, L. (2012). Coronavirus E protein forms ion channels with functionally and structurally-involved membrane lipids. Virology *432*, 485–494. https://doi.org/10.1016/j.virol.2012.07.005.

Versteeg, G.A., van de Nes, P.S., Bredenbeek, P.J., and Spaan, W.J. (2007). The coronavirus spike protein induces endoplasmic reticulum stress and upregulation of intracellular chemokine mRNA concentrations. J. Virol. *81*, 10981–10990.

Vervelde, L., Matthijs, M.G., van Haarlem, D.A., de Wit, J.J., and Jansen, C.A. (2013). Rapid NK-cell activation in chicken after infection with infectious bronchitis virus M41. Vet. Immunol. Immunopathol. *151*, 337–341. https://doi.org/10.1016/j.vetimm.2012.11.012.

Villarreal, L.Y. (2010). Diagnosis of infectious bronchitis: an overview of concepts and tools. Rev. Bras. Cienc. Avic. *12*, 111–114.

Villarreal, L.Y., Brandão, P.E., Chacón, J.L., Assayag, M.S., Maiorka, P.C., Raffi, P., Saidenberg, A.B., Jones, R.C., and Ferreira, A.J. (2007). Orchitis in roosters with reduced fertility associated with avian infectious bronchitis virus and avian metapneumovirus infections. Avian Dis. *51*, 900–904. https://doi.org/10.1637/7815-121306-REGR4.1.

von Brunn, A., Teepe, C., Simpson, J.C., Pepperkok, R., Friedel, C.C., Zimmer, [107] R., Roberts, R., Baric, R., and Haas, J. (2007). Analysis of intraviral protein-protein interactions of the SARS coronavirus ORFeome. PLOS ONE *2*, e459. https://doi.org/10.1371/journal.pone.0000459.

Walsh, D., and Mohr, I. (2011). Viral subversion of the host protein synthesis machinery. Nat. Rev. Microbiol. *9*, 860–875. https://doi.org/10.1038/nrmicro2655.

Wang, J., Fang, S., Xiao, H., Chen, B., Tam, J.P., and Liu, D.X. (2009). Interaction of the coronavirus infectious bronchitis virus membrane protein with beta-actin and its implication in virion assembly and budding. PLOS ONE *4*, e4908. https://doi.org/10.1371/journal.pone.0004908.

Wang, X., Rosa, A.J., Oliverira, H.N., Rosa, G.J., Guo, X., Travnicek, M., and Girshick, T. (2006). Transcriptome of local innate and adaptive immunity during early phase of infectious bronchitis viral infection. Viral Immunol. *19*, 768–774. https://doi.org/10.1089/vim.2006.19.768.

Wang, X., Liao, Y., Yap, P.L., Png, K.J., Tam, J.P., and Liu, D.X. (2009). Inhibition of protein kinase R activation and upregulation of GADD34 expression play a synergistic role in facilitating coronavirus replication by maintaining de novo protein synthesis in virus-infected cells. J. Virol. *83*, 12462–12472. https://doi.org/10.1128/JVI.01546-09.

Watters, T.M., Kenny, E.F., and O'Neill, L.A. (2007). Structure, function and regulation of the Toll/IL-1 receptor adaptor proteins. Immunol. Cell Biol. *85*, 411–419.

Wei, Y., Ji, Y., Guo, H., Zhi, X., Han, S., Zhang, Y., Gao, Y., Chang, Y., Yan, D., Li, K., *et al.* (2017). CD59 association with infectious bronchitis virus

particles protects against antibody-dependent complement-mediated lysis. J. Gen. Virol. *98*, 2725–2730. https://doi.org/10.1099/jgv.0.000962.

Wei, Y.Q., Guo, H.C., Dong, H., Wang, H.M., Xu, J., Sun, D.H., Fang, S.G., Cai, X.P., Liu, D.X., and Sun, S.Q. (2014). Development and characterization of a recombinant infectious bronchitis virus expressing the ectodomain region of S1 gene of H120 strain. Appl. Microbiol. Biotechnol. *98*, 1727–1735. https://doi.org/10.1007/s00253-013-5352-5.

Welihinda, A.A., Tirasophon, W., and Kaufman, R.J. (1999). The cellular response to protein misfolding in the endoplasmic reticulum. Gene Expr. *7*, 293–300.

Wesley, R.D., Woods, R.D., and Cheung, A.K. (1991). Genetic analysis of porcine respiratory coronavirus, an attenuated variant of transmissible gastroenteritis virus. J. Virol. *65*, 3369–3373.

Westerbeck, J.W., and Machamer, C.E. (2015). A coronavirus E protein is present in two distinct pools with different effects on assembly and the secretory pathway. J. Virol. *89*, 9313–9323. https://doi.org/10.1128/JVI.01237-15.

White, J.M., and Whittaker, G.R. (2016). Fusion of enveloped viruses in endosomes. Traffic *17*, 593–614. https://doi.org/10.1111/tra.12389.

Wickramasinghe, I.N., de Vries, R.P., Eggert, A.M., Wandee, N., de Haan, C.A., Gröne, A., and Verheije, M.H. (2015). Host tissue and glycan binding specificities of avian viral attachment proteins using novel avian tissue microarrays. PLOS ONE *10*, e0128893. https://doi.org/10.1371/journal.pone.0128893.

Wilson, N.S., Dixit, V., and Ashkenazi, A. (2009). Death receptor signal transducers: nodes of coordination in immune signaling networks. Nat. Immunol. *10*, 348–355. https://doi.org/10.1038/ni.1714.

Winter, C., Schwegmann-Wessels, C., Cavanagh, D., Neumann, U., and Herrler, G. (2006). Sialic acid is a receptor determinant for infection of cells by avian Infectious bronchitis virus. J. Gen. Virol. *87*, 1209–1216.

Winter, C., Herrler, G., and Neumann, U. (2008a). Infection of the tracheal epithelium by infectious bronchitis virus is sialic acid dependent. Microbes Infect. *10*, 367–373. https://doi.org/10.1016/j.micinf.2007.12.009.

Winter, C., Schwegmann-Wessels, C., Neumann, U., and Herrler, G. (2008b). The spike protein of infectious bronchitis virus is retained intracellularly by a tyrosine motif. J. Virol. *82*, 2765–2771.

Winterfield, R.W., and Albassam, M.A. (1984). Nephropathogenicity of infectious bronchitis virus. Poult. Sci. *63*, 2358–2363. https://doi.org/10.3382/ps.0632358.

Wong, H.H., Kumar, P., Tay, F.P., Moreau, D., Liu, D.X., and Bard, F. (2015). Genome-wide screen reveals valosin-containing protein requirement for coronavirus exit from endosomes. J. Virol. *89*, 11116–11128. https://doi.org/10.1128/JVI.01360-15.

Wong, S.K., Li, W., Moore, M.J., Choe, H., and Farzan, M. (2004). A 193-amino acid fragment of the SARS coronavirus S protein efficiently binds angiotensin-converting enzyme 2. J. Biol. Chem. *279*, 3197–3201. https://doi.org/10.1074/jbc.C300520200.

Woo, P.C., Huang, Y., Lau, S.K., and Yuen, K.Y. (2010). Coronavirus genomics and bioinformatics analysis. Viruses *2*, 1804–1820. https://doi.org/10.3390/v2081803.

Xiao, H., Xu, L.H., Yamada, Y., and Liu, D.X. (2008). Coronavirus spike protein inhibits host cell translation by interaction with eIF3f. PLOS ONE *3*, e1494. https://doi.org/10.1371/journal.pone.0001494.

Xu, G., Liu, X.Y., Zhao, Y., Chen, Y., Zhao, J., and Zhang, G.Z. (2016). Characterization and analysis of an infectious bronchitis virus strain isolated from southern China in 2013. Virol. J. *13*, 40. https://doi.org/10.1186/s12985-016-0497-3.

Xu, L., Khadijah, S., Fang, S., Wang, L., Tay, F.P., and Liu, D.X. (2010). The cellular RNA helicase DDX1 interacts with coronavirus nonstructural protein 14 and enhances viral replication. J. Virol. *84*, 8571–8583. https://doi.org/10.1128/JVI.00392-10.

Xu, L.H., Huang, M., Fang, S.G., and Liu, D.X. (2011). Coronavirus infection induces DNA replication stress partly through interaction of its nonstructural protein 13 with the p125 subunit of DNA polymerase δ. J. Biol. Chem. *286*, 39546–39559. https://doi.org/10.1074/jbc.M111.242206.

Xu, X., Liu, Y., Weiss, S., Arnold, E., Sarafianos, S.G., and Ding, J. (2003). Molecular model of SARS coronavirus polymerase: implications for biochemical functions and drug design. Nucleic Acids Res. *31*, 7117–7130.

Yachida, S., Aoyama, S., Takahashi, N., Iritani, Y., and Katagiri, K. (1978). Plastic multiwell plates to assay avian infectious bronchitis virus in organ cultures of chicken embryo trachea. J. Clin. Microbiol. *8*, 380–387.

Yachida, S., Iritani, Y., and Katagiri, K. (1979). Effect of incubation temperature on infectivity titration of mouse brain-passaged avian infectious bronchitis virus in laboratory host systems. Acta Virol. *23*, 398–402.

Yagyu, K., and Ohta, S. (1990). Detection of infectious bronchitis virus antigen from experimentally infected chickens by indirect immunofluorescent assay with monoclonal antibody. Avian Dis. *34*, 246–252.

Yamada, Y., and Liu, D.X. (2009). Proteolytic activation of the spike protein at a novel RRRR/S motif is implicated in furin-dependent entry, syncytium formation, and infectivity of coronavirus infectious bronchitis virus in cultured cells. J. Virol. *83*, 8744–8758. https://doi.org/10.1128/JVI.00613-09.

Yamada, Y., Liu, X.B., Fang, S.G., Tay, F.P., and Liu, D.X. (2009). Acquisition of cell-cell fusion activity by amino acid substitutions in spike protein determines the infectivity of a coronavirus in cultured cells. PLOS ONE *4*, e6130. https://doi.org/10.1371/journal.pone.0006130.

Yang, X., Chen, X., Bian, G., Tu, J., Xing, Y., Wang, Y., and Chen, Z. (2014). Proteolytic processing, deubiquitinase and interferon antagonist activities of Middle East respiratory syndrome coronavirus papain-like protease. J. Gen. Virol. *95*, 614–626.

Yang, Z., and Klionsky, D.J. (2010). Eaten alive: a history of macroautophagy. Nat. Cell Biol. *12*, 814–822. https://doi.org/10.1038/ncb0910-814.

Ye, J., Rawson, R.B., Komuro, R., Chen, X., Davé, U.P., Prywes, R., Brown, M.S., and Goldstein, J.L. (2000). ER stress induces cleavage of membrane-bound ATF6 by the same proteases that process SREBPs. Mol. Cell *6*, 1355–1364.

Ye, Y., and Hogue, B.G. (2007). Role of the coronavirus E viroporin protein transmembrane domain in virus assembly. J. Virol. *81*, 3597–3607.

Ye, Y., Hauns, K., Langland, J.O., Jacobs, B.L., and Hogue, B.G. (2007). Mouse hepatitis coronavirus A59 nucleocapsid protein is a type I interferon antagonist. J. Virol. *81*, 2554–2563.

Yoneda, T., Imaizumi, K., Oono, K., Yui, D., Gomi, F., Katayama, T., and Tohyama, M. (2001). Activation of caspase-12, an endoplastic reticulum (ER) resident caspase, through tumor necrosis factor receptor-associated factor 2-dependent mechanism in response to the ER stress. J. Biol. Chem. *276*, 13935–13940. https://doi.org/10.1074/jbc.M010677200.

Yoneyama, M., and Fujita, T. (2007). Function of RIG-I-like receptors in antiviral innate immunity. J. Biol. Chem. *282*, 15315–15318.

Yoshida, H., Haze, K., Yanagi, H., Yura, T., and Mori, K. (1998). Identification of the cis-acting endoplasmic reticulum stress response element responsible for transcriptional induction of mammalian glucose-regulated proteins. Involvement of basic leucine zipper transcription factors. J. Biol. Chem. *273*, 33741–33749.

Yoshida, H., Matsui, T., Yamamoto, A., Okada, T., and Mori, K. (2001). XBP1 mRNA is induced by ATF6 and spliced by IRE1 in response to ER stress to produce a highly active transcription factor. Cell *107*, 881–891.

Yoshikawa, T., Hill, T.E., Yoshikawa, N., Popov, V.L., Galindo, C.L., Garner, H.R., Peters, C.J., and Tseng, C.T. (2010). Dynamic innate immune responses of human bronchial epithelial cells to severe acute respiratory syndrome-associated coronavirus infection. PLOS ONE *5*, e8729. https://doi.org/10.1371/journal.pone.0008729.

Youn, S., Leibowitz, J.L., and Collisson, E.W. (2005a). *In vitro* assembled, recombinant infectious bronchitis viruses demonstrate that the 5a open reading frame is not essential for replication. Virology *332*, 206–215.

Youn, S., Collisson, E.W., and Machamer, C.E. (2005b). Contribution of trafficking signals in the cytoplasmic tail of the infectious bronchitis virus spike protein to virus infection. J. Virol. *79*, 13209–13217.

Youngner, J.S. (1954). Monolayer tissue cultures. I. Preparation and standardization of suspensions of trypsin-dispersed monkey kidney cells. Proc. Soc. Exp. Biol. Med. *85*, 202–205.

Yount, B., Curtis, K.M., and Baric, R.S. (2000). Strategy for systematic assembly of large RNA and DNA genomes: transmissible gastroenteritis virus model. J. Virol. *74*, 10600–10611.

Yount, B., Denison, M.R., Weiss, S.R., and Baric, R.S. (2002). Systematic assembly of a full-length infectious cDNA of mouse hepatitis virus strain A59. J. Virol. *76*, 11065–11078.

Yount, B., Curtis, K.M., Fritz, E.A., Hensley, L.E., Jahrling, P.B., Prentice, E., Denison, M.R., Geisbert, T.W., and Baric, R.S. (2003). Reverse genetics with a full-length infectious cDNA of severe acute respiratory syndrome coronavirus. Proc. Natl. Acad. Sci. U.S.A. *100*, 12995–13000. https://doi.org/10.1073/pnas.1735582100.

Yu, L., Zhang, X., Wu, T., Wang, Y., Meng, J., Liu, Q., Niu, X., and Wu, Y. (2017). The papain-like protease of avian infectious bronchitis virus has deubiquitinating activity. Arch. Virol. *162*, 1943–1950. https://doi.org/10.1007/s00705-017-3328-y.

Zalinger, Z.B., Elliott, R., Rose, K.M., and Weiss, S.R. (2015). MDA5 is critical to host defense during infection with murine coronavirus. J. Virol. *89*, 12330–12340. https://doi.org/10.1128/JVI.01470-15.

Zhai, Y., Sun, F., Li, X., Pang, H., Xu, X., Bartlam, M., and Rao, Z. (2005). Insights into SARS-CoV transcription and replication from the structure of the nsp7-nsp8 hexadecamer. Nat. Struct. Mol. Biol. *12*, 980–986.

Zhang, Y.T., and Whittaker, G. (2016). Productive infection of field strains of avian coronavirus infectious bronchitis virus in chicken peripheral blood-derived monocyte. bioRxiv, 041558.

Zhao, Q., Wang, X., Nelin, L.D., Yao, Y., Matta, R., Manson, M.E., Baliga, R.S., Meng, X., Smith, C.V., Bauer, J.A., *et al.* (2006). MAP kinase phosphatase 1 controls innate immune responses and suppresses endotoxic shock. J. Exp. Med. *203*, 131–140.

Zhao, Z., Thackray, L.B., Miller, B.C., Lynn, T.M., Becker, M.M., Ward, E., Mizushima, N.N., Denison, M.R., and Virgin, H.W.4th. (2007). Coronavirus replication does not require the autophagy gene ATG5. Autophagy *3*, 581–585.

Zheng, J., Yamada, Y., Fung, T.S., Huang, M., Chia, R., and Liu, D.X. (2018). Identification of N-linked glycosylation sites in the spike protein and their functional impact on the replication and infectivity of coronavirus infectious bronchitis virus in cell culture. Virology *513*, 65–74.

Zhong, Q., Hu, Y.X., Jin, J.H., Zhao, Y., Zhao, J., and Zhang, G.Z. (2016). Pathogenicity of virulent infectious bronchitis virus isolate YN on hen ovary and oviduct. Vet. Microbiol. *193*, 100–105. https://doi.org/10.1016/j.vetmic.2016.08.017.

Zhong, Y., Liao, Y., Fang, S., Tam, J.P., and Liu, D.X. (2012). Up-regulation of Mcl-1 and Bak by coronavirus infection of human, avian and animal cells modulates apoptosis and viral replication. PLOS ONE *7*, e30191. https://doi.org/10.1371/journal.pone.0030191.

Zhu, X., Wang, D., Zhou, J., Pan, T., Chen, J., Yang, Y., Lv, M., Ye, X., Peng, G., Fang, L., *et al.* (2017). Porcine deltacoronavirus nsp5 antagonizes type I interferon signaling by cleaving STAT2. J. Virol. *91*, e00003–17.

Ziebuhr, J., Snijder, E.J., and Gorbalenya, A.E. (2000). Virus-encoded proteinases and proteolytic processing in the Nidovirales. J. Gen. Virol. *81*, 853–879.

Zumla, A., Chan, J.F., Azhar, E.I., Hui, D.S., and Yuen, K.Y. (2016). Coronaviruses - drug discovery and therapeutic options. Nat. Rev. Drug Discov. *15*, 327–347. https://doi.org/10.1038/nrd.2015.37.

Züst, R., Cervantes-Barragan, L., Habjan, M., Maier, R., Neuman, B.W., Ziebuhr, J., Szretter, K.J., Baker, S.C., Barchet, W., Diamond, M.S., *et al.* (2011). Ribose 2'-O-methylation provides a molecular signature for the distinction of self and non-self mRNA dependent on the RNA sensor Mda5. Nat. Immunol. *12*, 137–143. https://doi.org/10.1038/ni.1979